SEDIMENT TRANSPORT AND DEPOSITION UNDER UPPER FLOW REGIME PLANE BED CONDITIONS

by

© RICHARD JAMES CHEEL, B.A., M.Sc.

A Thesis

Submitted to the School of Graduate Studies

in Partial Fulfillment of the Requirements

for the Degree

Doctor of Philosophy

McMaster University

May, 1984

SEDIMENT TRANSPORT AND DEPOSITION ON UPPER PLANE BEDS

DOCTOR OF PHILOSOPHY (1984) McMASTER UNIVERSITY
(Geology)

TITLE: Sediment Transport and Deposition Under Upper Flow Regime Plane Bed Conditions

AUTHOR: Richard James Cheel, B.A. (McMaster University)
M.Sc. (University of Ottawa)

SUPERVISOR: Professor G.V. Middleton

NUMBER OF PAGES: xiii, 183

ABSTRACT

Upper plane bed is a stable bedform which develops on mobile sand beds and results in the formation of horizontal laminae. An investigation of some characteristics of upper plane bed and its deposits is described in the thesis.

"Heavy mineral shadows" are described for the first time and defined as: irregular patches of heavy minerals, on bedding plane exposures of sandstones (or sands) deposited on an upper plane bed, which are characterized by the presence of an abrupt upstream boundary, with adjacent lighter minerals, and a gradual transition into the lighter minerals in the downstream direction. The directional significance of shadows is shown with examples from an ancient sandstone and from a flume. Flume experiments also showed that shadows wash out with increasing flow strength, suggesting their possible use in paleohydraulic interpretations.

Horizontal laminae formed under upper plane bed conditions are precisely described by a detailed examination of textural variations through laminated sands and sandstones as seen in thin section. The data show two types of structure: (1) "textural laminae", including both fining-upward (F.U.) and coarsening-upward (C.U.) laminae less than 1 mm thick, occuring in random sequence and extending generally less than 40 mm in the direction normal

to the depositing flow, and (2) laterally extensive "heavy mineral sheets'", consisting of layers (often only a few grain diameters thick) in which opaque heavy minerals are abundant in or making up coarsening-upward laminae. The characteristics of textural laminae are proposed to result from their formation by bursts (forming F.U. laminae) and sweeps (forming C.U. laminae) in the flow near the bed. Heavy minerals in sheets, however, are thought to move in patches (shadows?) on the bed largely in response to large eddies in the outer flow. Local erosion of the patches by sweeps incorporates the heavy minerals into C.U. laminae while the patches are resistant to the effects of bursts, so that heavy minerals are absent in F.U. laminae.

ACKNOWLEDGEMENTS

The author thanks Dr. G.V. Middleton for supervising the thesis and for suggestions for improvement on the various drafts that he suffered through. The list of others who are thanked for their help are: the supervisory committee of Dr. J. Kramer and Dr. A. Smith, Dr. R.G. Walker for both positive and negative comments on the work during its development, Dr. B. Kendrick (University of Waterloo) for allowing access to his computer and graphics board, Dr. B.R. Rust (University of Ottawa) for providing laboratory facilities during the flume work in Ottawa, Dana Naldrett (University of Ottawa) for help with some of the more tedious jobs during the flume work, the Geological Survey of Canada for allowing access to their flume and esspecially to Paul Egginton and John Luscombe, and Len Zwicker who developed the technique for impregnating unconsolidated sands and prepared exellent thin sections for textural analysis. Thanks also to the faculty, staff and students of the Geology Department at McMaster University for their many and varied contributions over the years. The Faculty of Science and, especially the Department of Geology, Brandon University, are gratefully acknowledged for support and encouragement in the final stages of writing the thesis.

A special thanks to Charlotte, Celine and Nigel for putting up with me during work on this thesis, and to my mother and father for their support. The thesis is

dedicated to my father and to my son Nigel who was born during this work.

TABLE OF CONTENTS

	Page
I. INTRODUCTION	1
II. PREVIOUS WORK ON UPPER FLOW REGIME PLANE BEDS	4
INTRODUCTION	4
BEDFORMS ON MOBILE SEDIMENT BEDS	
Fluid flows	4
Initiation of sediment movement	6
Bedforms on mobile sediment beds	10
UPPER FLOW REGIME PLANE BED AND SEDIMENTARY ENVIRONMENTS	21
DESCRIPTION OF UPPER FLOW REGIME PLANE BEDS	24
EROSION AND DEPOSITION ON UPPER FLOW REGIME PLANE BEDS	27
The sediment continuity equation and erosion and deposition	27
Small scale variations in erosion and deposition	29
SUMMARY	38
III. HEAVY MINERAL SHADOWS, A NEW SEDIMENTARY STRUCTURE FORMED UNDER UPPER FLOW REGIME CONDITIONS:ITS DIRECTIONAL AND HYDRAULIC SIGNIFICANCE	40
INTRODUCTION	40
PREVIOUS WORK	41

page

HEAVY MINERAL ACCUMULATIONS IN THE
WHIRLPOOL SANDSTONE 42

Geological setting 42

Heavy mineral accumulations 44

FLUME EXPERIMENTS 48

DISCUSSION 56

CONCLUSIONS 66

IV. HORIZONTAL LAMINAE FORMED BY DEPOSITION ON UPPER FLOW REGIME PLANE BEDS 68

INTRODUCTION 68

PREVIOUS THEORIES 69

(1) Velocity fluctuations 70

(2) Like-seeks-like 70

(3) Combined velocity fluctuations and like-seeks-like 71

(4) Superposition of current lineations 72

(5) Migration of low bed forms 73

(6) The bursting mechanism 74

DESCRIPTION OF HORIZONTAL LAMINAE 76

Field examples 76

Locations 76

Methods 78

Description of laminae 81

Experimentally formed horizontal laminae 105

page

Methods 105

Description of laminae 113

DISCUSSION 120

CONCLUSION 135

V. CONCLUSIONS AND SUGGESTIONS FOR FUTURE WORK 138

REFERENCES CITED 143

APPENDICES 151

APPENDIX I. LIST OF SYMBOLS 151

APPENDIX II. DESCRIPTION OF EXPERIMENTAL APPARATUS AND METHODS 153

A. 12.2 metre McMaster recirculating flume 153

B. The Geological Survey of Canada sedimentation flume 157

C. The collection and impregnation of box cores 162

APPENDIX III. TEXTURAL DATA 164

LIST OF FIGURES

Figure II-1. Schematic illustration of bed forms. 11

Figure II-2. Ripple and dune morphology. 12

Figure II-3. Depth-velocity diagrams. 17

Figure II-4. Velocity-grain-size diagram. 18

		page
Figure II-5.	Variation in bed shear stress ratio over dimensionless time.	34
Figure III-1.	Location map: Rice and McNarg quarry.	43
Figure III-2.	Heavy mineral shadows on bedding planes.	45
Figure III-3.	Paleocurrent directions associated with heavy mineral shadows.	47
Figure III-4.	Heavy mineral shadows on flume bed.	50
Figure III-5.	Grain size versus distance through a heavy mineral shadow.	52
Figure III-6.	Heavy minerals on standing wave crests in flume.	54
Figure III-7.	Bed profiles for flume Runs 1 to 4.	55
Figure III-8.	Large heavy mineral shadow in Shubenacadie River.	65
Figure IV-1.	Location of collection sites in Nova Scotia.	77
Figure IV-2.	Thin section sampling layout.	80
Figure IV-3.	Horizontal laminae in the Whirlpool Sandstone.	82
Figure IV-4.	Horizontal laminae in trenches.	84
Figure IV-5	A to H. Vertical sections of grain size variation through	

		page
	horizontal laminae.	85
Figure IV-6.	Horizontal laminae in polished section and thin section.	99
Figure IV-7.	Lateral correlation diagram, sample MB-03.	100
Figure IV-8.	Lateral correlation diagram, sample RM-05.	101
Figure IV-9.	Grain size distribution, flume runs G-05 to G-07.	106
Figure IV-10.	A, B and C. Velocity profiles.	109
Figure IV-11.	Bed profiles.	112
Figure IV-12.	A, B and C. Vertical sections showing variation in grain size through horizontal laminae.	115
Figure IV-13.	Schematic illustration of horizontal laminae.	122
Figure IV-14.	Plot of relative sizes of light and heavy minerals in laminae.	124
Figure IV-15.	Variation in average grain size in laminae through sample MB-02.	133
Figure IIA-1.	Schematic of McMaster flume.	154
Figure IIB-1.	Schematic of G.S.C. flume.	158
Figure IIB-2.	Vertical and cross channel velocity profiles.	161

LIST OF TABLES

		page
Table III-1.	Hydraulic data for flume runs 1 to 4.	49
Table IV-1.	Summary of laminae abundance and thickness.	93
Table IV-2.	Transition difference matrices based on laminae sequences.	95
Table IV-3.	Textural data for laminae with light and heavy minerals.	96
Table IV-4.	Hydraulic data for flume runs G-05 to G-07.	114

CHAPTER I

INTRODUCTION

The major aim of the research described in this thesis was to provide a first detailed description of horizontal laminae formed by deposition under upper flow regime plane bed conditions. It had been hoped that by identifying textural trends which define laminae and by determining the hydraulic equivalence of light and heavy minerals in laminae that it would be possible to unequivocally interpret the specific processes which formed the laminae. As will be seen in later chapters, however, this goal was not completely attained although data are presented which strongly suggests two particular mechanisms of laminae formation. After preliminary flume work over plane beds of mixed light and heavy minerals a new primary sedimentary structure was discovered while on a field trip to examine the Whirlpool Sandstone near Georgetown, Ontario. Structures of this type are named "heavy mineral shadows" in the thesis and are shown to be useful in determinining paleocurrent direction from bedding plane exposures of horizontally laminated sandstones.

The format of the thesis is meant to allow the presentation of results in independant chapters which will

make for easier separation of the material for the purpose of publication (a modified version of Chapter III is in press in the Journal of Sedimentary Petrology at the time of writing). Chapter II reviews the previous work on upper flow regime plane beds which is relevant to later chapters, and this chapter is intended to introduce the thesis topic to the reader who is not specialized in sedimentology (although some previous knowlege of fluid mechanics and sediment transport would be useful). Previous work which is relevant to specific chapters is reviewed in the appropriate chapter. In Chapter II the relationship between upper plane beds and other bedforms is described and a brief survey is made of the sedimentary environments in which this bedform is commonly preserved. The characteristics of upper flow regime plane beds are then described, followed by a discussion of the processes of erosion and deposition on mobile sand beds.

In Chapter III "heavy mineral shadows" are described in an ancient sandstone (from the Whirlpool Sandstone near Georgetown, Ontario) and on active upper flow regime plane beds in a flume. They are shown to exhibit characteristics which are useful in determining paleocurrent directions in sandstones on which they are exposed. The flume experiments also suggest that the presence or absence of shadows or other types of heavy mineral accumulations on plane beds may have paleohydraulic implications.

Chapter IV comprises the main body of the thesis and is concerned with the nature and origin of horizontal laminae formed under upper flow regime plane bed conditions. First, theories of formation of these laminae are reviewed. Data showing textural variations in horizontally laminated sands and sandstones are decribed in samples collected from the Whirlpool Sandstone, from intertidal sand bars in Nova Scotia, and from a plane bed formed in a flume. The implications of these first detailed descriptions of horizontal laminae are discussed in terms of existing theories of their formation and a new hypothesis is proposed on the basis of the data.

The concluding chapter (V) summarizes the findings of the work described and highlights the new contributions which have been made in the thesis. Suggestions are made for future research which should provide answers to the questions left unanswered in the thesis. The Appendices include: (I) a list of symbols used in the text, (II) a description of apparatus and methods used in the work described in both Chapters III and IV, and (III) a summary of all of the textural data collected during the work.

CHAPTER II

PREVIOUS WORK ON UPPER FLOW REGIME PLANE BEDS

INTRODUCTION

This chapter reviews previous work by others which is relevant to later chapters on specific aspects of upper flow regime plane beds (syn. upper plane beds). The chapter begins with a brief introduction to some aspects of fluid flows, in the absence of a mobile sediment bed, which are important to later discussion of bedforms and sediment transport. Criteria for the initiation of transport of grains under fluid flows are then described. The significance of upper plane bed is shown first by a description of its relationship to other bedforms and then by a discussion of the sedimentary environments in which it may be preserved. The characteristics of upper plane beds are described in detail, followed by a discussion of the processes of erosion and deposition which may be important to later consideration of the formation, movement and preservation of structures associated with upper plane beds.

BEDFORMS ON MOBILE SEDIMENT BEDS

Fluid Flows

The flow of water over a mobile bed of sediment

results in the development of bedforms and their associated internal stratification. To fully understand the significance of bedforms and stratification it is necessary to first consider the nature of fluid flows over immobile beds which are smooth. In this section important flow variables are introduced which will be useful in the later discussion of bedforms.

Fluid flows with a free water surface over smooth, rigid beds may be described in terms of the following variables:

d	the flow depth
U	the mean flow velocity
ρ	the density of the fluid
μ	the viscosity of the fluid
g	the acceleration due to gravity.

By dimensional analysis these variables may be combined into various dimensionless numbers, the most important of which, for the present discussion, are the Reynolds number (R) and the Froude number (F). The Reynolds number is defined by:

$$R = \frac{U\ d}{\nu} \qquad (1)$$

where ν is the kinematic viscosity (μ/ρ). The Reynolds number is proportional to the ratio between inertial forces and viscous forces acting on the fluid. It was shown on the basis of experiments by Reynolds (1883) that in the case of flow through pipes (where d in equation 1 is replaced by the

pipe diameter) that at values of R less than about 2000 flow is laminar, fluid particles move in the flow along paths which are parallel to the boundary. At Reynolds numbers greater than 2000 flow is turbulent, fluid particles follow a more-or-less random path in the flow direction. The same relationship between the nature of the flow and the Reynolds number is true of open channel flow. More will be said on the characteristics of turbulent flows in the section on erosion and deposition later in this chapter.

The Froude number is defined by:

$$F = \frac{U}{\sqrt{g\ d}} \qquad (2)$$

and is proportional to the ratio between inertial forces and gravity forces acting on an open channel flow. An important implication of the Froude number is that it defines the relationship between the average flow velocity and the velocity of gravity waves (water surface waves) which is equal to $\sqrt{gd}$. At Froude numbers less than 1 water surface waves will travel both downstream and upstream while at Froude numbers greater than 1 surface waves will travel upstream. These types of flow are termed "tranquil" ($F<1$) and rapid ($F>1$) flow regimes, respectively. The rapid flow regime is characterized by the presence of water surface waves.

The Initiation of Sediment Movement

Flow over flat beds of mobile particles (e.g. sand)

is similar to flow over rigid boundaries until the bed material begins to be transported. The condition for the initiation of movement on a flat bed depends on the relationship between forces acting to keep the grains on the bed and the fluid forces (lift and viscous drag) which act to move the grains. The important variables which determine the magnitude of the resultant force are: $g(\rho_s - \rho)$, the submerged weight of the grains (ρ_s is the density of the sediment particles); the size of the particles (as represented by their average diameter, D); the boundary or bed shear stress applied by the flow (τ_o); the fluid viscosity; and the fluid density. (See Middleton and Southard, 1977, for a comprehensive discussion of the forces acting on grains which determine the conditions at which movement begins.) By dimensional analysis of these variables Shields' (1936) determined that:

$$\frac{\tau_{ocrit}}{(\rho_s - \rho)gD} = f(R^*) \qquad (3)$$

The left hand side is the ratio of the applied shear stress to the submerged weight of the grains and is referred to as Shields' β where τ_{ocrit} is the critical shear stress for the intiation of movement of the grains. The right hand side is a form of Reynolds number which is specifically known as the boundary or grain Reynolds number (R*) in which the average velocity in equation 1 is replaced by the shear velocity (U*, which is equal to $\sqrt{\tau_o/\rho}$) and the flow depth is replaced

by the average grain diameter.

The boundary Reynolds number describes the relationship between the size of the grains on the bed and the thickness of the "viscous sublayer" of the flow, a thin region extending away from the bed in which the flow is neither fully turbulent nor laminar but exhibits a mixture of characteristics of both. The flow becomes fully turbulent above the viscous sublayer and is termed the "outer region". At a boundary Reynolds number of about 12 the grain size of the bed material approximately equals to the thickness of the sublayer. The viscous sublayer begins to break up, except around the grains themselves, as R* exceeds this value. Boundaries are said to be hydrodynamically smooth (i.e., the viscous sublayer is fully devloped) at values of R*<5, and rough (i.e., the viscous sublayer is fully disrupted) at values of R*>70. At values of R* between this range the flow is said to be transitionally rough (i.e., thin and discontinuous). The value of Shields' beta, therefore, depends in part on whether the grains are entirely within the viscous sublayer or protruding into the outer turbulent flow.

Shields (1936) experimentally determined the value of β for flat beds of sand of uniform size and density, using a wide range of sand sizes and density, and plotted the data against R* on what is now known as a "Shields' diagram" (for example see Blatt, Middleton, and Murray,

1980, page 102). From this diagram the critical bed shear stress for the intiation of movement of sand grains may be calculated. However, while Shields' criterion for the initiation of movement was meant to apply to grains of a wide range of density, work by Ward (1969), and more recently by Collins and Rigler (1982), has shown that at low boundary Reynolds numbers (i.e., smooth flows) it underestimates the critical shear stress for the initiation of movement of "heavy minerals" which have a density greater than that of quartz (2650 Kg/m^3).

The Shields' criterion defines the condition for the initiation of movement of grains in contact with the bed (termed "bed load"). This type of sediment transport is characterized by sliding or rolling over the bed or by short "hops" between points on the bed, a type of movement termed saltation. Under greater bed shear stress than that required to just initiate motion the grains are carried up into the flow and undergo transport in suspension, supported by the upward-moving component of the fluid turbulence. This "suspended" load may be subdivided into two components: the "wash load", very fine grained sediment which remains in suspension even during periods of weak flow and which is not found in the bed material, and an "intermittent suspension load" which is the part of the bed material which goes into suspension when a critical flow strength is exceeded. Middleton (1976) has shown that the coarsest grains within

the intermittent suspension load have settling velocities (w) which are equal to the value of U* for the flow. The criterion for the initiation of transport of bed material in suspension, therefore, is w=U*.

Bedforms On Mobile Sand Beds

With the beginning of sediment movement the bed becomes molded by the flow into the bedforms, along with their internal stratification, which are of interest to geologists. Figure II-1 illustrates the types of bedforms which may develop on a mobile sand bed under unidirectional flows with a free water surface (in full pipes not all of the structures will form). The position of each type of bedform, from top to bottom, represents the sequence of forms which might develop with increasing flow velocity and constant depth (although, as will be shown later, the components of the sequence vary with the size of the bed material and the flow depth). The distinctive features of each bedform are summarized as follows (note that terms for describing ripples, dunes and sandwaves are defined in figure II-2):

(1) Lower plane bed. A flat, featureless sand bed over which sediment is transported strictly as bed load.

(2) Ripples. Small, asymmetrical bed waves (heights up to a few centimetres, lengths centimetres to decimetres) with irregular, short crests. Downstream migration occurs by deposition of bed load on their lee slopes which are at the

Figure II-1. Schematic illustration of bedforms which develop on mobile sand beds with increasing flow strength (after Blatt, Middleton, and Murray, 1980).

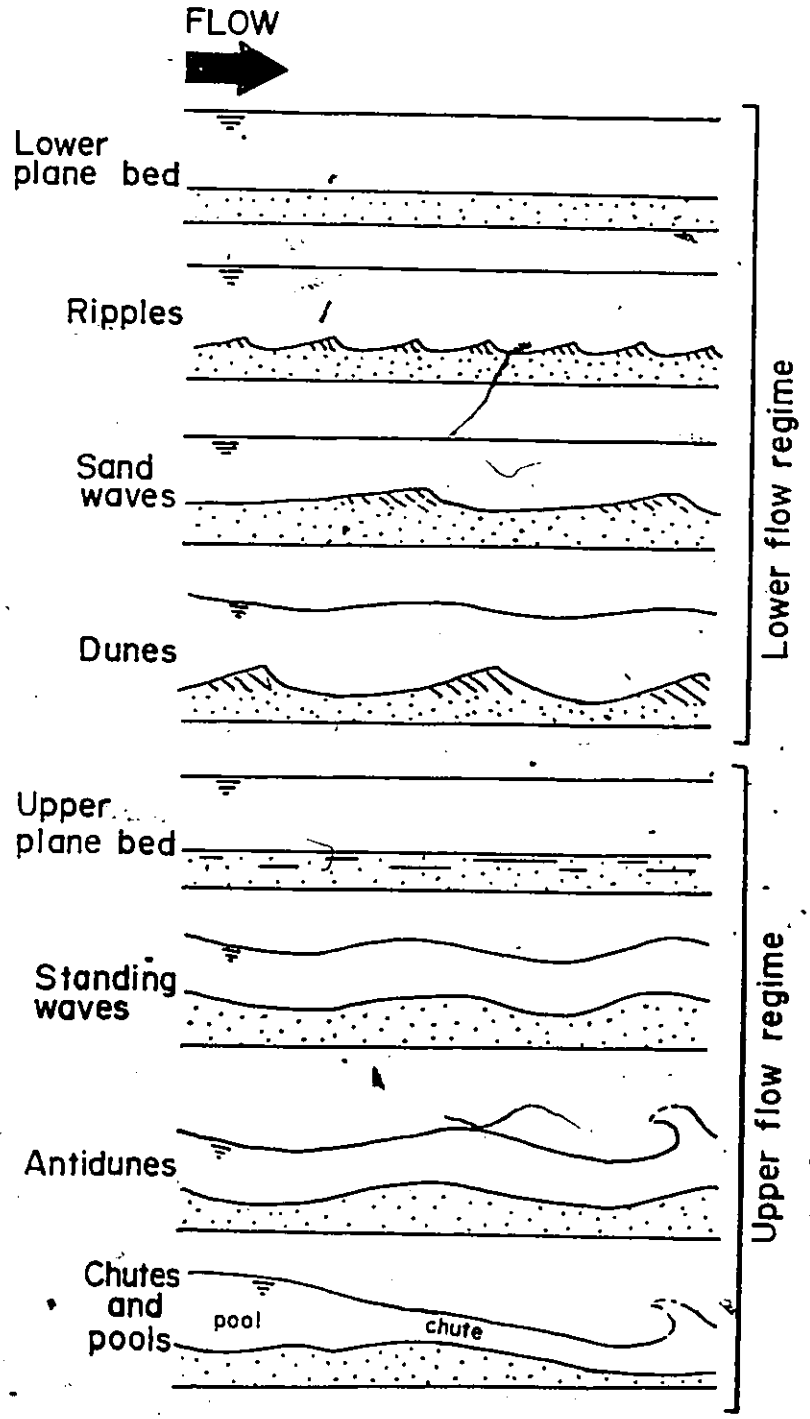
FLOW
Lower plane bed
Ripples
Sand waves
Dunes
Lower flow regime
Upper plane bed
Standing waves
Antidunes
Chutes and pools
pool
chute
Upper flow regime

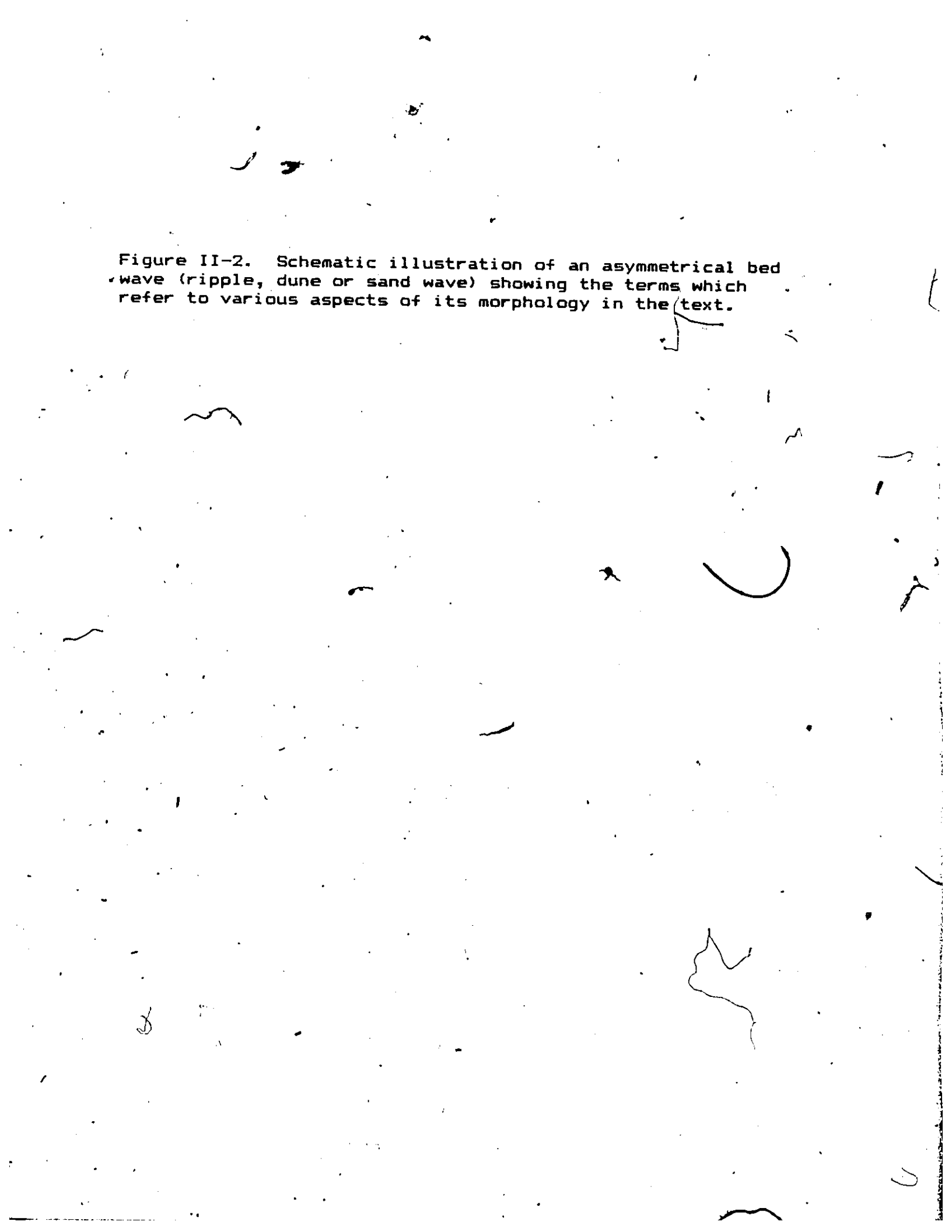

Figure II-2. Schematic illustration of an asymmetrical bed wave (ripple, dune or sand wave) showing the terms which refer to various aspects of its morphology in the text.

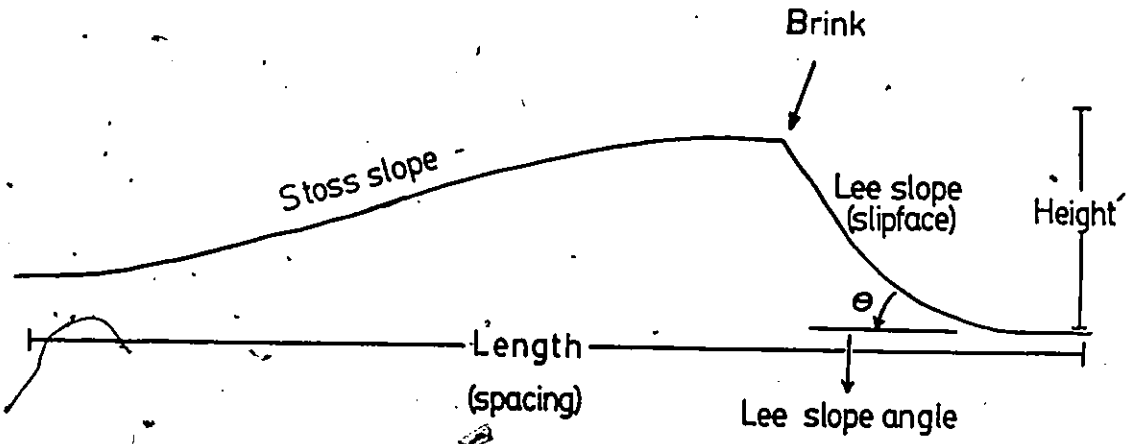
Brink
Stoss slope
Lee slope
(slipface)
Height
θ
Length
(spacing)
Lee slope angle

approximate angle of repose for the sand.

(3) Sand waves. Much larger than ripples (decimetres to metres high and metres to hundreds of metres long) with straight to sinuous crests and lee slopes which are less than angle of repose.

(4) Dunes (syn. megaripple, large ripple). Morphologically similar to ripples but significantly larger (centimetres to tens of metres high and decimetres to tens of metres in length).

(5) Upper plane bed. A flat, almost featureless bed surface over which sediment transport is intense, both as bed load and suspended load.

(6) Standing waves (syn. standing wave antidunes). Symmetrical waves on the bed surface which are in phase with water surface waves which do not move upstream or downstream.

(7) Antidunes. Similar to standing waves but form under water surface waves which move upstream and may periodically break by oversteepening as the wave heights become excessively high. With breaking of the water surface waves sediment is deposited on the upstream side of the bed wave.

(8) Chutes and pools. A bedform characterized by reaches of shallow, accelerating flow over mounds of sand (chutes) alternating with reaches of deeper, decelerating flow (pools). Flow from chutes enters the pools through a hydraulic jump.

The above descriptions of bedforms are based largely on those by Harms, Southard, and Walker (1983) and Simons, Nordin, and Richardson (1965). For a more detailed description the reader is referred to those papers.

The broad classification of bedforms into those of upper and lower flow regime (Fig. II-1), was first proposed by Simons and Richardson (1963). They had earlier classified bedforms according to whether the flow was tranquil ($F<1$) or rapid ($F>1$) (Simons and Richardson, 1962). However, further work on bedforms in flumes suggested that a more logical classification was that of lower and upper flow regimes which only roughly correspond to tranquil and rapid flow regimes, respectively. This classification was not based on a critical value of F but on the "...magnitude of the resistance to flow, bed, and water surface configuration, and mode and magnitude of sediment transport" (Simons and Richardson, 1963, p. 288). Lower flow regime was characterized by a high resistance to flow due to the bedforms, which included ripples and dunes, the sediment transport rates were relatively low and the water surface was out of phase with the bed. Upper flow regime was characterized by lower flow resistance, intense sediment transport, and the water surface was in phase with plane, standing wave or antidune bedforms. An unfortunate aspect of this classification is the emphasis on the relationship between the bed and water surfaces. Ripples, dunes and

plane bed will develop in full pipes with no free water surface (McDonald and Vincent, 1972) and, therefore, are independent of the water surface. Standing waves, antidunes and chutes and pools, however, will not form in the absence of a free water surface. Classification of bedforms on the basis of their relationship to the water surface would group upper plane bed in the lower flow regime. Upper plane bed does share the other characteristics of upper flow regime bedforms and is properly classified with the above restriction noted.

Other attempts have been made to classify bedforms on the basis of flow parameters in order to predict the formation of bedforms under various flow conditions. The most successfull of these attempts was that of Southard (1971). He reasoned that the most important variables which control the type of bedform under a given flow are: d, U, ρ, μ, D, ρ_s, and g. By dimensional analysis Southard reduced these seven variables to four dimensionless products:

$$\left(\frac{\rho^2 g}{\mu^2}\right)^{1/3} d \qquad \text{a dimensionless depth} \qquad (4)$$

$$\left(\frac{\rho}{\mu g}\right)^{1/3} U \qquad \text{a dimensionless velocity} \qquad (5)$$

$$\left(\frac{\rho^2 g}{\mu^2}\right)^{1/3} D \qquad \text{a dimensionless grain size} \qquad (6)$$

$$\frac{\rho_s}{\rho} \qquad \text{a dimensionless grain density} \qquad (7)$$

For natural sands the dimensionless grain density is constant if it is assumed that the predominant mineral is quartz (ρ_s = 2650 kg/m^3) and the fluid is water (ρ = 1000 kg/m^3), so that the range of bedform stability can be described by the three remaining dimensionless products. This scheme is made even more attractive if it is assumed that ρ, μ, and g, do not vary significantly so that it is possible to show the fields of bedform stability in terms of d, D and U. (Note that while this assumption simplifies the interpretation of the dimensionless products it also causes some scatter of points in plots of d versus D and d versus U based on flume data from flows of varying temperature because μ varies considerably with water temperature). Figures II-3 and II-4 are examples of depth-velocity and velocity-size diagrams for bedforms in flumes (so that only relatively shallow flow depths are represented).

As noted earlier in this chapter, these diagrams show that the sequence of bedforms which develops with increasing velocity (at constant flow depth) varies depending on flow depth and average grain size. An example of the effect of flow depth on the bedform sequence appears in figure II-3B which shows that upper plane bed does not form on beds of 0.45 mm to 0.55 mm sand at depths less than approximately 0.12 m. At shallower depths the bedform changes directly from dunes to antidunes (or standing

Figure II-3. Depth-velocity diagrams showing bedform stability fields in (A) fine sand (0.10 to 0.15 mm diameter) and (B) medium to coarse sand (0.45 to 0.55 mm diameter). Stability fields shown are from Harms, Southard and Walker (1983, figures 2-4A and B).

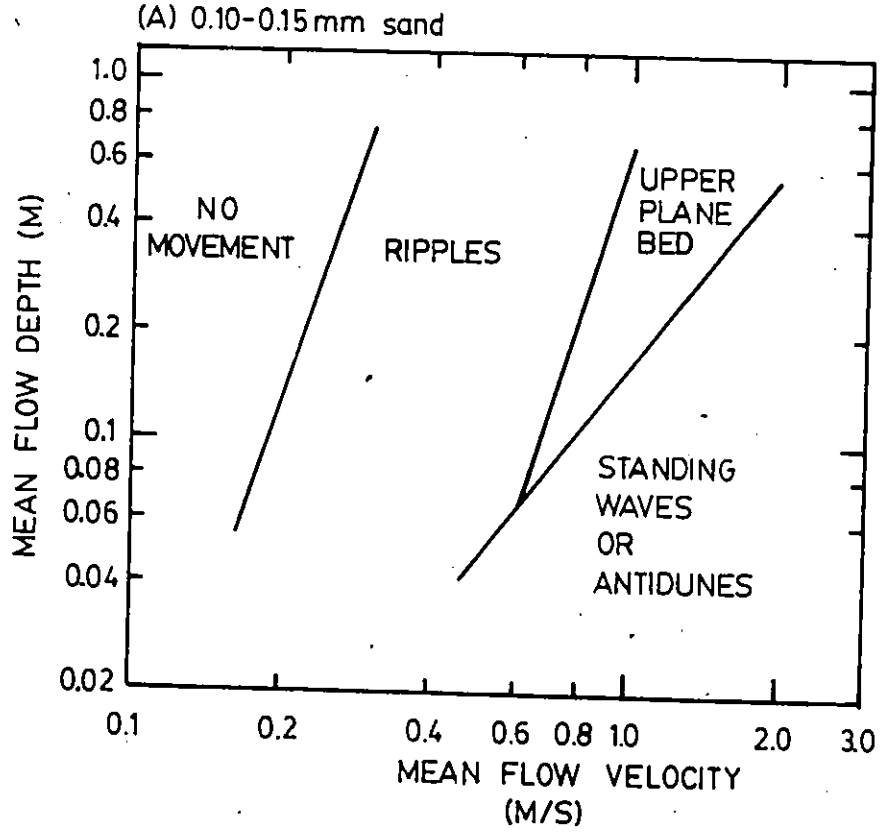
(A) 0.10-0.15 mm sand
MEAN FLOW DEPTH (M)
1.0
0.8
0.6
0.4
0.2
0.1
0.08
0.06
0.04
0.02
NO MOVEMENT
RIPPLES
UPPER PLANE BED
STANDING WAVES OR ANTIDUNES
0.1
0.2
0.4
0.6
0.8
1.0
2.0
3.0
MEAN FLOW VELOCITY (M/S)

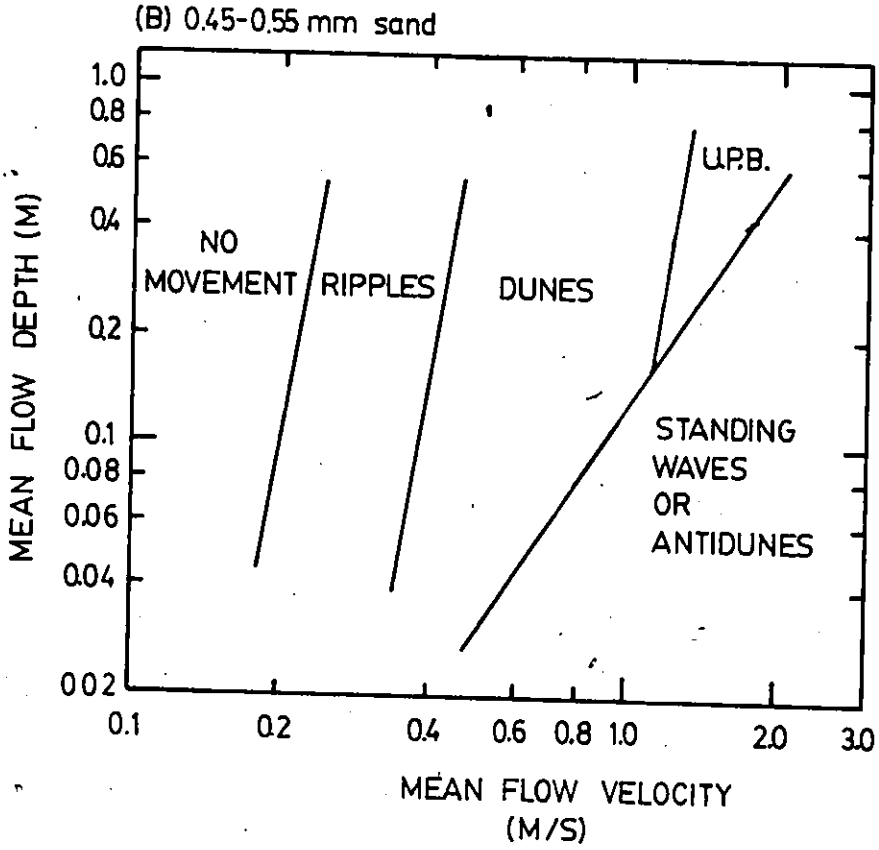
(B) 0.45-0.55 mm sand
MEAN FLOW DEPTH (M)
1.0
0.8
0.6
0.4
0.2
0.1
0.08
0.06
0.04
002
NO MOVEMENT
RIPPLES
DUNES
U.P.B.
STANDING WAVES OR ANTIDUNES
0.1
0.2
0.4
0.6
0.8
1.0
2.0
3.0
MEAN FLOW VELOCITY (M/S)

Figure II-4. Velocity-grain-size diagram showing bedform stability fields for flow depths between 0.18 and 0.22 metres. Stability fields shown are after Harms, Southard and Walker (1983, figure 2-5). The upper limit of upper plane bed and dunes has been changed from the original so that these bedforms do not exist at Froude numbers greater than 1. This modification is consistant with data shown in their figure 2-5 and better suits the findings of Kennedy (1963).

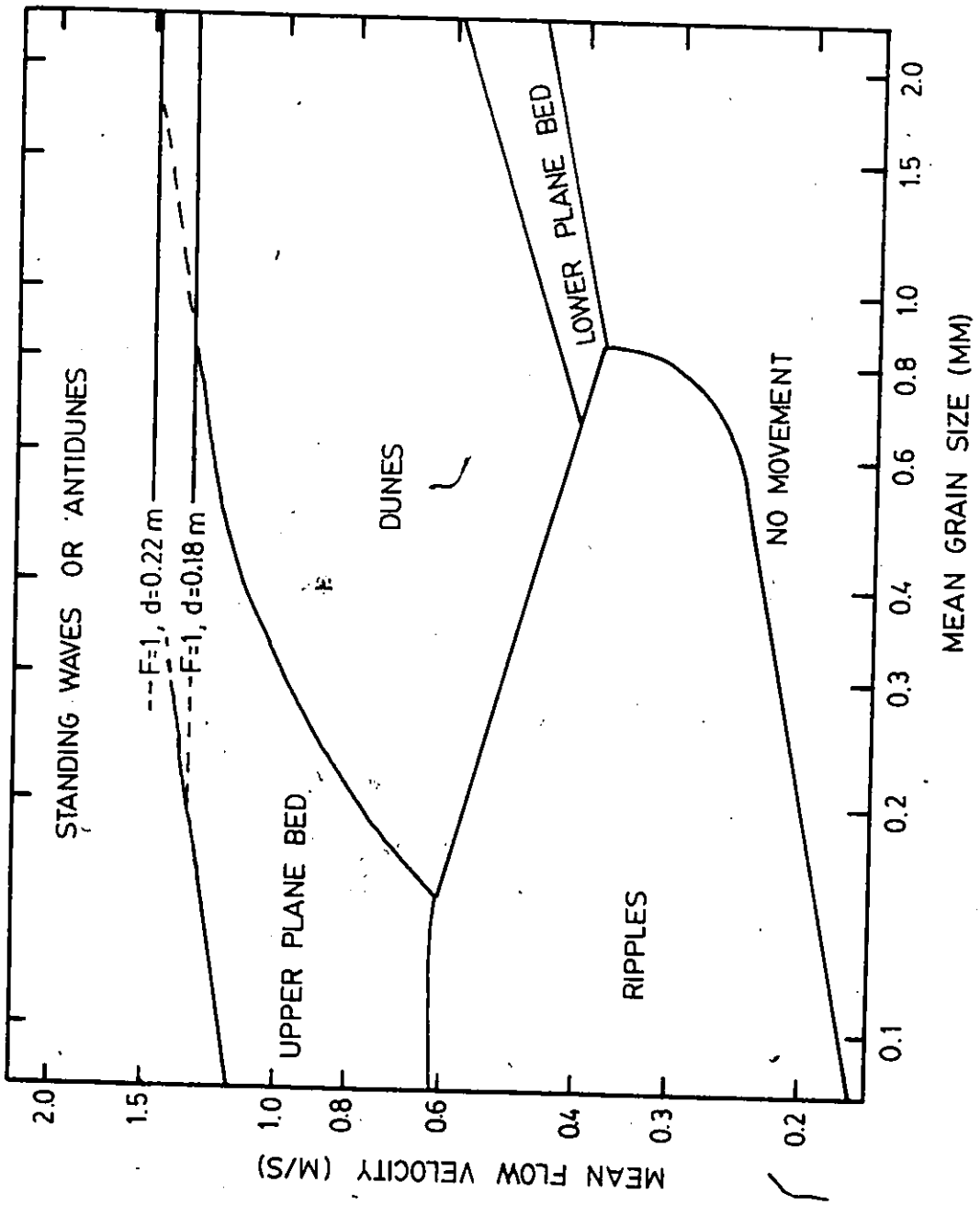
STANDING WAVES OR ANTIDUNES
--F=1, d=0.22 m
-F=1, d=0.18 m
UPPER PLANE BED
DUNES
LOWER PLANE BED
RIPPLES
NO MOVEMENT
MEAN FLOW VELOCITY (M/S)
MEAN GRAIN SIZE (MM)
2.0
1.5
1.0
0.8
0.6
0.4
0.3
0.2
0.1
0.2
0.3
0.4
0.6
0.8
1.0
1.5
2.0

waves). The absence of upper plane bed under shallow flow depths is due to the development of stationary water surface waves with increasing flow velocity as the flow Froude number approaches a critical value between 0.8 and 1.0 (Kennedy, 1963). These water surface waves mold the bed into standing wave bedforms, at lower flow velocities than are necessary for the development of an upper plane bed. At depths greater than 0.12 m, however, sufficient flow velocity is reached for an upper plane bed to form, before F reaches the critical value.

The effect of grain size on the sequence of bedforms is shown in figure II-4. On beds of fine sand, less than approximately 0.15 mm, dunes do not develop and the range of velocities over which upper plane bed is stable is quite large and increases with increasing flow depth (see figure II-3A). In coarser sand, greater than approximately 0.8 mm, ripples do not form and lower plane bed makes up the characteristic bedform at low velocities after the bed material begins to be transported by the flow. Leeder (1980) proposed that the absence of ripples on coarse-grained sand beds was due to the disruption of the viscous sublayer by the grains as they just begin to protrude above the viscous sublayer (i.e., R*>12). The protrusions of grains was thought to inhibit flow separation over bed defects which might otherwise develop into ripples. The upper plane bed occurs over a narrow range of flow

velocities in coarse sand (i.e., coarser than 0.5 mm) although this range increases for deeper flows where F is less than one, even at velocities which are high enough for the development of upper plane bed.

The change in bedform from dunes to upper plane bed was described by Simons and Richardson (1963, p. 289) as being characterized by "...long dunes of small amplitude..." which decrease in amplitude as the flow velocity (at constant depth) increased. They termed these bedforms "washed out dunes" or "transitional bedforms". Saunderson and Lockett (1983) have described three types of transitional dunes which differ from those reported by Simons and Richardson (1963) and exhibit a mixture of the attributes of both dunes and plane beds (i.e., angle of repose lee slopes and plane bed on the dune tops). Southard and Harms (1972) and Jopling and Forbes (1979) described the transition from ripples to upper plane bed on beds of silt-size sediment (i.e., less than 0.0625 mm diameter). They found that like washed out dunes, ripples become lower and more rounded (having less well defined lee slopes) with velocity increasing towards that required for upper plane bed. Another noteworthy feature of the transition is that the velocity at which the transition occurs depends on whether the change in bedform is from ripples or dunes to plane bed (with increasing velocity) or from plane bed to ripples or dunes (with decreasing velocity). Flume

experiments have shown that upper plane beds persist down to considerably lower velocites if the transition is downward to dunes or ripples. Whether the downward transition is from plane bed to dunes or ripples is thought to depend on the relationship between the grain size of the bed material and the viscous sublayer thickness (Engelund and Hansen, 1972; Allen and Leeder, 1980). In flumes the observed transition is to ripples when $R^* < 12$ and to dunes when $R^* > 12$.

The causes of the change from ripples or dunes to plane bed are not well understood. Engelund and Fredsoe (1974) have shown that the transition most likely depends on the ratio between the suspended load and the bed load in transport over the bed. As the ratio increases plane beds are stable to lower Froude numbers. This explains the wider range of stability of upper plane beds in fine sands (with relatively small settling velocities) which will more readily go into suspension than coarser sands. Other theories of plane bed stability (or instability) have been proposed (Bagnold, 1956, 1966; Kennedy, 1963; Hill, 1966; Hill, Srivinasan, and Unny, 1969; Allen and Leeder, 1980) but none of these explain the observed stability of upper plane beds as well as Engelund and Fredsoe (1974).

UPPER PLANE BEDS AND SEDIMENTARY ENVIRONMENTS

This section provides a general summary of the types

of sedimentary environments in which the deposits of upper plane bed (i.e., horizontally laminated sands) may be preserved and does not aim to catalog the occurrences of horizontal laminae which have been reported in the literature. From the above discussion it is apparent that upper plane bed is a common bedform under relatively fast flows in which the Froude numbers are less than the critical value for standing waves or antidunes. Bed materials of fine sand and silt (less than 0.25 mm) are most likely to develop and preserve the deposits of upper plane beds, especially sands which are too fine to form large dunes which might rework earlier deposited horizontally laminated sands during their downstream migration. The development of upper plane beds on medium size sand (0.25 to 0.5 mm) requires fast, deep flows. In any sedimentary environment under flows which are slow, shallow and/or over coarse sands (greater than 1.0 mm) the experimental results described earlier suggest that horizontal laminae formed by deposition on upper flow regime plane beds will be absent.

Upper plane bed and its associated stratification are reported in the flood deposits of rivers. McKee, Crosby, and Berryhill (1967) described up to 4 m of horizontally laminated sands in the deposits of a single flood event of Bijou Creek in Colorado. Similarly, the Whirlpool Sandstone (Silurian), which is locally dominated by horizontally laminated sandstone, is interpreted to be

the deposit of an ancient braided river system (Middleton, Salas, and Martini, 1983). In the marine environment horizontal laminae are commonly found in the deposits of strong currents in tidal channels (Reinson, 1979) and of storm-generated currents on continental shelves (Walker, 1979; Dott and Bourgeois, 1982). Near horizontal, subparallel laminae are typical of beach-face deposits and may resemble horizontal laminae. These laminae form in response to the swash and backwash of water up the beach and are genetically different from the laminae of interest to this thesis. In deep marine deposits horizontal laminae are common in turbidites (Bouma, 1962; and interpreted as being formed by deposition on upper flow regime plane beds by Harms and Fahnestock, 1965). Laminae formed by deposition from turbidity currents (on the continental slope and rise and on the continental shelf where they may be storm generated) may differ from those found in the deposits of rivers or tidal currents where the concentration of suspended sediment in transport is lower. The effects of the higher concentration of suspended sediment is possibly two-fold: (1) in damping the turbulent structure of the flow, and (2) increasing the rate of deposition on the bed from fallout from suspension as the competence of the turbidity current wanes. As a result the laminae described later in this thesis may differ from those found in the deposits of turbidity currents.

DESCRIPTION OF UPPER FLOW REGIME PLANE BEDS

Kennedy et al. (1966, p. 53) defined flat (or plane) bed as "A bed surface devoid of bed forms." However, a number of features of upper plane beds have been described in the literature. These features are described below.

Qualitative observations of bed load movement over a plane bed have been reported by a number of workers. The zone of bed load movement is described as comprising a layer up to several millimeters thick (Moss, 1972), in which particles are moving in very high concentrations. This layer reportedly has a visible upper surface which marks the boundary with the overlying suspension load. Several names have been applied to this type of bed load layer, including: "zone of saltation" (Gilbert and Murphy, 1914); "traction carpet" (Dzulynski and Sanders, 1962); "collision region" (Hill, 1966); "heavy fluid layer" (Jopling, 1967); "rheologic layer" (Moss, 1972). Moss (1972, p. 192) described the rheologic layer in which "Particles move collectively, not individually, gravitationally pulled towards the bed but maintained in a dispersed state ... (by) the pressure generated by particle collisions ...". This supporting force was termed "dispersive pressure" by Bagnold (1954) and is a force per unit area acting at right angles to the bed which arises due to the downward transfer of momentum from colliding grains. The intensity of dispersive

pressure (P) was related to properties of the flow and the material in transport (Bagnold, 1954, equation 3) by:

$$P = A\rho_s f(\lambda) D^2 \left(\frac{\partial G}{\partial y}\right) \cos\alpha \qquad (8)$$

where the new terms are: A, a constant for specific conditions of the collisions in the sediment in transport, λ the linear concentration of grains, $\partial G/\partial y$ the shear strain in the layer of moving grains, and α an angle related to the conditions of collision among the grains.

Allen (1964) described bed load on plane beds as being distributed in parallel rows (which he called "windrows") extending along the direction of flow. In a flume these windrows were observed to be 2 to 5 mm wide and 5 to 35 cm long and were characterized by a relatively slow moving bed load. Between windrows were regions (two or three times as wide as the windrows) in which bed load was less concentrated and faster-moving. Allen (1970) found that the spacing of windrows was a function of U^* and ν. Jackson (1976) noted that the spacing of the windrows was approximately equal to the spacing (S) of alternations of low and high speed streaks of fluid which had been recognized in the viscous sublayer of clear water flows (Kline, Reynolds, Schraub and Rundstadler, 1967) which is given by:

$$S \approx \frac{100\nu}{U^*} \qquad (9)$$

Jackson (1976) suggested that the sand in windrows was in transport within low speed streaks. Furthermore, he suggested that the reported absence of windrows over beds of sand coarser than approximately 0.35 mm (Allen, 1968) was consistent with this theory because over coarser sands the viscous sublayer would be disrupted (i.e., under transitional to rough turbulent flows) and fluid streaks would not be stable. More recent work by Weedman and Slingerland (1983) has suggested that the spacing of windrows (or "sand streaks" as they chose to call them) increases with increased concentration of sediment in transport.

The surfaces of plane beds in the field commonly exhibit low linear ridges a few grain layers high which are approximately parallel to the depositional flow direction. These structures are referred to as "primary current lineation" (first named in English by Stokes, 1947; synonymns include: parting lineation, Crowel, 1955 and parting plane-lineation, McBride and Yeakle, 1963). These are believed to reflect the existence of windrows on the bed during deposition (Allen, 1964). Commonly associated with primary current lineation is "parting-step lineation" (McBride and Yeakle, 1963) which is made up of a series of parallel steps in the broken depositional surface of the cemented deposits of upper plane beds. Like primary current

lineation the steps are also aligned parallel to the direction of the depositing flow.

EROSION AND DEPOSITION ON UPPER FLOW REGIME PLANE BEDS

The preservation of the structures described in the following chapters depends on whether the upper plane bed is aggrading (i.e., undergoing net deposition) or degrading (i.e., undergoing net erosion). If the bed material is being eroded the probability is small that structures which form on or within the material at the surface of the bed will be preserved. This section will first describe the conditions which determine whether the bed is aggrading or degrading over time and then briefly discuss some characteristics of the flow which may cause small scale variation in the distribution of areas on the bed which undergo erosion and deposition.

Sediment continuity equation: erosion and deposition

Whether the elevation of an area of a bed over which particles are in transport will increase (aggrade) or decrease (degrade) depends on (1) the difference between the rate at which particles enter the region over that area and the rate at which they are transported out of the region, and (2) the difference in the concentration of sediment in suspension above the area over time. This condition can be written for an area of unit width on the bed in the form of a differential equation which is known as the "sediment

continuity equation":

$$\frac{\partial h}{\partial t} = -V \left(\frac{\partial q_s}{\partial x} + d\frac{\partial c}{\partial t}\right) \qquad (10)$$

where $\partial h/\partial t$ is the rate of change of the bed elevation, V is the bulk volume of sediment, $\partial q_s/\partial x$ is the change in the sediment transport rate in the downstream direction, $\partial c/\partial t$ is the rate of change in the concentration of sediment in suspension above the bed. (See Middleton and Southard, 1977, for an example of the derivation of this equation.) When the sum of the expressions in brackets is negative the bed will undergo deposition and when they are positive there will be erosion. If, for the sake of simplicity, we assume that the fallout from suspension is of negligible importance compared to deposition from bed load, equation 10 can be reduced to:

$$\frac{\partial h}{\partial t} = -V\left(\frac{\partial q_s}{\partial x}\right) \qquad (11)$$

This assumption is probably reasonable when considering the formation of laminae in upper plane beds which are aggrading relatively slowly because q_s represents only the particles which are near the bed and which will most readily deposit.

From equation 11 it can be seen that if $\partial q_s/\partial x$ is negative (i.e., less sediment is in transport in the downstream direction) there must be net deposition on the bed ($\partial h/\partial t$ is positive). To consider possible causes of net

deposition on a bed the factors which control q_s must be recognized. Gessler (1971) states that most sediment transport equations can be written in the form:

$$q_s = k(\tau_o - \tau_{ocrit})^p \qquad (12)$$

where k is a constant, τ_{ocrit} is the critical bed shear stress for the initiation of motion of grains of a given diameter on the bed (based on equation 3) and p is some power. If we consider a bed of uniform grain size the critical bed shear stress will vary little in comparison to the possible variation in the acting bed shear stress. As a result q_s will vary directly with τ_o (at least down to the limiting value $\tau_o = \tau_{ocrit}$, below which no movement of bed grains will occur so that $q_s=0$). Therefore, with this restriction noted, it can be stated that $\partial q_s/\partial x$ will vary with $\partial \tau_o/\partial x$, which implies that if $\partial \tau_o/\partial x$ is negative there will be net deposition on the bed and if it is positive there will be erosion.

Small scale variation in erosion and deposition

In the above discussion the value of τ_o is the time averaged bed shear stress at a point in the flow. However, under conditions for which upper plane bed is the stable bedform the flow will be complex. Secondary flows and/or elements of the turbulent flow structure will cause local variation in the bed shear stress above or below the time averaged value by an amount τ_o' (termed the turbulent or

Reynolds shear stress) due to the vertical transfer of fluid momentum towards and away from the bed. The turbulent shear stress combines with τ_o in equation 12 to either increase or decrease the sediment transport rate locally so that at any instant in time $\partial\tau_o'/\partial x$ will vary over the bed and result in a complex pattern of local erosion and deposition.

Secondary flows act in the plane normal to the downstream flow (primary flow) direction and are recognized in the component of flow velocity in that plane. They form in both straight and curved channels and combine with the primary flow to form vortices or spiral flow "cells" with horizontal axes parallel to the primary flow direction. In alluvial channels these may consist of single cells which extend over the entire flow depth and across most of the channel width or multiple cells, each individual cell extending across part of the channel width. In meandering rivers there is often a large single cell at meander bends and two large cells at the inflection point between bends (Thorne and Hey, 1979). Spiral secondary flows cause regions of downwelling and upwelling in the flow which result in local increase and decrease, respectively, in the shear stress acting on the the bed. Over mobile sediment beds this causes variation in the sediment transport rate and, therefore, alternating regions of potential deposition and erosion in the direction transverse to the flow. Einstein and Li (1958, p. 1086) suggested that some sand

bars in channels were formed due to the variation in rates of sediment transport that results from secondary flows.

The results of many studies of the organized structure of turblence has been the subject of a recent review by Cantwell (1981). He summarized the characteristics of four major constituents of the structure: (1) a pattern of streamwise counter rotating vortices in the region nearest the wall (associated with streaks which were mentioned earlier in regard to windrows and current lineations), (2) ejections of fluid (bursting) and injections of fluid (sweeps) away from and into, respectively, the region just above the streaks, (3) small scale "typical eddies" which occur in the outer region of the flow and are found on the upstream facing portions of (4) large scale eddies. The large eddies of the outer flow region and the actions of the burst/sweep process appear to be responsible for most of the variation in boundary shear stress and are discussed in more detail below.

Large eddies rotate about horizontal axes oriented normal to the primary flow direction. As summarized by Cantwell (1981, p. 482-483), at a height of approximately 0.8d above the bed large eddies range in length (in the downstream direction) from 1d to 2d and in width from 0.5d to 1d. The centres of individual eddies are spaced 2d to 3d apart in the direction normal to the flow and move downstream at approximately $0.8U_\infty$ (U_∞ = free stream

velocity)..

The action of bursts and sweeps near the boundary have been the object of a large number of studies since they were first identified by Kline et al. (1967). In recent years they have been discussed in the geological literature concerning bedforms, sedimentary structures and stratification, and sediment transport (e.g. Jackson, 1976; Bridge, 1978; Leeder, 1983). The burst/sweep process involves the quasiperiodic uplift and ejection of fluid from low speed streaks in the viscous sublayer (bursting) alternating with the inrush of relatively high speed fluid from the outer region (sweeps) generally towards high speed streaks in the viscous sublayer. The process has been observed in flows over a wide range of boundary Reynolds numbers, under smooth to rough turbulent flows (Grass, 1971). The number of bursts and sweeps which occur over a given period of time is approximately equal and their periodicity (T) has been found, by Rao, Narasimha, and Narayanan (1971), to be approximated by:

$$T \approx \frac{5d}{U_\infty} \qquad (13)$$

An important implication of the observed periodicity of the burst/sweep process is that it is a function of properties of the outer flow. Rao et al. (1971) suggested that the process is in response to the interaction of the outer flow structure with the viscous sublayer. The size of the

packages of fluid which make up bursts and sweeps is less than that comprising large eddies. Cantwell (1981, p. 480) describes estimates of the length of the fluid packages as being from 20ν/U* to 100ν/U* and with heights ranging from 15ν/U* to 20ν/U*. He also cites estimates of the width as being up to "several" times the length and height.

The effects of the organized structure of turbulence on the bed shear stress are shown in figure II-5 in terms of variation in the ratio τ_0'/τ_0 with time (or rather a dimensionless time T*, in the form $T^*=TU_\infty/d$, where T is time measured in seconds) at a fixed point in the flow. While the data shown in figure II-5 are based on measurements made in a wind tunnel (Brown and Thomas, 1977) the results are similar to those which would be expected from water flows. Two scales of variation in τ_0'/τ_0 correspond to the two scales of turbulence described above (Brown and Thomas, 1977): (1) a small scale, slowly varying fluctuation due to large eddies in the outer flow (Figs II-5a and b), and (2) a high frequency, large amplitude fluctuation due to bursts and sweeps (Figs. 5a and c). Note that essentially the same form of distribution in τ_0'/τ_0 would appear if simultaneously measured values of τ_0' were plotted against distance along the flow (in figure II-5 the flow would be from left to right). These would appear in the downstream direction as relatively sharp, closely spaced, local variations in bed shear stress, due to bursts and sweeps, superimposed onto a

Figure II-5. Record of the ratio τ'/τ_o, based on measurements made in a wind tunnel, over dimensionless time (after Brown and Thomas, 1971). (a) shows a slowly varying conponent of τ'/τ_o onto which is superimposed a high frequency, high amplitude fluctuation in τ'/τ_o. (b) shows only the slowly varying component and (c) shows only the high frequency, high amplitude component.

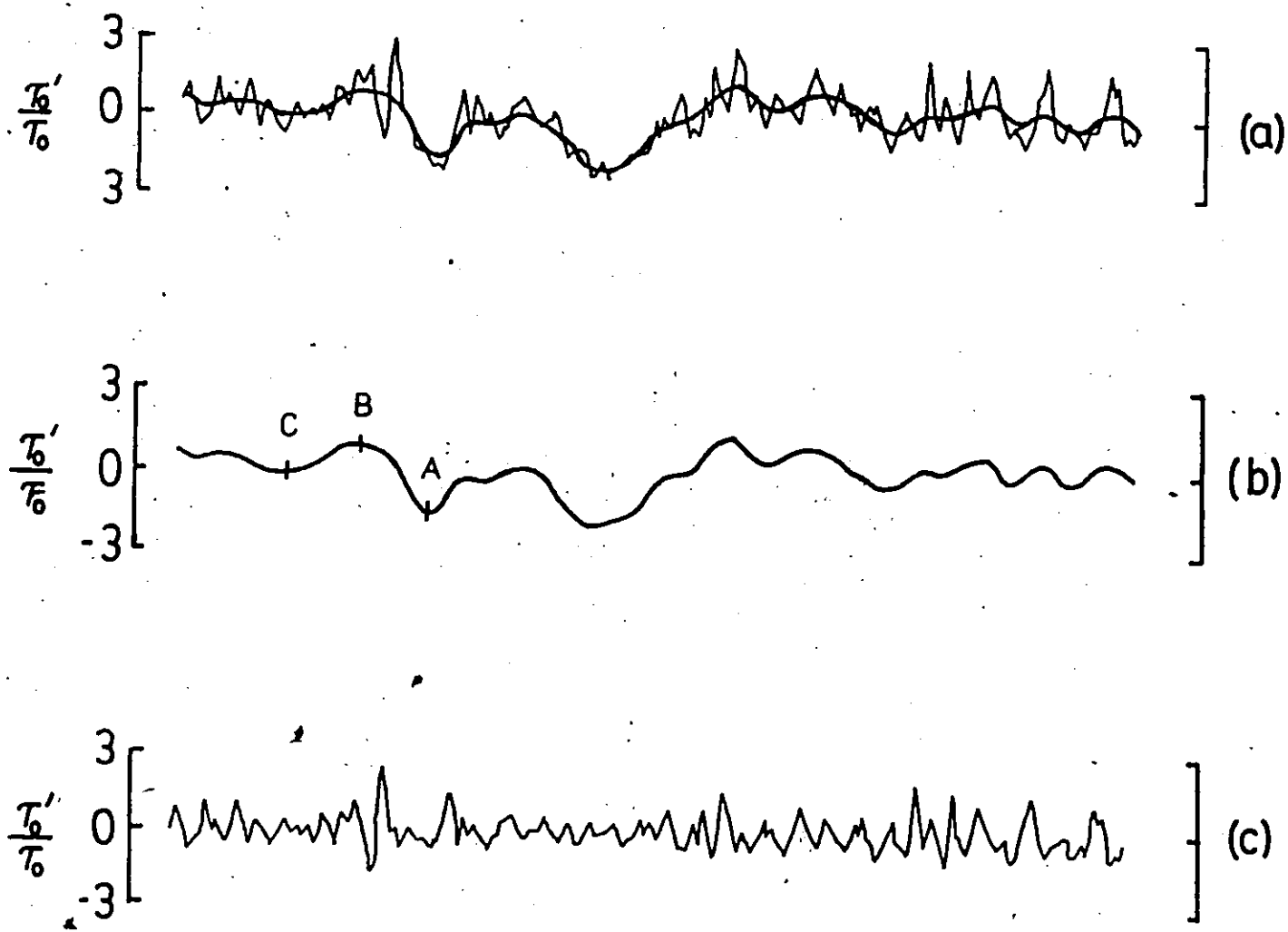
3
0
3
(a)
3
C
B
A
0
-3
(b)
3
0
-3
(c)
0
20
40
60
80
TU₀/h

larger, less intense variation due to large eddies.

The effect of the downstream variation in bed shear stress on sediment transport rate along the flow is of importance to this discussion. Taking the variation in τ_o'/τ_o shown in figure II-5b to represent downstream variation in τ_o' it is possible to recognize the distribution of turbulent shear stress acting on the bed in the direction parallel to the flow due to large eddies. The segment A-C of the line in figure II-5b represents the distribution of instantaneous bed shear stress associated with a single large eddy. Segment A-B repesents the upstream portion of the eddy, beneath which $\partial\tau_o'/\partial x$ increases downstream so that the bed beneath that part of the eddy will undergo erosion. On the downstream portion of the eddy (segment B-C) $\partial\tau_o'/\partial x$ is negative so that deposition will occur on the bed. Preservation of the deposit on the downstream side of a large eddy depends on the duration of the period of interaction between the eddy and the bed. If the eddy maintains the same distribution of bed shear stress as it moves downstream the regions of erosion and deposition will also move downstream. As a result the site of deposition will undergo subsequent erosion as the eddy moves with the flow. However, Southerland (1967) suggested that eddies in the outer region only briefly interact with the bed as they move along the flow and then are deflected back away from the bed. In this case the resulting deposit on the

downstream side of an eddy will not undergo subsequent erosion as the eddy continues with the flow. The ultimate preservation of this type of deposit will depend on the net rate of deposition on the bed due to the downstream variation in the time averaged bed shear stress ($\partial\tau_o/\partial x$). The size of the deposit will be some fraction of the size of the eddy itself.

The burst/sweep process, which is superimposed onto the action of large eddies in the flow, has a complex effect on local erosion and deposition. The approach of a sweep towards the bed locally increases the bed shear stress by up to 5 times τ_o (Grass, 1971) producing a shear stress maximum on the bed and changing the local shear stress gradient ($\partial\tau_o'/\partial x$). This, in turn, will alter the distribution of areas of erosion and deposition on the bed in a manner which is similar to that produced by eddies (though over a smaller area of the bed). Just upstream of the point of maximum bed shear stress associated with the sweep $\partial\tau_o'/\partial x$ is positive so that the bed will undergo erosion. Downstream of the maximum, where $\partial\tau_o'/\partial x$ is decreasing, the sediment transport rate will also decrease, causing deposition. As the fluid in the sweep moves in the flow direction near the bed it loses momentum and dissipates so that it is likely that the newly deposited bed material will be preserved (unless it is reworked by a later sweep).

The distribution of areas of erosion and deposition

due to bursting is more difficult to predict. At the point on the bed where ejection occurs there is a local minimum in τ_o' so that from the upstream direction to the burst $\partial\tau_o'/\partial x$ is negative and deposition will occur. From the point of bursting to some point downstream $\partial\tau_o'/\partial x$ is positive so that erosion should take place. However, the ejection of fluid away from a bed over which sediment is in transport carries grains briefly upward where they begin to settle back towards the bed (Sumer and Deigaard, 1979). This complicates the situation downstream of the burst because along the section of the bed which should be undergoing erosion due to the positive shear stress gradient there will also be an addition of grains due to fallout from the burst (similar to the term $\partial c/\partial t$ which was included in equation 10). Whether erosion or deposition occurs, therefore, depends on the relative importance of the positive shear stress gradient and the rate at which grains fall out of the fluid ejected during bursting.

In summary, for the condition of interest to later discussion of the formation, movement and preservation of structures formed on an upper plane bed (i.e., deposition), there must exist a downstream decrease in bed shear stress. Furthermore, the amount, or thickness, of sediment which is deposited will depend on the magnitude of $\partial\tau_o'/\partial x$ and the length of time that this condition persists (because the

thickness increases at the rate $\partial h/\partial t$). These deposits should exhibit the effects of smaller scale variations in the distribution of the turbulent bed shear stress due the effects of secondary flows and/or the turbulent structure of the flow.

SUMMARY

Upper flow regime plane bed is a stable bedform which develops on mobile sand beds under higher bed shear stress than ripples and dunes and lower Froude numbers than standing waves or antidunes. The development of upper plane bed is favoured in any environment in which fine grained sediment is transported under relatively deep, fast flows. The factors which control the stability of upper plane beds are presently not well understood.

Active upper plane beds are characterized by intense sediment transport near the bed which is often described as a distinct layer with a relatively sharp boundary with the suspended sediment at higher levels in the flow. A common characteristic of this bed load layer are alternating, flow parallel windrows of slow moving, sediment-rich fluid and faster moving fluid in which the concentration of sediment is lower. On bedding plane exposures of sandstone deposited on upper plane beds these windrows are preserved as primary current lineations.

The preservation of structures associated with

active upper plane beds will depend on whether the bed is undergoing net erosion or deposition. This depends on the net change in sediment transport rate over the bed which, in turn, is a function of the rate of change of time average bed shear stress in the direction of sediment transport (i.e., downstream). Small scale variations in the shear stress acting on the bed will also cause local variations in the sediment transport rate and result in a complex pattern of erosion and deposition along the bed.

CHAPTER III

HEAVY MINERAL SHADOWS, A NEW SEDIMENTARY STRUCTURE FORMED UNDER UPPER FLOW REGIME PLANE BED CONDITIONS: ITS DIRECTIONAL AND HYDRAULIC SIGNIFICANCE

INTRODUCTION

The determination of paleoflow direction from bedding plane exposures of sandstones believed to have been deposited on an upper plane bed is often made in the field by measuring the orientation of lineations on the bedding surface. These may be parting-plane lineations (syn. current lineations; Allen, 1964) or parting-step lineations (McBride and Yeakel, 1963), both of which provide only a sense of the paleocurrent direction if no other sedimentary structures of known directional significance are available for measurement nearby. Where lineations are the only structure it is possible to infer the flow direction from the upstream imbrication of sand grains as seen in thin section cut perpendicular to bedding and parallel to the lineations (Allen, 1964).

This chapter describes heavy mineral accumulations on bedding planes in sandstones which exhibit both types of parting lineation. The accumulations form structures on the bedding surface which are shown to provide a means of

determining paleocurrent direction in the field. To further understand the implications of the heavy mineral accumulations a set of flume experiments is described in which a sand containing heavy minerals comprised the bed material under flows within the range of stability of upper plane bed.

PREVIOUS WORK

Most of the information available in the literature, on the nature of heavy mineral accumulations under unidirectional flows, is derived from direct observations of heavy mineral transport and deposition in flumes. The accumulation of heavy minerals on ripples has been described by McQuivey and Keefer (1969) who showed that magnetite sand in a bed of predominantly quartz sand tended to form relatively high concentrations just upstream of the ripple crests. They reasoned that the less mobile magnetite grains move up the stoss slope of ripples and deposit near their crests where the intensity of velocity fluctuations (and maximum instantaneous bed shear stress) is lowest. Brady and Jobson (1973) described similar magnetite accumulations between the crest and brink points of dunes. They also reported "... thin ripple (form) accumulations or very thin almost sheetlike accumulations ..." (Brady and Jobson, 1973, p. K16) on the stoss slopes of dunes and washed out dunes. On an upper plane bed, near the upper limit of plane bed

stability, Brady and Jobson noted that there were no accumulations of magnetite sand on the bed surface. Kuenen (1966) reported the development of "patches" of both light and heavy minerals on a plane bed in a circular flume in which the flow velocity was decelerating, depositing sediment from suspension to simulate deposition from a turbidity current. He attributed the development of these accumulations to the tendency for grains of similar susceptibility to entrainment (i.e., similar size, density and shape) to be transported and deposit together.

HEAVY MINERAL ACCUMULATIONS IN THE WHIRLPOOL SANDSTONE

Setting

The structures described below occur in the Whirlpool Formation (Silurian) at the Rice and McHarg Quarry, approximately 4 km south of Georgetown, Ontario (Fig. III-1). The Whirlpool is the basal Formation of the Cataract Group (Alexandrian Series) and is exposed along the Niagara escarpment and in quarries from Medina, New York to near Collingwood, Ontario. It is defined by Bolton (1957, p. 9) as "...typically a massive to thick-bedded, white to light grey, fine-grained, crossbedded, compact, unfossiliferous quartzose sandstone or orthoquartzite." Bolton interpreted the Whirlpool Formation as a shallow marine facies laid down during a marine transgression. More recent work, however, has led to its reinterpretation as the

Figure III-1. Location map showing quarry in which the structures described in the text are exposed.

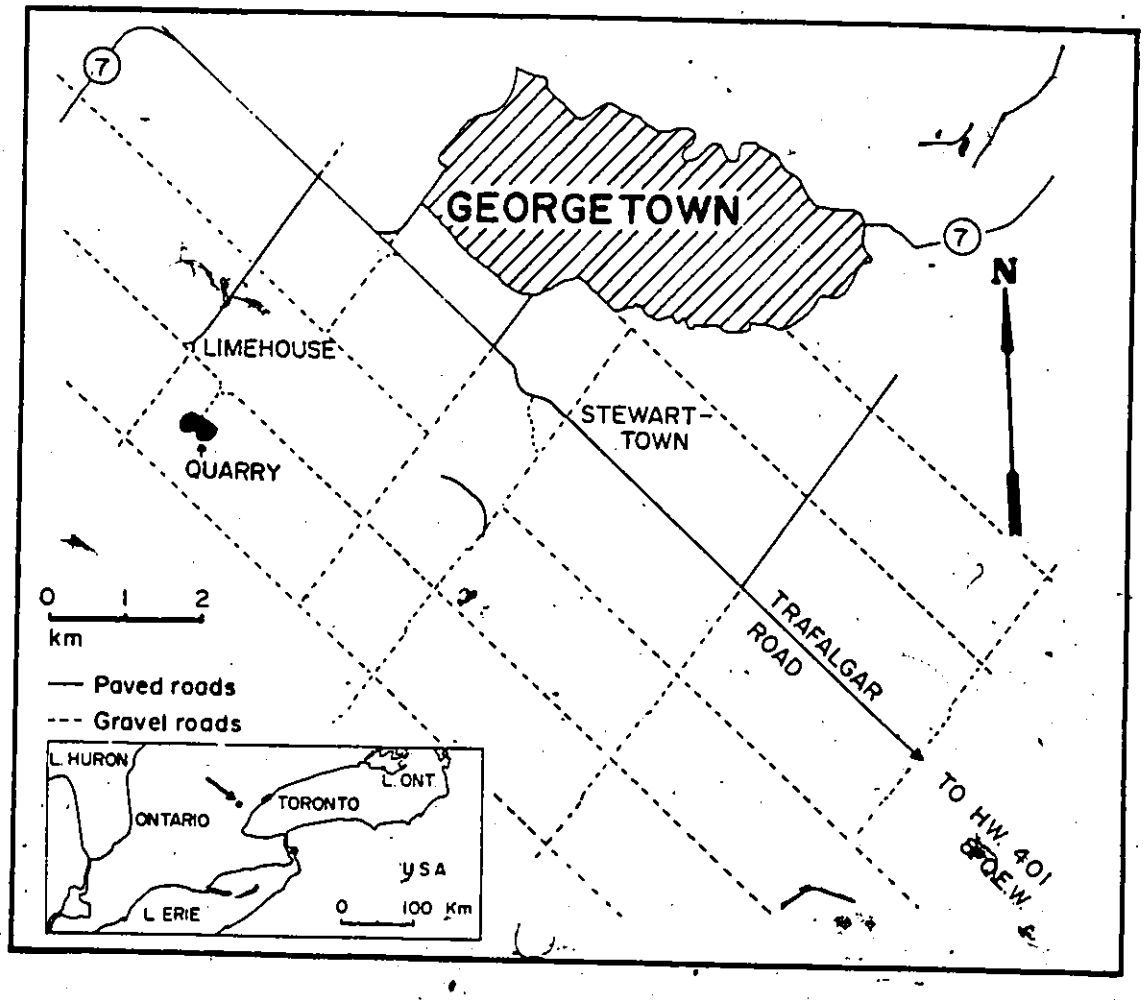
7
GEORGETOWN
7
N
LIMEHOUSE
QUARRY
STEWART-
TOWN
0 1 2
km
— Paved roads
--- Gravel roads
TRAFALGAR
ROAD
TO HW. 401
L. HURON
ONTARIO
TORONTO
L. ONT.
USA
L. ERIE
0 100 Km

product of deposition in a braided fluvial environment (Middleton, Salas and Martini, 1983).

Heavy Mineral Accumulations

The heavy mineral accumulations described below occur on part of an exposed bedding surface of horizontally laminated sandstone in the Rice and McHarg quarry. Within the quarry are isolated units of large-scale trough and planar cross-bedding exposed on bedding surfaces showing rib and furrow structures and parting lineation. The vertical sequence of structures seen in the wall of the quarry reflects the relationships observed in plan: horizontally laminated sandstone cut by isolated scours filled with cross-bedded sandstone, and, less commonly, by beds of ripple trough cross-strata sets. All of the directional structures in the quarry indicate paleoflow to the west or north-west.

One horizontal bedding surface which displays parting lineation extends over several hundred square metres and is much darker in colour than other parting lineated surfaces due to a relatively high concentration of opaque heavy minerals (leucoxene, hematite, and magnetite). Over much of the surface the opaque minerals are uniformly distributed although in one relatively small area they occur in distinct patches with no detectable relief. Figure III-2 shows a number of these heavy mineral accumulations with respect to the line of the parting lineation. Note that along any line parallel to the parting lineation there is

Figure III-2. (a) Heavy mineral accumulations on a parting-plane lineated bedding plane in the Rice and McHarg quarry. Note that along lines parallel to the lineation (parallel to the top the the photograph) on one side of the accumulations there is commonly a sharp boundary with the lighter toned sandstone while the transition is gradational on the opposite side. (b) A freshly quarried slab showing very well preserved heavy mineral accumulations on a lineated surface (parallel to top of photograph). Note that inferred flow direction is from right to left (see text).

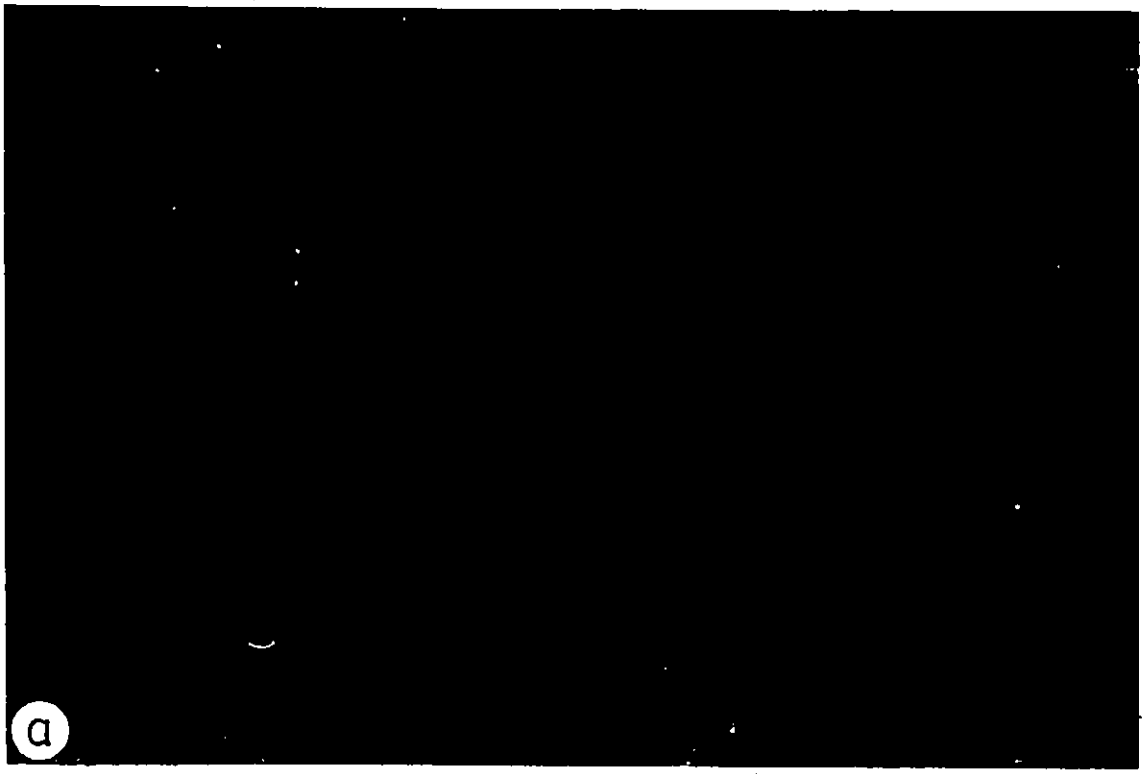
a

b

commonly one side of the heavy mineral accumulations which has sharp boundaries with the lighter coloured quartz-rich areas while on the other side the accumulations become gradually lighter. The difference in the two boundaries reflects the asymmetry of the heavy mineral concentration gradient along lines parallel to the parting lineation. This characteristic of the accumulations suggested that they may be useful in determining paleocurrent directions in the field. In this example paleocurrent directions were determined from the large scale troughs and casts of imbricate lutite clasts exposed on the quarry floor. Figure III-3 (a and b) shows rose diagrams and resultant vectors derived from the paleocurrent data compared with the form of the heavy mineral accumulations. These observations suggest that the flow was approximately parallel to the parting lineation from light areas towards the sharp boundary of the heavy mineral acumulations. To verify this the dip of imbrication of grains was measured within a few millimetres of the bedding plane on which the accumulations are exposed in a thin section cut perpendicular to bedding and parallel to the parting lineation. Figure III-3c shows that, on average, grains dip towards the east along the line of lineation and indicate that flow was to the west, from the light areas towards the sharp boundary of the heavy mineral accumulations.

Figure III-3. Figure showing the relationship between the orientation of the parting lineation and the asymmetry of the heavy mineral concentration in an accumulation compared to the local paleocurrent direction inferred from: (a) large scale trough axes, (b) casts of imbricate pebbles, and (c) grain imbrication just below a bedding plane on which the heavy mineral accumulations are exposed. Note that the orientation of all of the structures are shown in plan, with respect to north, while the rose diagram for the grain imbrication shows the dip of grains as seen in a thin section cut normal to the bedding plane and parallel to the lineations.

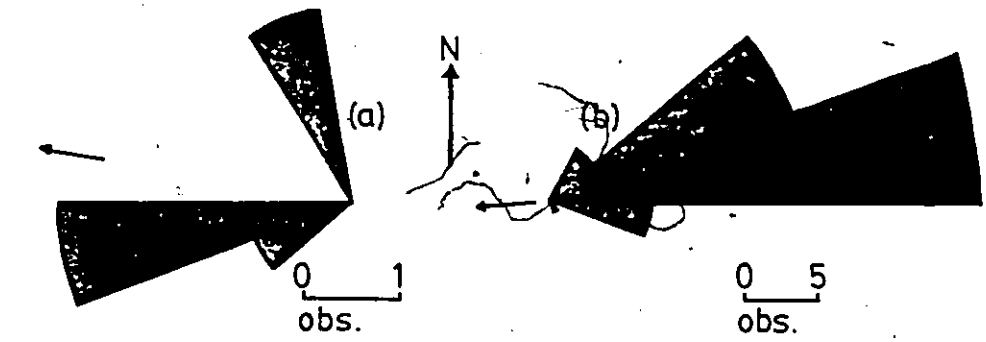
(a)
N
(b)
0 1
obs.
0 5
obs.

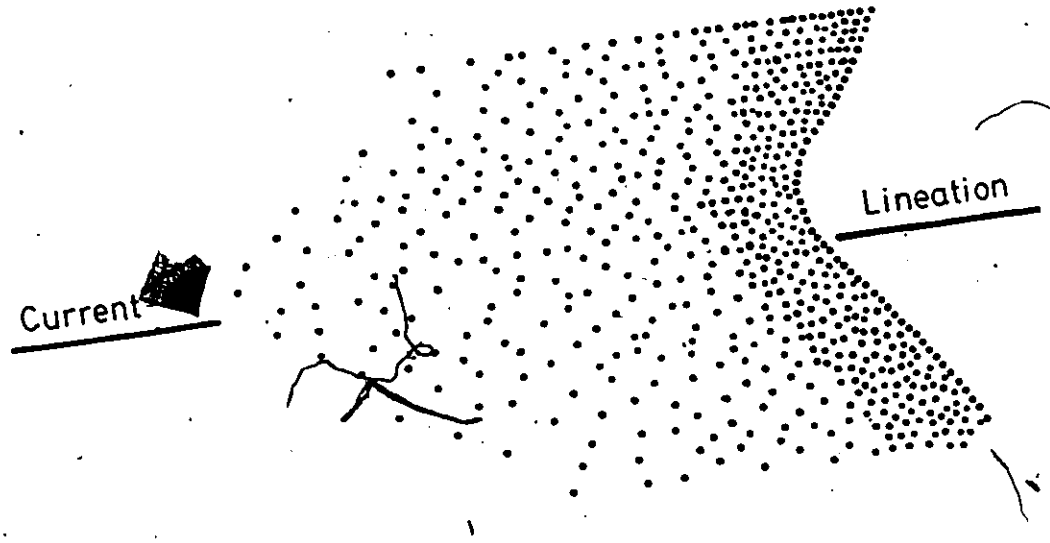
Current
Lineation

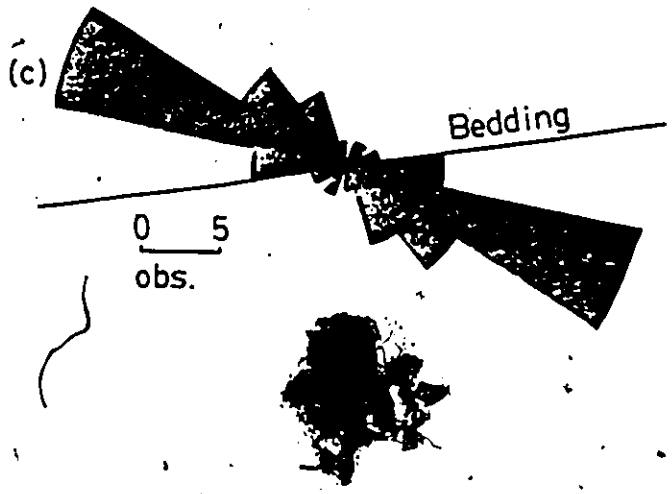
(c)
Bedding
0 5
obs.

FLUME EXPERIMENTS

To further investigate the heavy mineral accumulations, a series of flume runs were undertaken. The flume used for these experiments is described in Appendix II-A. Quartz sand (average size: 2.52 ϕ or 0.17mm) was mixed with chromite sand (average size: 2.75 ϕ or 0.15mm) to make up a homogenous bed for the flume that consisted of 3% by weight heavy minerals. A set of four runs were made at slightly varied velocities and depths. The flow data are summarized in Table III-1 (note that corrections have been made for side-wall effects using the method of Johnson, 1942). An attempt was made to determine if the heavy mineral accumulations observed in the field had a limited range of stability under plane bed conditions. Unfortunately because of the restriction to relatively shallow flow depths in the narrow flume the plane bed was only stable over a restricted range of velocities.

During Run 1, at the lowest stream power in the plane bed stability field of the four flume runs, heavy mineral accumulations like those in the Whirlpool Sandstone were present on what appeared to be a plane bed. The accumulations had a sharp upstream boundary with the quartz-rich sand with a more gradual transition downstream (Fig. III-4). They remained intact as they moved downstream, beneath a layer of faster moving quartz sand, by intermittent erosion of their upstream edges and deposition

Table III-1. Hydraulic data for flume runs.

Run	U (m/s)	d (m)	τ_o (N/m^2)	U* (m/s)	$\tau_o U$ (N/ms)	F
1	0.67	0.0993	1.66	0.041	1.102	0.67
2	0.67	0.1013	1.68	0.041	1.120	0.67
3	0.67	0.0987	1.68	0.041	1.316	0.68
4	0.79	0.0871	1.66	0.041	1.316	0.87

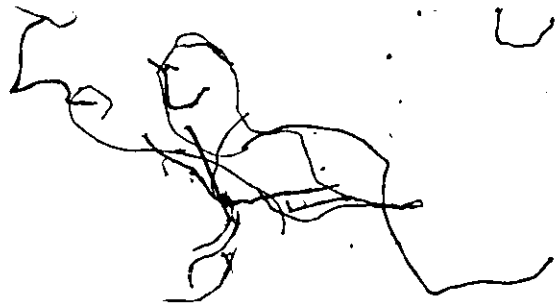

Figure III-4. Heavy mineral accumulations on the flume bed during Run 1. Arrow indicates the direction of flow. The length of the section of bed shown is approximately 15 cm.

a few centimetres downstream. To determine if any textural variations exist along the accumulations a thin section was cut from an impregnated box core oriented perpendicular to bedding and parallel to the flow direction through one accumulation (see Appendix II-C for a description of the impregnating technique). The long axes of all chromite grains making up the accumulation (as seen on the thin section) were measured, and are plotted in figure III-5 as averages for each 0.4 mm segment along the length of the thin section. Grain size through the accumulation neither decreases or increases significantly along the measured length.

During Run 2 heavy mineral accumulations similar to those of Run 1 were present near the upstream end of the channel but became increasingly diffuse downstream where they were entirely absent. There the chromite appeared to be distributed like the quartz sand in flow-parallel rows in constant transport ("windrow" in the terminology of Allen, 1964). It could not be determined if the chromite sand was actually distributed in rows or if it was uniformly distributed on the bed and was being partially masked by the moving quartz sand. In Run 3, at a slightly greater stream power, the bed along the entire length of the flume was like that at the downstream end of the channel during Run 2. At the greatest stream power and at a considerably higher Froude number (Run 4) the chromite sand appeared to

Figure III-5. Plot of grain size versus distance downstream through a heavy mineral accumulation in the flume bed (run 1) as determined from the measurement of chromite grain long axes in thin section cut parallel to the flow direction. The equation for the best-fit line through points is:

$$Dc = 0.1686 + 2.4248 \times 10^{-5} X$$

where Dc is the average chromite grain long axis and X is the horizontal distance along the thin section. The correlation coefficient of the line is equal to 0.0135.

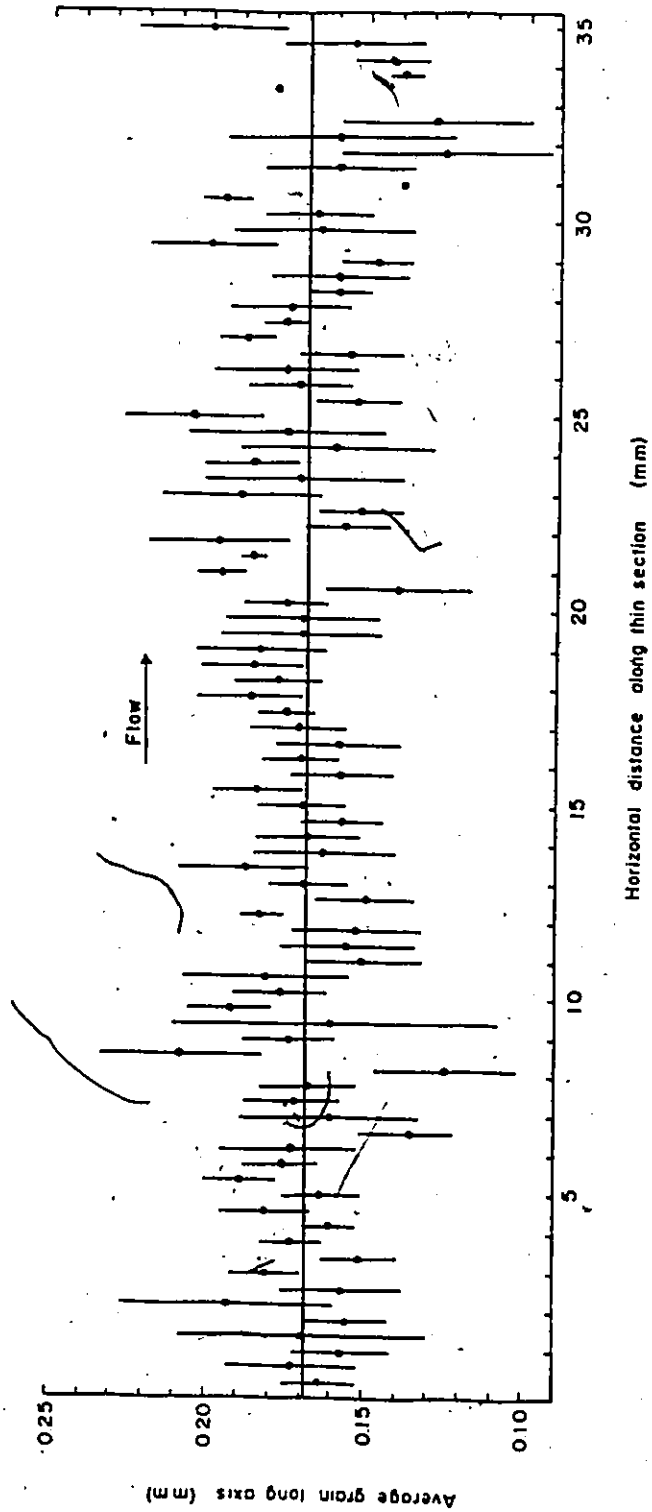
Flow
0.25
0.20
0.15
0.10
5
10
15
20
25
30
35
Horizontal distance along thin section (mm)
Average grain long axis (mm)

accumulate in lower concentrations than in Run 1 and without the asymmetry in the concentration gradient. These accumulations were evenly spaced approximately 0.2 m apart (from the downstream end of one accumulation to the upstream end of the next) and extended across most of the channel width (Fig. III-6).

While the bed appeared to be flat during each Run detailed bed profiles, constructed from measurements of bed height made with a point gage mounted on the flume rails, indicate that low bedforms were present at the end of runs 1, 2, and 4 (Fig. III-7). During Run 1 the working section of the channel contained two long, very low bedforms (length to height ratios were 790 for the upstream form and 651 for the downstream form). These may be extremely washed out dunes (Simons and Richardson, 1961) although they more closely resemble plane bed than dunes due to their low relief and the very low angle lee slopes (0.4° maximum). They also differ from "low amplitude sand waves" described by Smith (1971) by the absence of avalanche faces. Similar low bedforms were present on the upstream part of the bed following Run 2 although downstream of 2.5 m (Fig. III-7) the bed was essentially flat. It is notable that the heavy mineral accumulations of Run 2 occurred only on the part of the bed where these bedforms are present. The profile for Run 3 shows no recognizable bedforms, the bed being flat along the length of the channel, the random variations in

Figure III-6. View of the flume bed following Run 4. Note the alternations of light (quartz-rich) and dark (chromite-rich) areas along the channel. Flow was towards the bottom of the photograph.

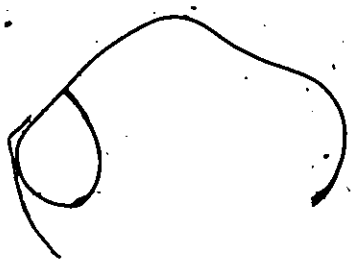

Figure III-7. Bed profiles along the flume channel following runs 1 to 4 based on bed heights measured with a point gage mounted onto the flume rails. Note that above the Run 4 profile heavy dark lines indicate the position along the channel where chromite was concentrated.

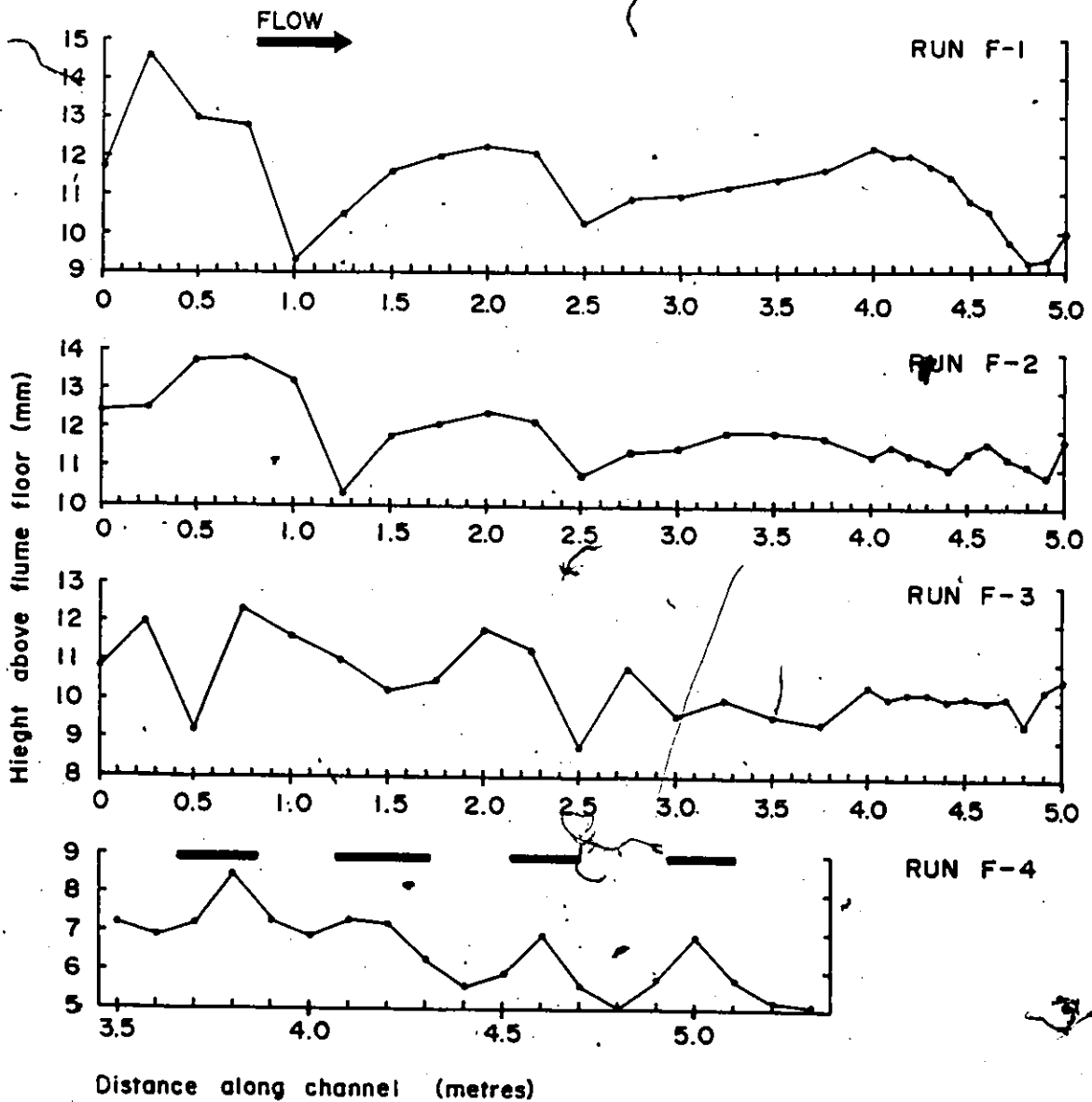
FLOW
RUN F-1
RUN F-2
RUN F-3
RUN F-4
Hieght above flume floor (mm)
Distance along channel (metres)

relief decreasing downstream. The bed following Run 4 was made up of low symmetrical waves with average length and height of 0.35 m and 0.0016 m, respectively. Chromite sand was concentrated on the crests of the wave forms (Fig. III-7). While water surface waves were not recognized during Run 4 it was believed that the symmetrical waves are low standing wave bedforms. To verify this assumption the flow velocity was calculated from the formula relating velocity and antidune spacing (derived from Kennedy, 1961):

$$U = \sqrt{\frac{gL}{2\pi}} \qquad (14)$$

where U is the average stream velocity, g is the acceleration due to gravity and L is the minimum length of the waves. Taking L to be equal to 0.35 m, U is calculated as 0.74 m/s, within 7% of the measured average velocity for Run 4, and suggesting that the bed surface waves formed in response to low water surface waves.

DISCUSSION

The term "heavy mineral shadow" is proposed for the heavy mineral accumulations described from the Whirlpool Sandstone (Fig. III-2) and flume runs 1 and 2 (Fig. III-4). This structure may be formally defined as an irregular patch of heavy minerals, on a bedding plane exposure of sandstone (or sand) deposited on an upper plane bed, which is

characterized by the presence of an abrupt upstream boundary, with adjacent lighter minerals, and with a gradual transition into the lighter minerals in the downstream direction. It may be appropriate to extend this definition to include identical structures on the flat backs of dunes (as shown in Figure 14B of Brady and Jobson, 1973). The term "ripple form" used by Brady and Jobson (1973) to describe these structures is not favoured because the word "ripple" suggests that the abrupt boundary (like the brink of a ripple) is on the downstream side of the structure (and was mistakenly drawn with such an orientation in their figure 13).

The presence of low bedforms in association with the heavy mineral shadows formed in the flume is of questionable significance because they would not be recognized in ancient sedimentary rocks. The existence of this previously unreported bedform does, however, warrant further investigation because of its potential relevance to discussion of the ripple or dune to plane bed transition.

The asymmetry of the heavy mineral concentration gradient probably develops due to the mode of movement of the shadows, that is by intermittent erosion along a well-defined upstream margin and deposition within a few centimetres downstream. A decrease in the heavy mineral concentration downstream results from a decreasing number of grains depositing with distance from the upstream edge of

the shadows. It is likely that the relatively heavy grains in the shadows are "out of phase" with the mode of transport and the bed state of the much larger population of lower density quartz grains. Evidence for this is the intermittent transport of heavy minerals while the lighter grains are in more-or-less constant transport over the plane bed.

The sudden movements of the leading edge of shadows, observed during flume experiments, must reflect an increase in bed shear stress past some critical value for the movement of chromite grains in the shadows The value of β, based on Shields' criterion (equation 3) for chromite grains of the diameter moving in shadows (from Fig. III-5), is 0.257 N/m^2 while its average value for Run 1 is 1.66 N/m^2 (from table I). The intermittent movement of shadows suggests that they respond to some critical bed shear stress which is greater than the average, suggesting that the grains in shadows are much more resistant of movement than one would expect. The underestimation by Shields' criterion is probably due in part to the fact that it is based on experimentally determined values of β for grains moving in low concentration over a bed material of the same size and density. It is also possible that the greater than predicted resistance to movement by the chromite grains is due to the fact that they are on the stationary bed and are overlain by a moving bed load of

predominantly quartz sand. The weight of the bed load may be transmitted to the bed (including the chromite grains in shadows) by dispersive pressure, thereby increasing the resistance to movement of grains in shadows (this was suggested to be the case for upper plane beds by Bagnold, 1956, 1966, and Hill, 1966)

The cause of fluctuations in shear stress acting on the grains in shadows which cause their intermittent movement may be attributed to the passing of eddies over the bed and/or to the approach of high speed sweeps towards the upstream edges of shadows. Because the size of large eddies is a function of the flow depth the effects of eddies in the shallow flow in the flume would be difficult to distinguish from the effects of sweeps. However, the scale of the shadows (i.e., of the lateral extent shown in Fig. III-4) is greater than the scale of sweeps. According to the relationship expressed in equation 9, Chapter II, the lateral spacing of streaks during Run 1 would have been approximately 2.5 mm. This suggests that the larger eddies are more likely responsible for the observed movement along the fronts of shadows.

The precise mode of transport during the movement of a shadow is a matter for speculation. One might expect that grains are lifted into the moving bedload layer during erosion (i.e., during the bed shear stress maximum associated with an eddy) and subsequently settle out

downstream where the local bed shear stress is lower. If this is the case it would be predicted that the distance which each grain is transported during a single erosional event will be inversely proportional to its settling velocity (and, in the case of grains of similar shape and density, its size). This mode of movement would result in a decrease in the size of heavy minerals in the downstream direction through a heavy mineral shadow. This variation in chromite long axis is not evident in the data shown in figure III-5. The apparent discrepancy might result from one (or more) of the following: (1) The long axes shown in figure III-5 are from the central 30% of the total length of a heavy mineral shadow; it is possible that in the downstream 35% of the length the predicted fining may be detectable. (2) Settling of grains may occur too rapidly for segregation according to settling velocity to become well developed (this is especially possible if heavy mineral grains are in sufficiently high concentrations to inhibit segregation according to their settling velocity). (3) The heavy mineral grains may not be completely lifted off the bed but become dilated in response to the additional shear as the eddy passes. In this case dispersive pressure (Bagnold, 1954) provides the support mechanism during transport so that sorting according to settling velocity will not take place. Bagnold (1954) proposed that the intensity of dispersive pressure acting on a grain is

proportional to its size (equation 8) and will result in the largest grains being pushed upwards through the dispersion. If the heavy minerals in shadows are supported by dispersive pressure during movement it would be expected that with deposition the cessation of movement will begin at the base of the dispersed layer. The largest grains (at the top of the layer), therefore, may continue downstream after the finer grains (in the lower part of the layer) have stopped. This could result in a coarsening of heavy mineral grains in the downstream direction, a trend which is very vaguely reflected in the slightly positive slope of the regression line through the points in figure III-5. (4) The majority of grains may only roll over the bed rather than being lifted off the bed. In this case the downstream variation in heavy mineral size through a shadow will reflect the relative ease of rolling over the bed (grains that roll more easily than others will move farther downstream with every movement of the heavy mineral shadow). Experiments by Everts (1973) showed that sand of a given size will more readily roll over a bed of finer sand than over a bed of sand of the same size. This is due to the greater exposure of the large grains to the flow (Fenton and Abott, 1977). In the case of the heavy mineral shadows one would expect the larger grains to roll the farthest so that in the downstream direction through the shadow there would be some increase in the size of heavy mineral grains. Determination

of which of the four possible means of heavy mineral shadow movement is correct may be possible through further experimentation.

The action of the high bed shear stress due to eddies may also be important in the initial formation of the patches of heavy minerals. The bed shear stress maximum, associated with an eddy, acting on a bed which is composed of a homogenous mixture of light and heavy minerals will cause a brief period of local erosion. Light minerals will travel farther than the heavy minerals which will deposit a short distance downstream. Such deposits will form areas enriched with heavy minerals which will be more resistant to movement relative to the surrounding lighter grains. In natural sands heavy minerals are generally finer than lighter minerals so that the enriched areas on the bed would remain so as they are overpassed (Everts, 1973) by the larger light grains. Heavy minerals, however, would be of a size similar to those in the shadows and would tend to deposit. These areas of enrichment would be sites of positive relief (i.e., on the order of a few grain diameters), due in part to their local armouring of the bed, and would be most prone to erosion on their upstream edges (as was observed in the flume).

The above ideas regarding the movement of the heavy mineral shadows and their postulated origin require the existence of eddies in the flow. The "washing out" of

shadows (Run 2) may reflect the damping of the turbulent structure of the flow by an increase in the concentration of suspended sediment with increased flow strength. The damping of turbulence by suspended sediment load has been well documented (Einstein and Chien, 1955; Vanoni and Brooks, 1957; Coleman, 1981). With the decrease in the variation in bed shear stress caused by the eddies, the heavy mineral shadows will no longer segregate into patches but will become a more diffuse component of the bed load. Due to their greater density the heavy minerals remain below the lighter minerals in the bed load and may have greater opportunity to deposit because they no longer occupy topographic highs on the bed. Brady and Jobson (1973) found that heavy minerals did tend to deposit slowly on an upper plane bed on which heavy mineral shadows were not present. The exact condition under which shadows will wash out is a matter for further study as this will depend on the size, density and concentration in the bed, of the heavy minerals and on the availability of fine sand to go into suspension.

The onset of heavy mineral accumulation on the crests of symmetrical bed waves (run 4) occurs with the development of waves on the water surface at Froude numbers between 0.8 and 0.9 (Kennedy, 1963). The distribution of heavy minerals on the bed during Run 4 may be in part due to their deposition during Run 3. With the development of low waves on the water surface scour occurs on the bed below

wave troughs. Heavy minerals deposited during Run 3 would then be eroded, leaving relatively quartz rich areas between the crests where the earlier deposit of heavy minerals are preserved.

The sequence of modes of heavy mineral transport described above has some relavence to the development of economic placers in environments where upper plane bed is a common bed state. Heavy mineral shadows represent a type of transport in which heavy minerals are concentrated while they are still part of the bed load. Those described from the Whirlpool Sandstone and flume experiments are relatively small (covering areas of several square centimetres) although similar forms have been observed by the author which extend over several square metres in the estuary of the Shubenacadie River, Nova Scotia, where flow depth exceeds 6 metres (Fig. 8). These large shadows have measurable relief (greater than 0.02 m) and when trenched are observed to contain a several centimetre thick layer of heavy minerals in very high concentration. Where large heavy mineral shadows are preserved as vertically stacked sequences they might provide deposits of economic minerals. The diffuse type of heavy mineral transport (run 3) would more likely deposit and preserve heavy minerals, although in lower concentrations than in the shadows. Finally, in the low standing wave phase the bed is locally reworked, remobilizing any heavy minerals contained in the bed. If

Figure III-8. Very large heavy mineral shadow on a flat bed in the Shubenacadie River, N.S., as seen at low tide. Flow was towards the bridge in the background.

the bed waves were to migrate over time the entire bed would be reworked over a depth equal to the bed wave height, and heavy minerals which were contained in that part of the bed would be transported downstream.

CONCLUSIONS

Distinct accumulations of heavy minerals on an upper plane bed have been named "heavy mineral shadows" and are shown to be useful as paleocurrent indicators when used in conjunction with the sense of paleoflow direction inferred from parting lineation. The shadows appear to be stable in the lower part of the plane bed stability field and wash out at greater flow strengths. Washing out may be due to the damping of turbulence by increased suspended sediment load. The range of conditions over which heavy mineral shadows are stable probably depends on the size, density and concentration in the bed of the heavy minerals and the availability of fine sand for suspension. At greater flow strength (just beyond the critical Froude number for antidunes) the development of low water surface waves causes heavy minerals to be eroded out of the bed in the wave troughs and preserved on the crests (assuming that the waves do not migrate) and appear as regularly spaced accumulations oriented transverse to the flow on a bed that otherwise appears flat. Recognition of these various types of heavy mineral accumulation in ancient sedimentary rocks may make

possible a more precise interpretation of hydraulic conditions during deposition.

CHAPTER IV

HORIZONTAL LAMINAE FORMED BY DEPOSITION ON AN UPPER FLOW REGIME PLANE BED

INTRODUCTION

Horizontal stratification (syn. plane or parallel lamination) as defined by Harms and Fahnestock (1965, p. 104), consists of "... sets of laminae in sand-sized material within which the laminae are horizontal, or nearly so...". Most such stratification is formed by deposition on an upper flow regime plane bed or in the presence of low standing waves (p. 116). Sets of horizontal laminae formed by deposition on upper plane beds can extend over tens of metres in outcrop although most individual laminae are faint and difficult to distinguish in the field. Where opaque minerals define a particular lamina, however, it may be traced over tens of metres (e.g. in the Katberg Sandstone of South Africa, Stavrakis, 1980, reports dark laminae which are continuous for up to 100 m).

Unlike cross stratification formed by the migration of ripples, dunes and sandwaves horizontal stratification has not been the subject of detailed study. However, many ideas regarding its mode of formation are recorded in the literature. These ideas are briefly reviewed in the

following section. Next, variations in grain size measured on thin sections through horizontally laminated deposits formed under upper flow regime plane bed conditions are described with examples from an ancient fluvial (?) sandstone and modern intertidal sand bars. The textural variations which are recognized are interpreted in terms of the form of horizontal laminae which they are believed to represent. Textural variation through sands deposited on upper plane beds in a flume are then described and compared to the examples from the field. In the final section the characteristics of laminae which were inferred from the grain size data are summarized and the theories of laminae formation are discussed. A new theory is proposed in light of these first detailed descriptions of the structure of laminae formed by deposition on upper plane beds.

PREVIOUS THEORIES OF HORIZONTAL LAMINAE FORMATION

In this section the more popular ideas of the origin of horizontal laminae are summarized. Largely excluded from this summary are theories which were developed to explain laminae which formed by deposition from turbidity currents where conditions may be considerably different from those over an upper flow regime plane bed. Note that while the theories are listed in the chronological order in which they appeared in the literature they may be broadly classified into two basic types: (i) those that attribute laminae

formation directly to fluctuations in the flow (theories 1, 3, and 6), and (ii) those that attribute laminae formation to segregation of grains on the bed into some bed structure (theories 2, 4, and 5). In all of the theories it must be assumed that the bed is undergoing net deposition (i.e., $\partial q_s/\partial x$ is negative) in order for laminae to be preserved.

1. Velocity fluctuations

Pettijohn (1957, 1975) attributed laminae formation in sands to deposition from a current in which the velocity fluctuates over time. Presumably in a flow in which the velocity was decreasing with time increasingly finer sediment would deposit on the bed. The laminae which would form from such velocity fluctuations would be fining-upward. The main objection to this theory is that horizontal laminae have been formed in flumes where flow is steady (e.g., Jopling, 1967).

2. Like-seeks-like

A theory proposed by Moss (1963) and Kuenen (1966) is now commonly referred to as the like-seeks-like hypothesis of laminae formation. Both observed that sand grains in transport on a bed appear to segregate into patches of grains with similar susceptibility to movement (i.e., similar size, shape and density). For example, when heavy minerals of a given size are available to an active

bed they will form local concentrations which will repel larger or smaller grains regardless of their density (larger grains will stick up into the flow and more readily roll away and finer particles will be more likely lifted off the bed). According to Moss (1963, p.324) a large number of local patches of similar grains may grow until they dominate the bed (if sufficient quantities of that particular size, shape and density are available). With net aggradation of the bed the large patch or group of patches will become an internal lamination and new patches will begin to develop on the active bed. Kuenen (1966) noted similar patches of like grain which, when buried by continued deposition, became distinct laminae in the deposit. Sequences of laminae formed by the superposition of patches of similar grains would predictably form randomly alternating layers of grains of similar size, shape, and density.

3. Combined Velocity Pulsations and Like-seeks-like

Frostick and Reid (1977) combined the theories of Pettijohn (1957, 1975) and Moss (1963) and Kuenen (1966) to explain alternating light and dark laminae in the deposits of an ephemeral stream in northern Kenya. They argued that in response to rainstorms passing over the basin catchment laminae couplets formed by deposition of sediment in transport during periods of high stream discharge. Fallout of medium sand from suspension was postulated to occur as

the flood waned and was followed by deposition of increasingly finer material. As sediment reached the bed segregation of grains was believed to occur by the "like-seeks-like" process, further enhancing the difference between layers in the deposit. Opaque heavy minerals, which were more abundant in the finest part of the suspended load, were among the last grains to settle out with continued decrease in discharge and were concentrated during transport as bed load. Laminae formed by the process envisioned by Frostick and Reid would be fining-upward with fine grained heavy minerals making up the top of each lamination (or light and dark couplet).

4. Superposition of Current Lineation

Jopling (1967) attributed the formation of horizontal laminae on an upper flow regime plane bed in a flume to the superposition of "longitudinal striations", or current lineations of Allen (1964). Jopling noted that there were slight variations in grain size between striations (i.e., some were coarser grained than others). He suggested that, as a bed aggraded, these texturally different striations would become superimposed and appear as laminae of different grain size in the deposit. As in the case of the Moss-Kuenen hypothesis for laminae formation the mechanism described by Jopling would produce a random sequence of layers of sand, each layer containing grains of

similar size.

5. Migration of Low Bedforms

In deposits of the Platte River, Nebraska, Smith (1971) observed horizontal laminae which formed by deposition during migration of low amplitude sand waves with lengths up to 4.5 m and heights less than 0.018 m. The foresets were at angle of repose for that sand and were produced by avalanching of grains down the lee slope during wave migration. Internally, cross-stratification formed by avalanching was not evident in trenches cut into the sand waves and the structure observed was horizontal lamination which was normally graded. Smith observed a bed approximately 30 cm thick which was made up of horizontal laminae presumably formed by sand wave migration and described the stratification as "...an alternation of horizontal coarse and fine laminae" (Smith, 1971, p. 71). The thickness of laminae ranged from 0.13 cm to 1.0 cm for the coarse laminae and 0.68 cm to 1.7 cm for the fine laminae.

McBride, Shepherd, and Crawley (1975) reported similarly formed horizontal laminae from flume experiments. Those laminae formed by the migration of low "ripples", 2 mm to 6 mm high and spaced 15 cm to 35 cm apart, and low "in-phase wave bedforms", 2 mm to 8 mm high and spaced 10 cm to 20 cm apart. Unlike the bedforms described by Smith

(1971) those described by McBride et al. (1975) lacked avalanche faces. However, grains were segregated so that coarse grains occupied the lee faces and fine grains were located on the stoss sides of the bedforms. With migration the finer grains overrode the coarser sand forming fining-upward lamination.

This particular type of lamination has been termed "subcritically climbing translatent strata" by Hunter (1977). Similar laminae are reported from ancient sedimentary rocks by Lindholm (1982) who proposed the term "flat stratification" for horizontal laminae formed by the migration of low ripples. In that study small ripple forms could be recognized on bedding planes so that this type of lamination can be differentiated from that formed by deposition on a plane bed.

6. The Bursting Mechanism

Bridge (1978) proposed a model for the formation of horizontal laminae on upper flow regime plane beds as a response of the bed material to the bursting process on smooth or transitional rough beds (i.e., $Re_* < 70$). Bridge (1978, p. 7) suggested that following the brief period of high bed-shear stress due to the approach of a high speed sweep the coarsest grains in the bed load would settle out and deposit on the bed. With continued dissipation of the sweep, the size of grains which are deposited would decrease

with time, forming a fining-upward lamination. A subsequent burst was predicted to reduce the rate of deposition locally and, in cases where the rate of deposition is high, allow deposition of progressively coarser sediment to form a coarsening-upward unit on top of the earlier formed fining-upward lamination. The coarsening-upward deposits were predicted only for flows in which the rate of deposition was "high" and would make up only thin tops of fining-upward laminae in medium to fine sand while in very fine sand the coarsening-upward units would make up entire laminae. Bridge noted that grains of different density would have equal settling velocities if they were deposited together by this mechanism.

Hesse and Chough (1980) suggested a similar model for laminae formation in silt and clay on levees formed by the spillover of turbidity currents from the Northwest Atlantic Mid-ocean Channel of the Labrador Sea. They objected to the "single bursting cycle" model of Bridge (1978) because there would be insufficient time between successive bursts and sweeps to allow the clay size sediment, the finest part of the laminae they observed, to settle out. They proposed a "multiple bursting cycle mechanism" which suggested that silt was deposited over a number of burst and sweep events. Clay was believed to deposit during periods when the bursting process was not active due to the suppression of turbulence in the viscous

sublayer by the presence of the very fine sediment in relatively high concentrations. Multiple bursting cycles are not necessary to explain horizontal laminae formed in clay-free sands, where there is time for settling of grains between bursts and sweeps. Hesse and Chough (1980) also objected to the single bursting cycle mechanism because the lateral extent of laminae that they observed was greater than the reported spacing of streaks.

DESCRIPTIONS OF HORIZONTAL LAMINAE

Field examples

Locations

Horizontal laminae are described from three field locations. Samples labled "RM" are from the Whirlpool Sandstone (Silurian) at the Rice and McHarg quarry in Southern Ontario (Chapter III, Fig. III-1). Sample RM-01 is from approximately 1 cm below the bedding plane on which the heavy mineral shadows are exposed and RM-05 was collected from the northeast end of the same bedding plane and includes dark layers which are rich in opaque heavy minerals. Heavy minerals included leucoxene, hematite and magnetite.

Samples labled "MB" are modern sands from the southern end of Mitchener Bar, an intertidal sand bar in the Avon River estuary near Mount Denson, Nova Scotia (Fig. IV-1). Bedforms on Mitchener Bar include dunes at the

Figure IV-1. Location map showing collection sites of horizontally laminated sands from intertidal sand bars in Nova Scotia.

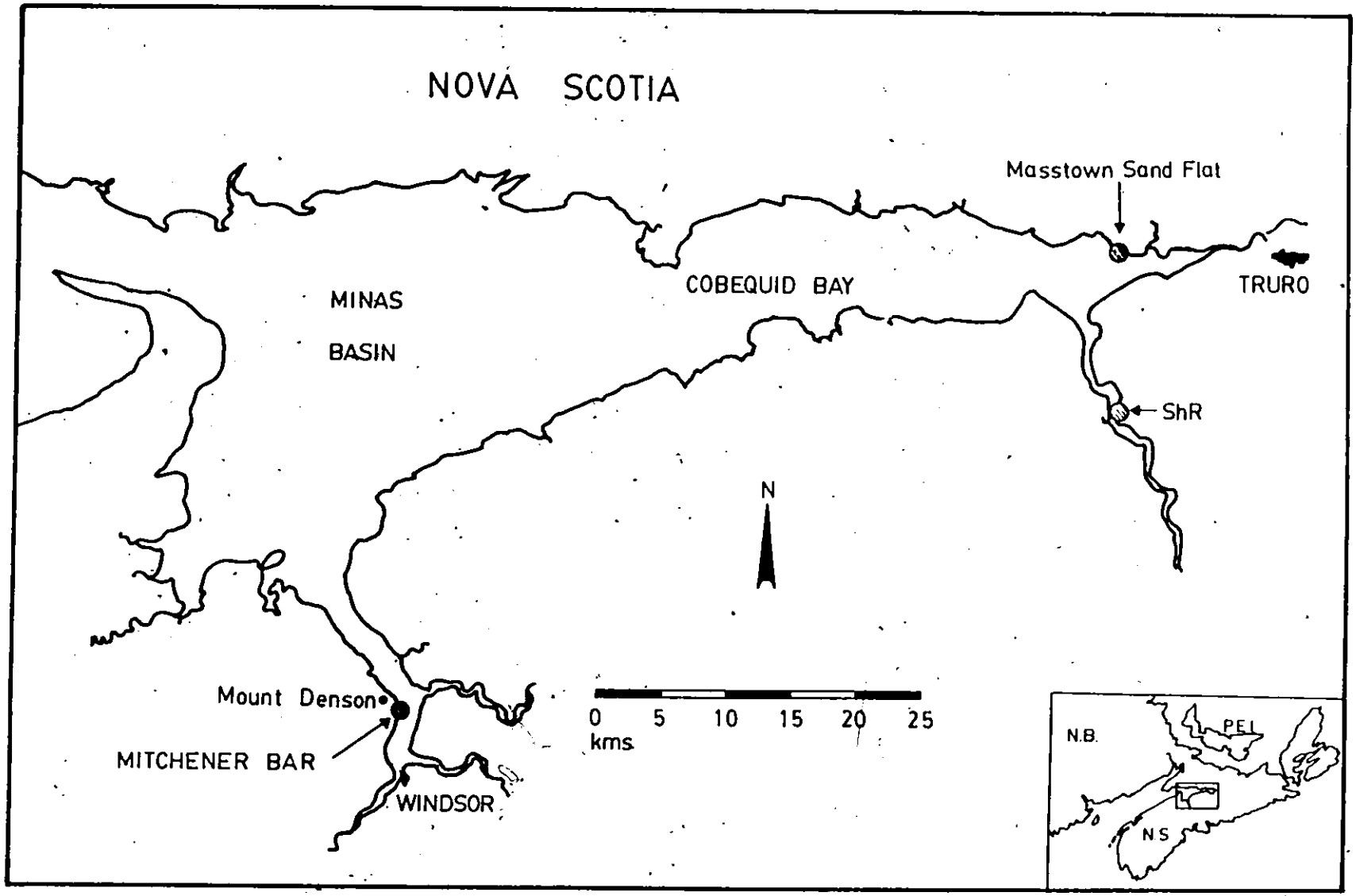
NOVA SCOTIA
Masstown Sand Flat
COBEQUID BAY
TRURO
MINAS
BASIN
ShR
N
Mount Denson
MITCHENER BAR
WINDSOR
0 5 10 15 20 25
kms
N.B.
P.E.I.
N.S.

northern end, transverse bars in the central portion and small scale ripples on the southern end. Lambiase (1977) reported that internal stratification in the southern end of Mitchener Bar consisted of horizontal laminae formed by deposition on upper plane beds and that the ripples on the surface were the result of late stage flow.

Samples labled "SR" are from the Inner Sand Flats, near Masstown, Nova Scotia, near the headwaters of Cobequid Bay. This is an extensive sand body covered with small scale ripples, formed during late stage flow, and internally dominated by horizontal laminae formed by deposition on an upper flow regime plane bed (Dalrymple, Amos, and McCann, 1983). One sample, ShR-01, is from a lobe of sand which was deposited at the mouth of a small tidal creek which emptied into the estuary of the Shubenacedie River, Nova Scotia. Internally the lobe was horizontally laminated with many prominent dark heavy mineral laminae. The opaque heavy minerals were predominantly magnetite.

Methods

All of the textural data on horizontal laminae are based on measurements of grain long axes as seen in thin section. Thin sections were cut, normal to the flow direction, from oriented samples from the Whirlpool Sandstone and from impregnated box cores collected from sand bars in Nova Scotia. The box cores were collected

approximately 10 cm below the rippled surfaces of sand bars, to avoid sampling of crossbedded sands, and were impregnated by the method described in Appendix II-C. The aim was to construct vertical sections which might show systematic textural variation through the horizontally laminated sands. This was achieved by measuring all grains in contiguous rectangular areas, 2 mm wide by 0.2 mm high (referred to as "measured units") through the thin sections (Fig. IV-2). An attempt was made to include 2 or 3 grain layers in each measured unit so the height was varied to accomodate coarser or finer sand sizes. Grain long axes from samples RM-01 and RM-05 were measured with a ruler, on the image produced by a Shadowmaster microprojector fitted with a 100X lens, to within plus or minus 0.005 mm. All other samples were analyzed by measuring long axes of grains which were projected onto a digitizing (graphics) board by means of a television camera attached to a microscope. The digitizing board was interfaced with an Apple IIE computer which computed distances measured on the board, stored the data and calculated the summary statistics. Accuracy using the digitizing board was plus or minus approximately 0.005 mm. All of the summary statistics for the data collected are given in Appendix III.

Average long axis length and standard deviation of the mean were calculated for each measured unit and plotted versus height above the bottom of the measured section

Figure IV-2. Diagram illustrating the sequence of layers in which grain long axes were measured for the construction of vertical sequences to show textural variation through horizontally laminated sands seen in thin section. The outline of the thin section, cut normal to bedding, is shown as well as the vertical section over which measurements were made. The enlarged view on the right shows three rectangular areas over which measurements were made.

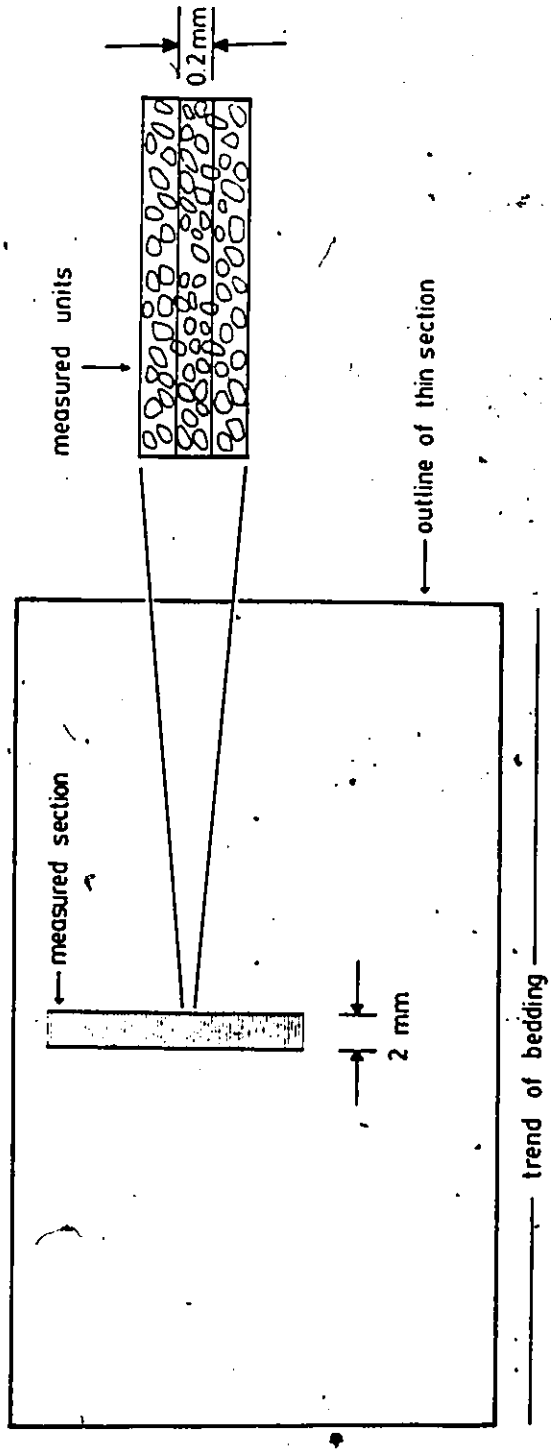
0.2 mm
measured units
outline of thin section
measured section
2 mm
trend of bedding

(Figs. IV-5A to H). When heavy minerals (predominantly magnetite and hematite) were present their average long axis lengths were calculated separately and plotted with the data for the lighter minerals (quartz and feldspar). Samples RM-05 and MB-03 were used to construct lateral correlation diagrams by measuring adjacent vertical sections (1 mm apart) with their bases along a line parallel to the lamination. Lines were drawn on the figures, connecting sequences of points which appeared to make up distinct textural units (i.e., if three or more points displayed a consistent change in grain size in vertical sequence). The lines were commonly based on the change in light mineral grain size upward. The trend of the heavy minerals was also considered in defining the trend of the textural unit, where they were present in a number of contiguous measured units.

Description of Horizontal Laminae

In outcrop and in polished section horizontal laminae from the Whirlpool Sandstone are well defined only where there are layers of opaque heavy minerals (Fig. IV-3). These layers of heavy minerals which can be traced over several metres in the field will be termed "heavy mineral sheets" because they appear to extend along horizontal planes in outcrop like a sheet of heavy minerals. Where heavy mineral sheets are absent there is only a vague sense of horizontal lamination. In trenches cut into the two

Figure IV-3. Photograph of outcrtop of the Whirlpool Sandstone at the Rice and McHarg quarry showing horizontally laminated sandstone with well defined heavy mineral sheets.

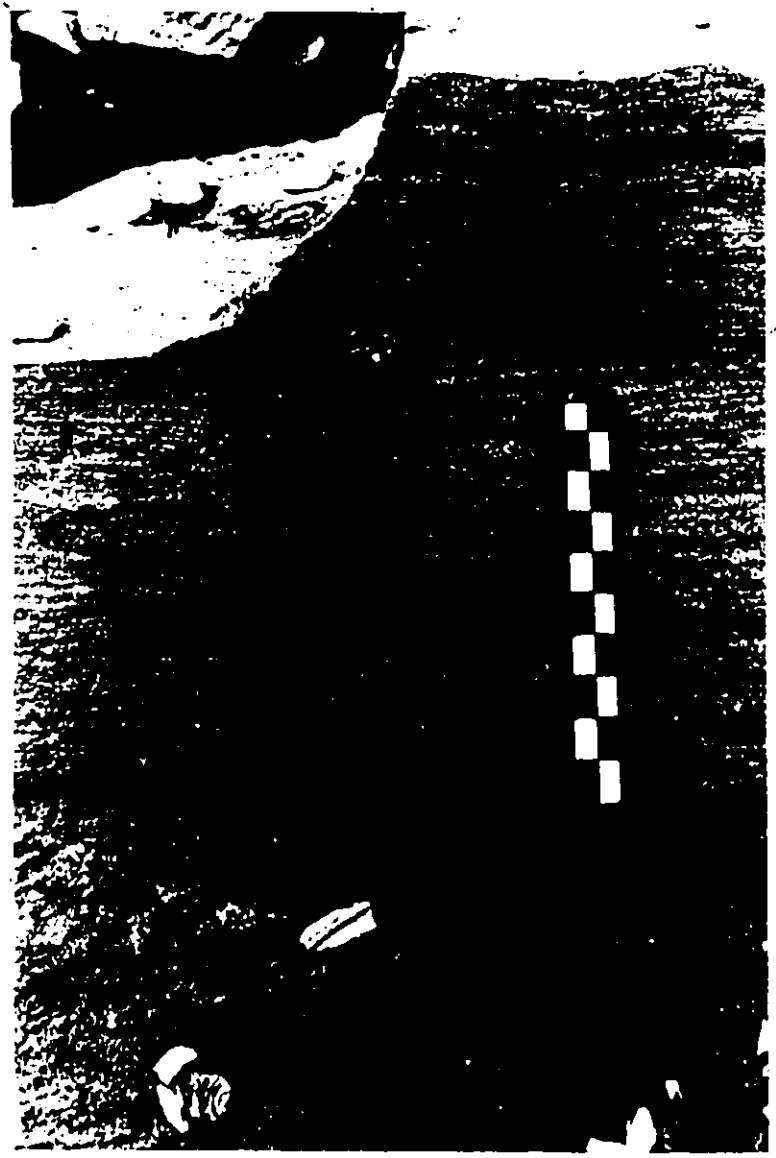

intertidal sand bars the horizontal laminae appeared only as occasional dark sheets of opaque heavy minerals (Fig. IV-4). The trench cut into the lobe of sand in the Schubenacedie River Estuary showed numerous, well-defined heavy mineral sheets.

In thin section only opaque heavy mineral sheets were obvious and areas which lacked heavy minerals appeared to be structureless. Plots of average grain size versus height above a fixed datum (or below in the case of samples RM-01 and RM-05) show the presence of fining-upward and coarsening-upward textural units (which are interpreted as laminae) which are generally less than 1 mm thick (Figs. IV-5 A to H). The difference in grain size between the top and base of the laminae is small, ranging from approximately 0.01 mm to 0.05 mm. Average grain size for fining- and coarsening-upward laminae are not significantly different. Table IV-1 summarizes the abundance and thickness of laminae. Taking all of the samples together, fining-upward and coarsening-upward laminae are equally abundant while the ungraded (or undeterminable) layers are relatively rare in the samples studied. Individual samples are sometimes dominated by one or the other type of lamination. Fining-upward laminae are significantly thicker than coarsening-upward laminae, their means being two standard deviations apart (only samples MB-02 and ShR-01 contained thicker coarsening-upward laminae). The apparently ungraded layers

Figure IV-4. Photographs of horizontal laminae in trenches cut into the deposits of intertidal sand bars, (a) Masstown Sand Flats, Cobequid Bay, (b) Mitchener Bar, Avon River estuary, and (c) a trench cut into a lobe of sand deposited in the Shubenacedie River estuary.

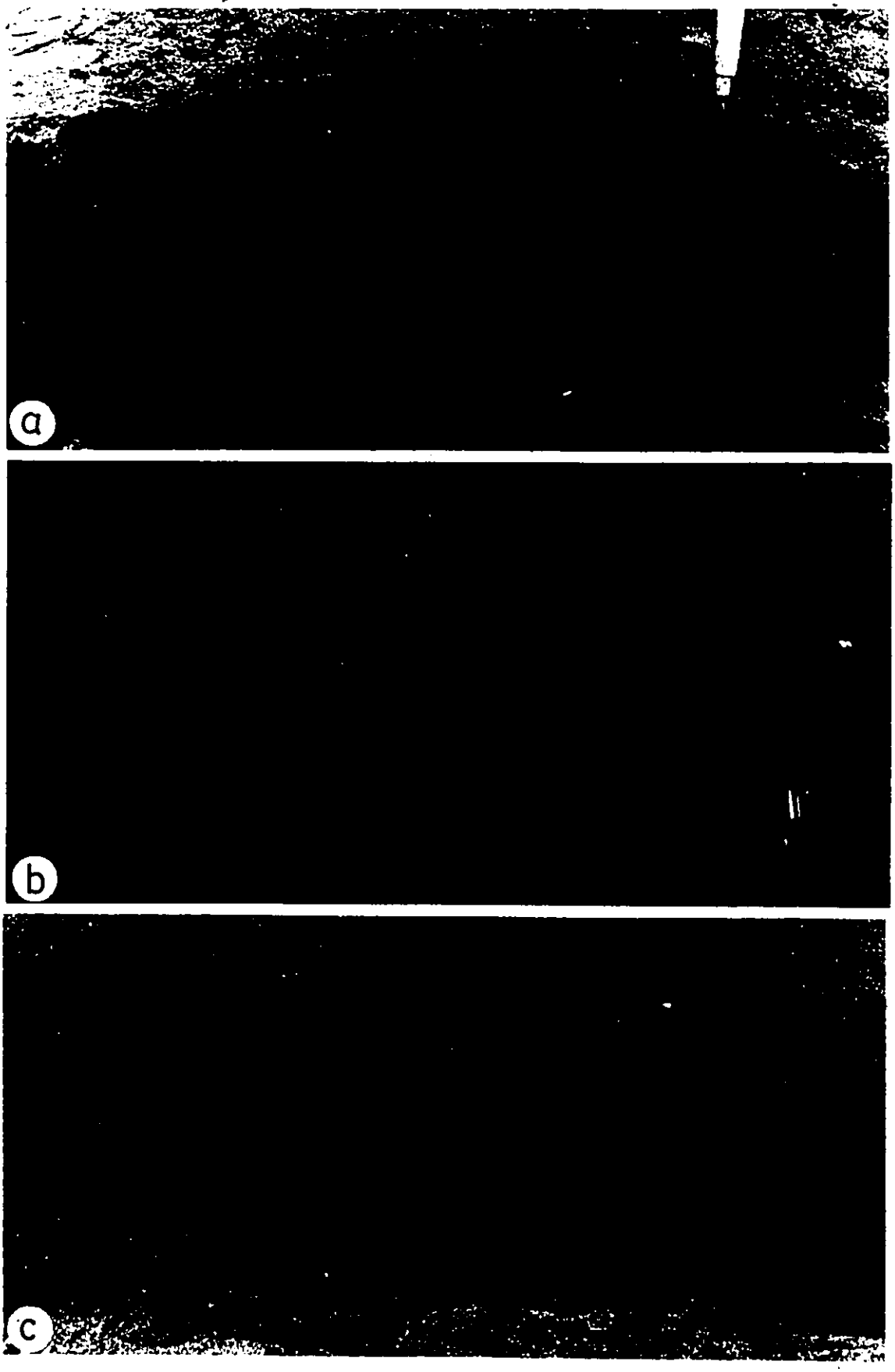
a
b
c

Figure IV-5A to IV-5H. Plots of average grain size versus distance above or below a fixed datum from thin sections cut from the Whirlpool Sandstone (Figs. IV-5A and IV-5B), from impregnated box cores from the Masstown sand flats (Figs. IV-5C and IV-5D), Mitchener Bar (Figs. IV-5E to IV-5G), and from the Shubenacedie River estuary (Fig. IV-5H). Textural units are defined as fining-upward (F.U.), coarsening-upward (C.U.) and ungraded or undeterminable (?). Lines were fitted by eye to sequences which appeared to make up distinct textural units. Error bars represent one standard deviation about the mean.

RM-01

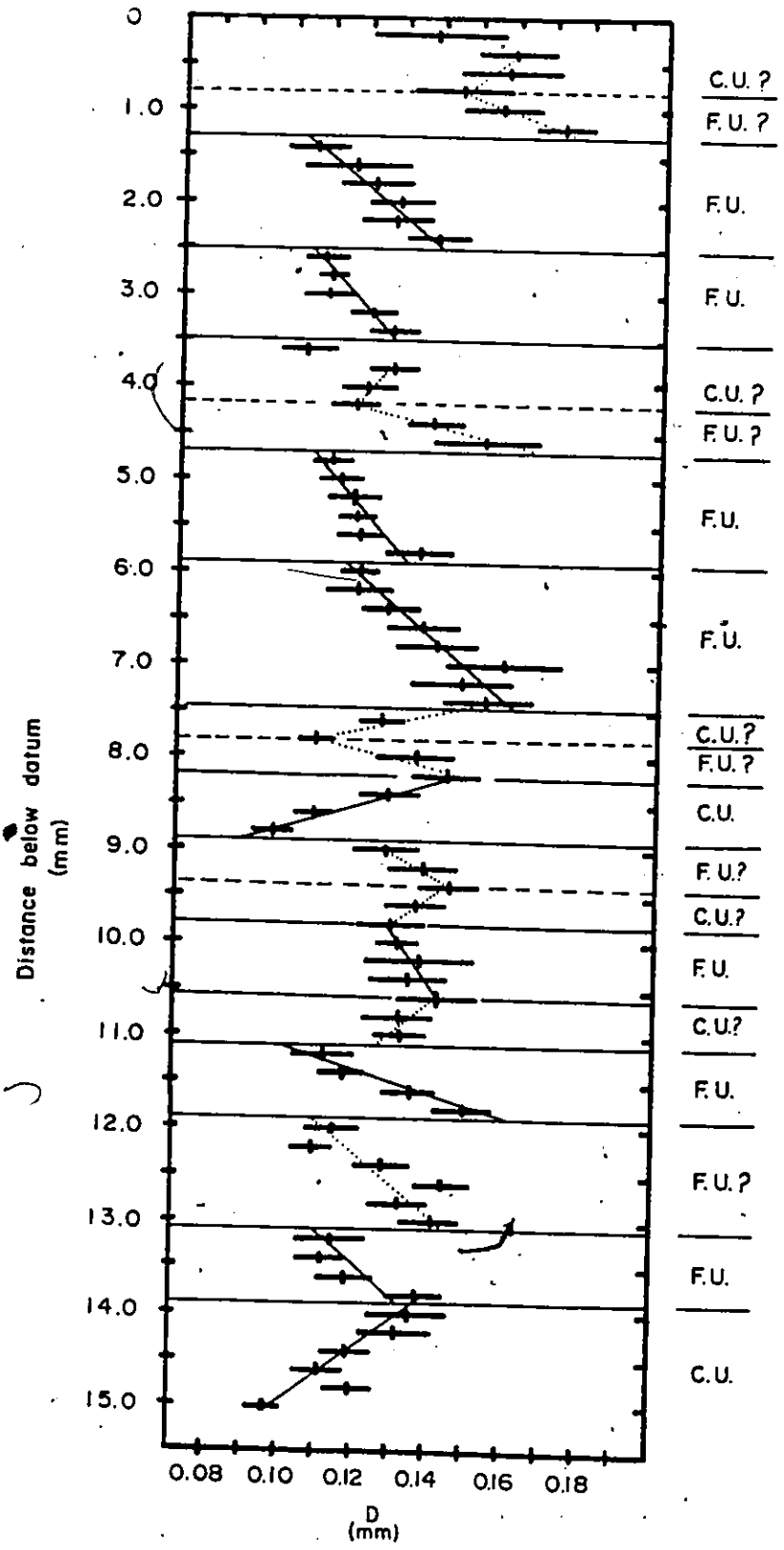
0
1.0
2.0
3.0
4.0
5.0
6.0
7.0
8.0
9.0
10.0
11.0
12.0
13.0
14.0
15.0
Distance below datum (mm)
0.08
0.10
0.12
0.14
0.16
0.18
D (mm)
C.U. ?
F.U. ?
F.U.
F.U.
C.U. ?
F.U. ?
F.U.
F.U.
C.U.?
F.U.?
C.U.
F.U.?
C.U.?
F.U.
C.U.?
F.U.
F.U.?
F.U.
C.U.

RM-05

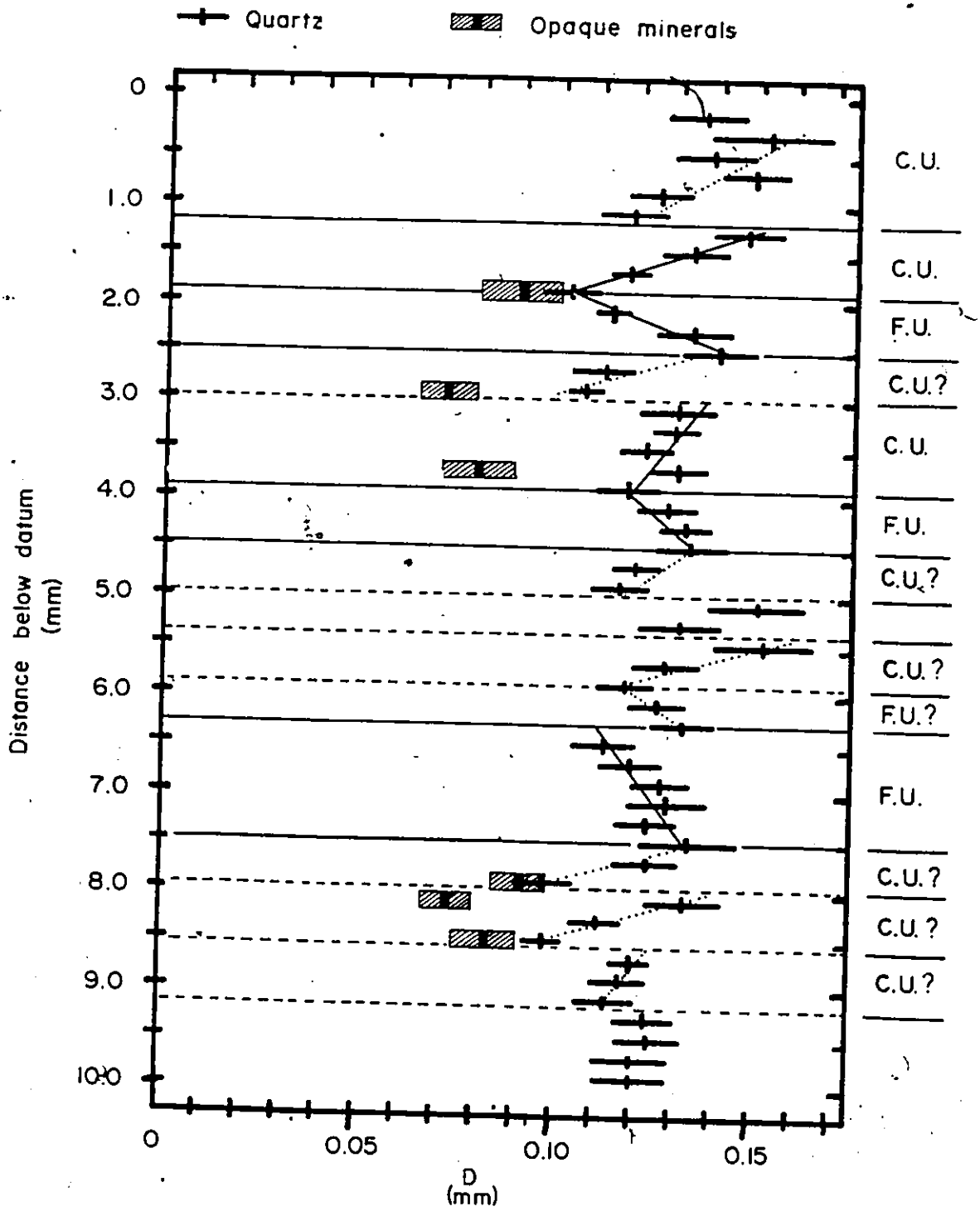
Quartz
Opaque minerals
Distance below datum (mm)
0
1.0
2.0
3.0
4.0
5.0
6.0
7.0
8.0
9.0
10.0
0
0.05
0.10
0.15
D (mm)
C.U.
C.U.
F.U.
C.U.?
C.U.
F.U.
C.U.?
C.U.?
F.U.?
F.U.
C.U.?
C.U.?
C.U.?

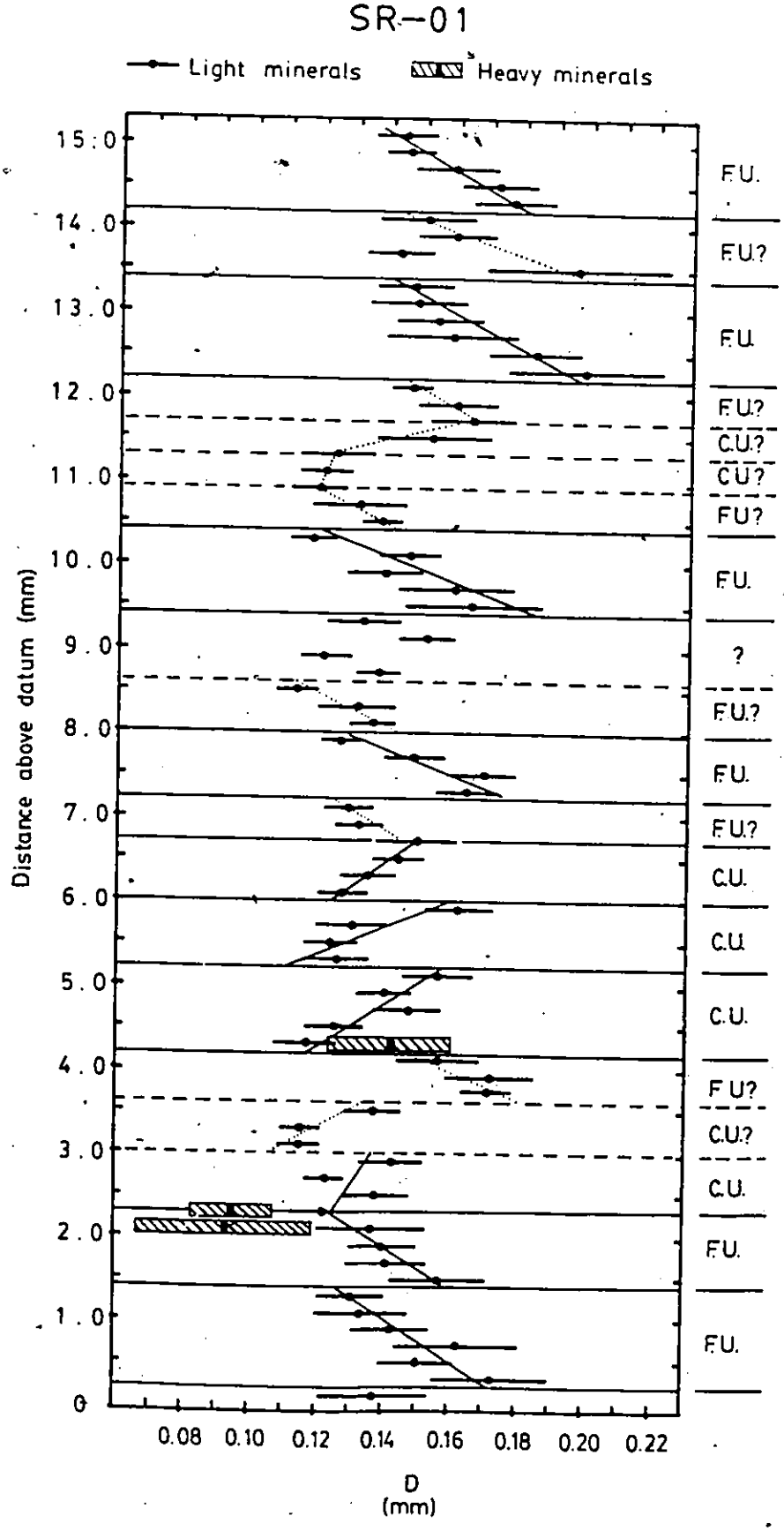
SR-01
Light minerals
Heavy minerals
Distance above datum (mm)
15.0
14.0
13.0
12.0
11.0
10.0
9.0
8.0
7.0
6.0
5.0
4.0
3.0
2.0
1.0
0
F.U.
F.U.?
F.U.
F.U.?
C.U.?
C.U.?
F.U.?
F.U.
?
F.U.?
F.U.
F.U.?
C.U.
C.U.
C.U.
F.U.?
C.U.?
C.U.
F.U.
F.U.
0.08
0.10
0.12
0.14
0.16
0.18
0.20
0.22
D
(mm)

SR–02

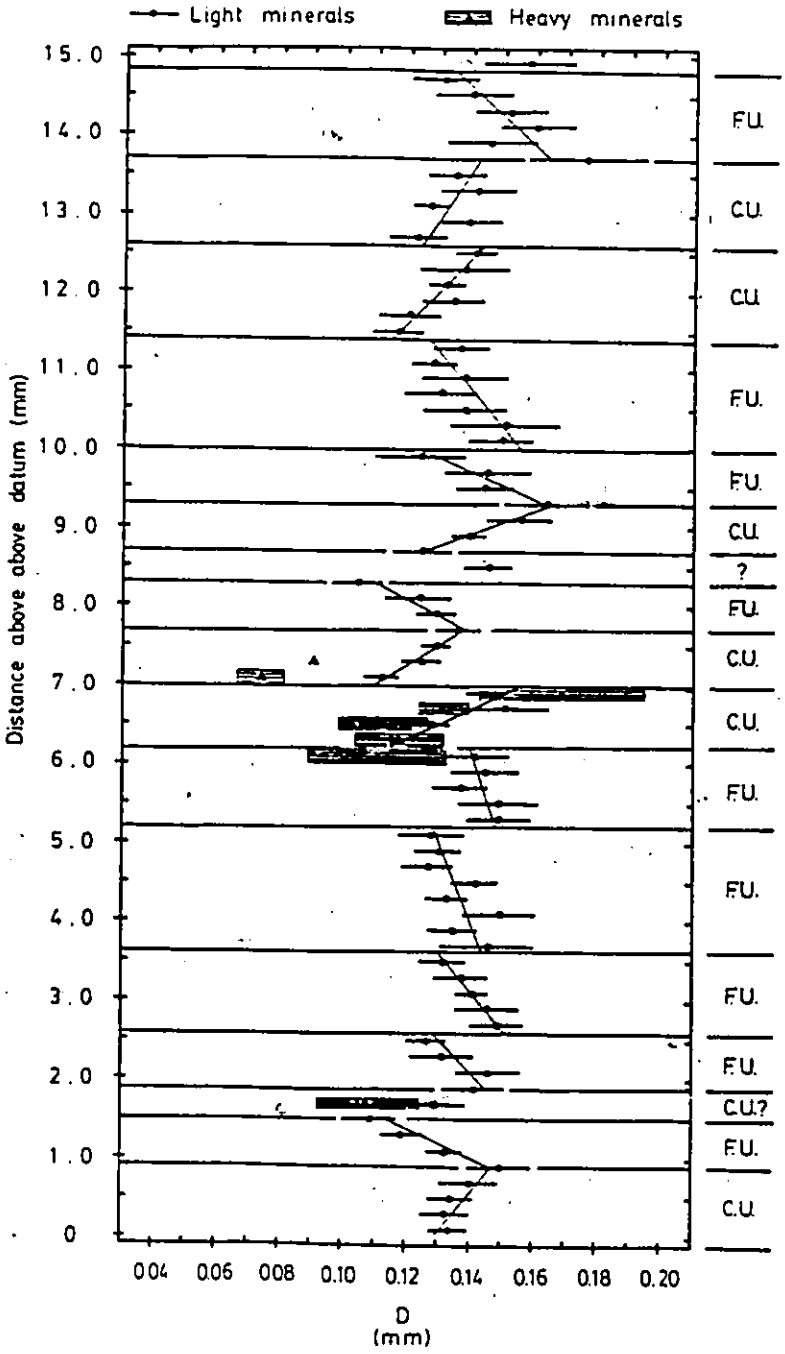
Light minerals
Heavy minerals
Distance above above datum (mm)
15.0
14.0
13.0
12.0
11.0
10.0
9.0
8.0
7.0
6.0
5.0
4.0
3.0
2.0
1.0
0
F.U.
C.U.
C.U.
F.U.
F.U.
C.U.
?
F.U.
C.U.
C.U.
F.U.
F.U.
F.U.
F.U.
C.U.?
F.U.
C.U.
0.04
0.06
0.08
0.10
0.12
0.14
0.16
0.18
0.20
D
(mm)

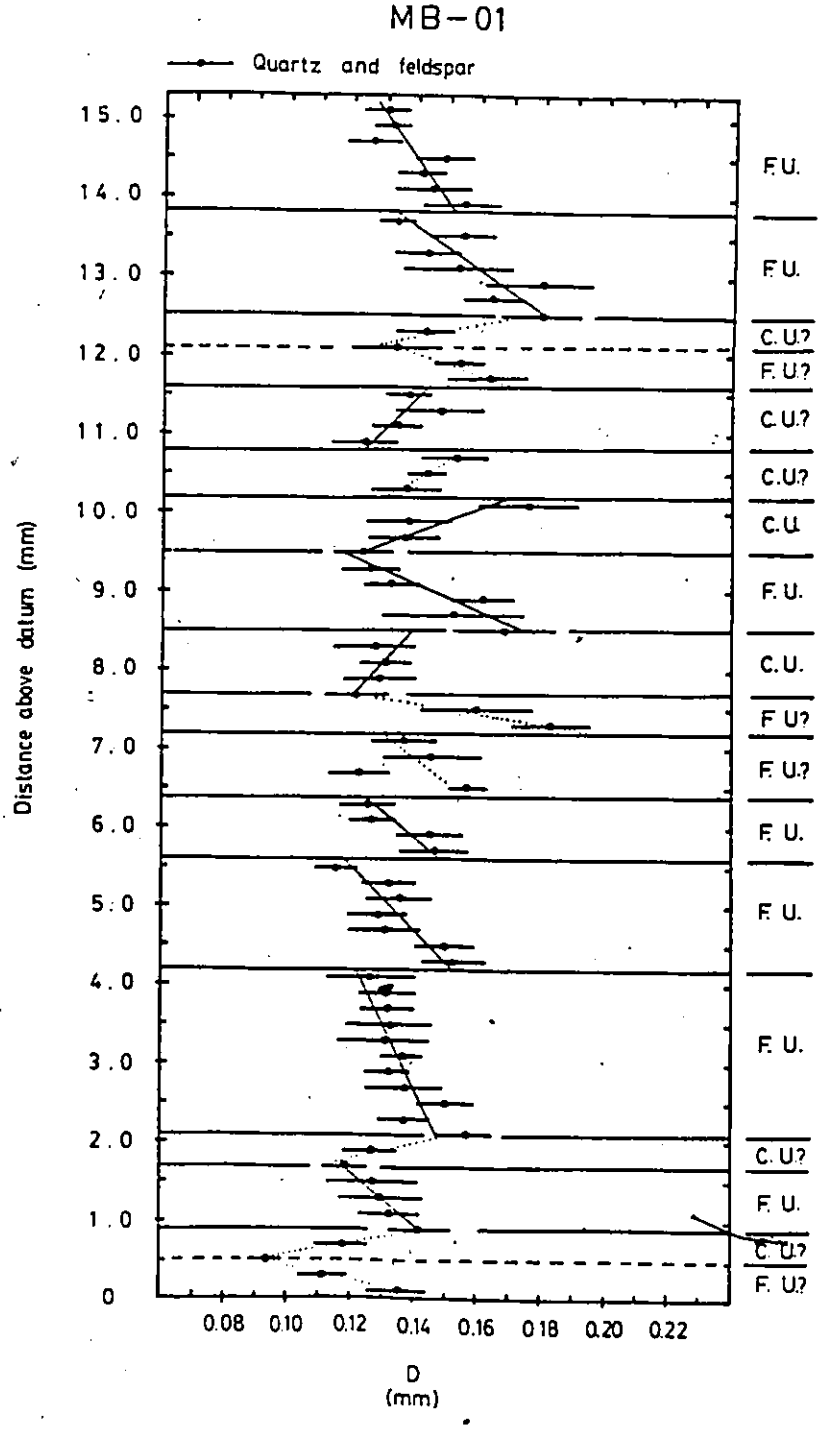
MB-01
Quartz and feldspar
Distance above datum (mm)
15.0
14.0
13.0
12.0
11.0
10.0
9.0
8.0
7.0
6.0
5.0
4.0
3.0
2.0
1.0
0
F.U.
F.U.
C.U.?
F.U.?
C.U.?
C.U.?
C.U.
F.U.
C.U.
F.U.?
F.U.?
F.U.
F.U.
F.U.
C.U.?
F.U.
C.U.?
F.U.?
0.08
0.10
0.12
0.14
0.16
0.18
0.20
0.22
D
(mm)

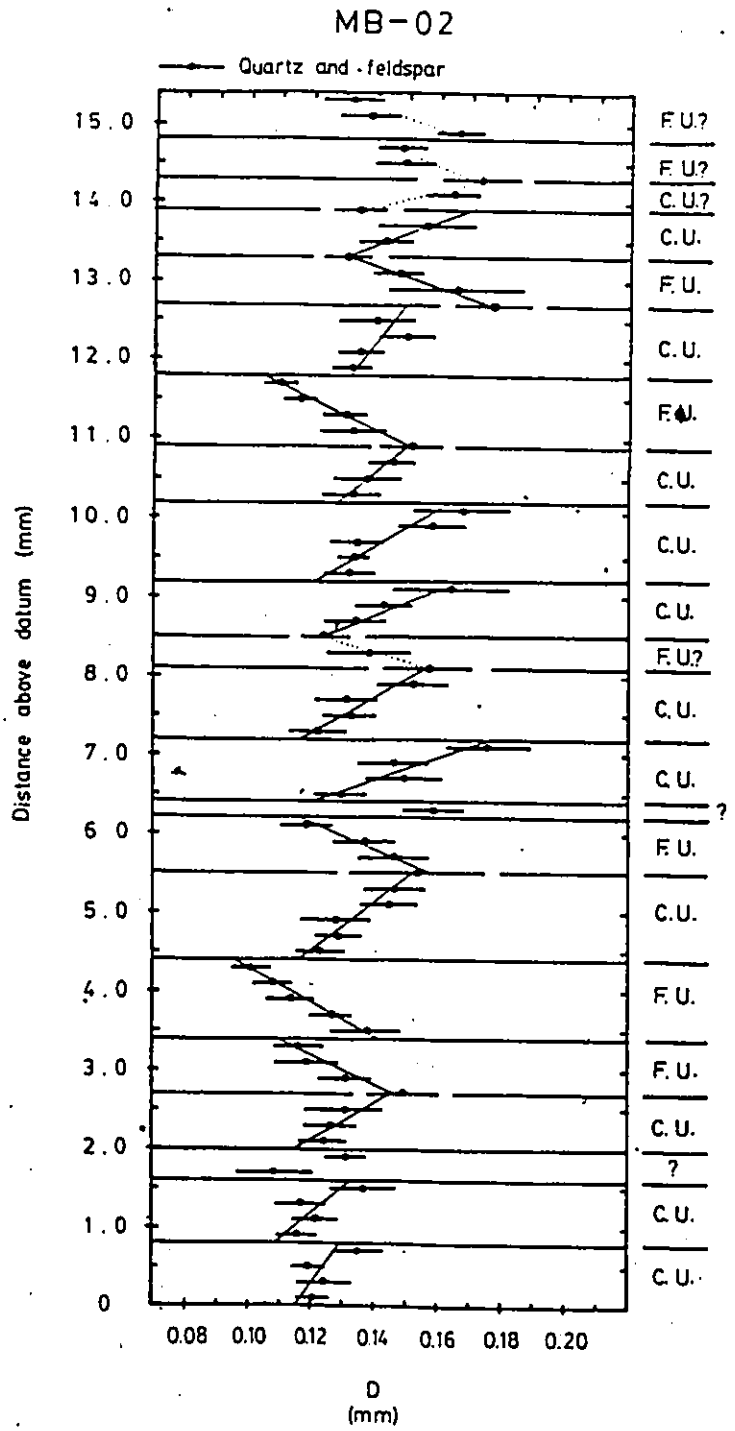
MB-02
Quartz and - feldspar
Distance above datum (mm)
15.0
14.0
13.0
12.0
11.0
10.0
9.0
8.0
7.0
6.0
5.0
4.0
3.0
2.0
1.0
0
0.08
0.10
0.12
0.14
0.16
0.18
0.20
D
(mm)
F.U.?
F.U.?
C.U.?
C.U.
F.U.
C.U.
F.U.
C.U.
C.U.
C.U.
F.U.?
C.U.
C.U.
?
F.U.
C.U.
F.U.
F.U.
C.U.
?
C.U.
C.U.

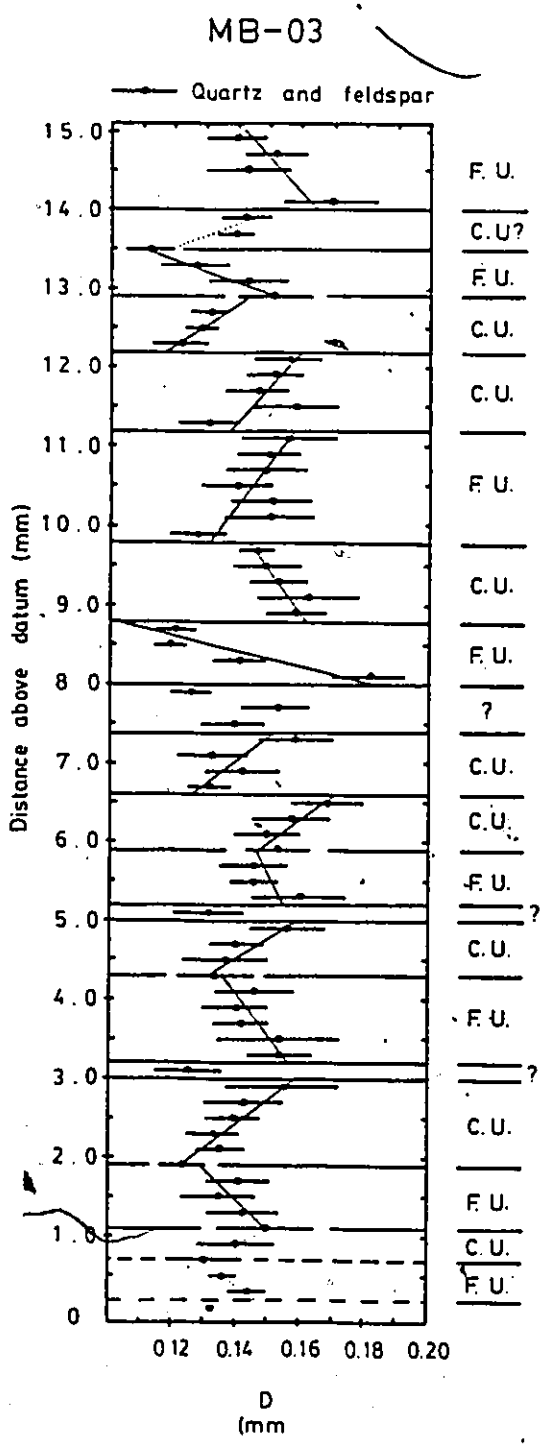
MB-03
Quartz and feldspar
Distance above datum (mm)
15.0
14.0
13.0
12.0
11.0
10.0
9.0
8 0
7.0
6.0
5.0
4.0
3.0
2.0
1.0
0
F. U.
C. U?
F. U.
C. U.
C. U.
F. U.
C. U.
F. U.
?
C. U.
C. U.
F. U.
?
C. U.
F. U.
?
C. U.
F. U.
C. U.
F. U.
0 12
0.14
0.16
0.18
0.20
D
(mm

ShR–01

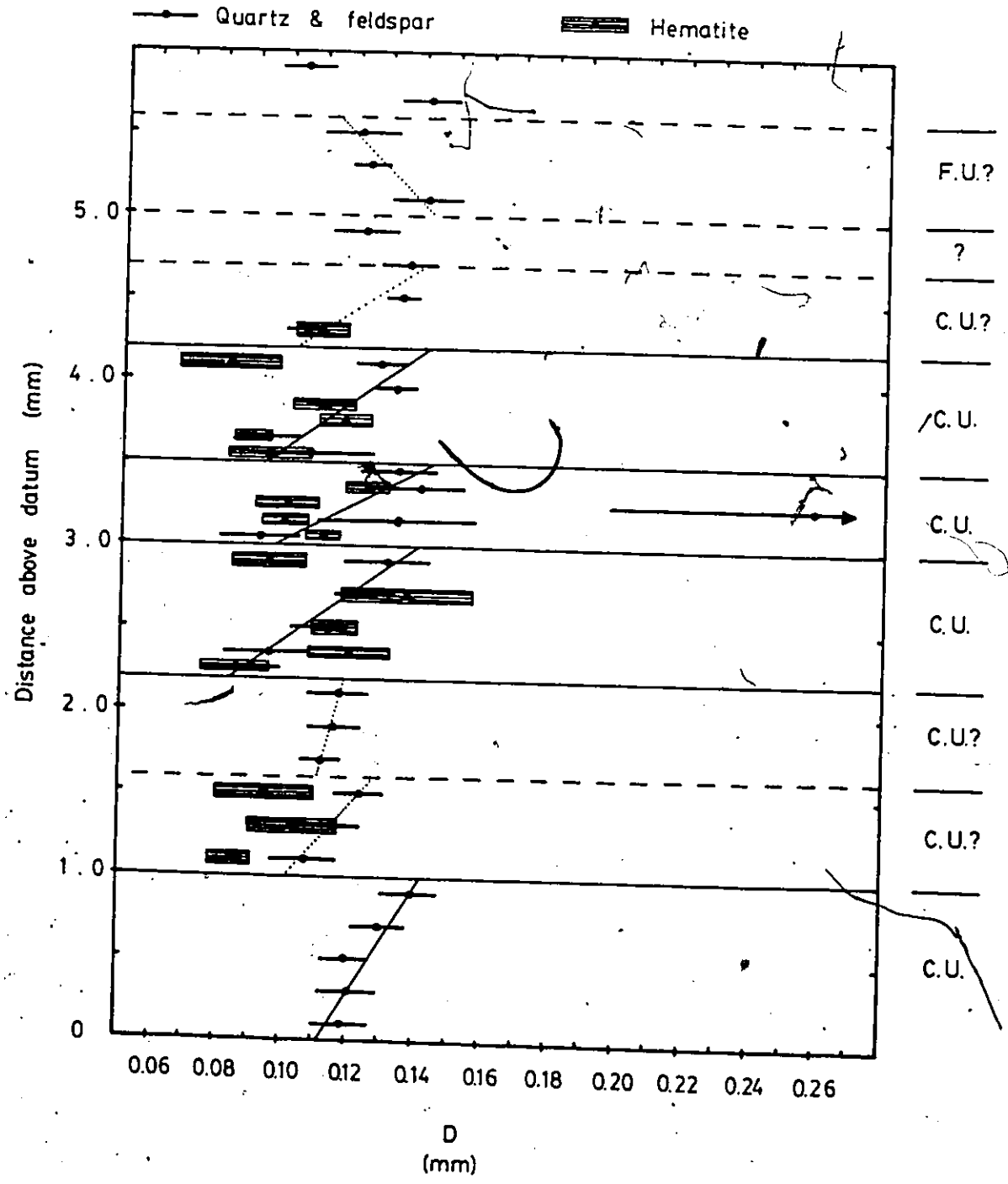
Quartz & feldspar
Hematite
Distance above datum (mm)
5.0
4.0
3.0
2.0
1.0
0
0.06
0.08
0.10
0.12
0.14
0.16
0.18
0.20
0.22
0.24
0.26
D
(mm)
F.U.?
?
C.U.?
/C.U.
C.U.
C.U.
C.U.?
C.U.?
C.U.

Table IV-1. Summary of laminae abundance and thickness.

	F.U.			C.U.			?		
Sample	N	$\bar{T}h$ (mm)	S/ N (mm)	N	$\bar{T}h$ (mm)	S/ N (mm)	N	$\bar{T}h$ (mm)	$S/\sqrt{N}$ (mm)
RM-01	12	0.87	0.10	7	0.66	0.13	1	0.20	
RM-05	4	0.70	0.17	9	0.65	0.07	2	0.76	0.36
SR-01	12	0.77	0.07	7	0.66	0.09	1	0.80	
SR-02	9	0.97	0.12	7	0.82	0.11	1	0.40	
MB-01	11	1.00	0.16	7	0.59	0.07	0		
MB-02	8	0.69	0.07	12	0.79	0.05	2	0.30	0.10
MB-03	8	0.86	0.10	9	0.77	0.08	3	0.33	0.13
ShR-01	1	0.60		7	0.67	0.07	1	0.30	
Total	65	0.85	0.04	65	0.71	0.03	11	0.50	0.11

are generally thinner than the graded laminae. There is no significant difference in laminae thickness between the four sets of samples.

To determine if the laminae occur in stacks of similar type, transition-difference matrices (Table IV-2) were constructed following the method of Miall (1973) for the case where transitions between like units are possible. Each matrix in Table IV-2 shows the difference between the observed frequency of transitions and the frequency if the transitions were strictly random. (Positive values indicate more frequent than random transitions and negative values are less frequent than random transitions.) Chi-square tests on the data (Harbaugh and Bonham-Carter, 1970) show that the transitions are independant (i.e., laminae are in random sequence at the 0.005 significance level).

A non-random feature of the data shown in figures IV-5A to H is the distribution of heavy minerals in the laminae. Opaque heavy minerals were present in 35 of the measured units in samples RM-05, SR-01, SR-02 and ShR-01, in a total of 18 laminae. Table IV-3 summarizes the location, size relationships between light and heavy minerals, and the number of grains of each mineral type in the measured units. A striking feature of the data in Table IV-3 is that 33 of the 35 units in which opaque heavy minerals occur are in coarsening-upward laminae. Where several measured units in a single coarsening-upward lamina contain heavy minerals the

Table IV-2. Transition difference matrices for textural sequences.

R.M. Samples (32 transitions)

Underlying \ Overlying	F.U.	C.U.	?
F.U.	-0.10	0.12	
C.U.	0.18	-0.23	0.04
?		0.56	

S.R. Samples (34 transitions)

Underlying \ Overlying	F.U.	C.U.	?
F.U.	0.05	-0.05	
C.U.	-0.02	0.08	0.05
?	-0.06	0.12	

M.B. Samples (56 transitions)

Underlying \ Overlying	F.U.	C.U.	?
F.U.	-0.15	0.24	-0.03
C.U.	0.09	-0.14	0.07
?	0.15	-0.06	

All samples. (123 transitions)

Underlying \ Overlying	F.U.	C.U.	?
F.U.	-0.08	0.09	-0.02
C.U.	0.08	-0.11	0.03
?	-0.06	0.12	

Table IV-3. Summary of textural data for laminae with heavy minerals.

Sample No.	Level	F.U. or C.U.	D (mm) Light	D (mm) Heavy	D_H/D_L	N Light	N Heavy
RM-05	8.5	C.U.	0.0977 ± 0.0049	0.0833 ± 0.0084	0.8526	31	6
	8.1	C.U.	0.1329 ± 0.0095	0.0733 ± 0.0067	0.5515	14	6
	7.9	C.U.	0.0973 ± 0.0071	0.0918 ± 0.0092	0.9435	22	11
	3.7	C.U.	0.1306 ± 0.0070	0.0800 ± 0.0091	0.6126	16	4
	2.9	C.U.	0.1063 ± 0.0050	0.0720 ± 0.0073	0.6773	24	5
	1.9	C.U.*	0.1026 ± 0.0073	0.0900 ± 0.0103	0.8772	27	6
SR-01	2.1	F.U.**	0.1361 ± 0.0161	0.0927 ± 0.0264	0.6811	21	3
	2.3	C.U.*	0.1220 ± 0.0102	0.0950 ± 0.0123	0.7787	24	5
	4.3	C.U.*	0.1164 ± 0.0095	0.1418 ± 0.0183	1.2182	21	3
SR-02	1.7	C.U.	0.1292 ± 0.0096	0.1082 ± 0.0158	0.8375	18	4
	6.1	F.U.**	0.1413 ± 0.0105	0.1108 ± 0.0151	0.7841	14	2
	6.3	C.U.	0.1149 ± 0.0065	0.1175 ± 0.0137	1.0226	20	4
	6.5	C.U.	0.1274 ± 0.0056	0.1123 ± 0.0137	0.8815	16	6
	6.7	C.U.	0.1507 ± 0.0140	0.1311 ± 0.0080	0.8699	11	4
	6.9	C.U.	0.1443 ± 0.0067	0.1689 ± 0.0267	1.1705	16	4
	7.1	C.U.	0.1119 ± 0.0055	0.0742 ± 0.0074	0.6631	24	2
	7.3	C.U.	0.1246 ± 0.0061	0.0904 ± 0.0013	0.7255	18	2

*Heavy minerals at the base of a coarsening upwards unit or at the top of a fining upwards unit.
**Heavy minerals are near the top of a fining upwards unit but may actually be associated with an overlying coarsening upward unit.

Table IV-3, continued.

Sample No.	Level	F.U. or C.U..	D (mm) Light	Heavy	D_H/D_L	N Light	Heavy
ShR-01	1.1	C.U.	0.1070 ± 0.0102	0.0849 ± 0.0063	0.7935	15	13
	1.3	C.U.	0.1116 ± 0.0087	0.1033 ± 0.0135	0.9256	17	8
	1.5	C.U.	0.1235 ± 0.0077	0.0950 ± 0.0147	0.7692	14	4
	2.25	C.U.	0.0908 ± 0.0087	0.0853 ± 0.0107	0.9394	11	12
	2.35	C.U.	0.0954 ± 0.0137	0.1197 ± 0.0124	1.2547	5	10
	2.5	C.U.	0.1110 ± 0.0091	0.1151 ± 0.0069	1.0370	12	8
	2.7	C.U.	0.1243 ± 0.0094	0.1370 ± 0.0200	1.1022	12	8
	2.9	C.U.	0.1309 ± 0.0130	0.0956 ± 0.0113	0.7303	15	7
	3.05	C.U.	0.1112 ± 0.0192	0.1347 ± 0.0238	1.2113	13	3
	3.15	C.U.	0.1347 ± 0.0238	0.0998 ± 0.0069	0.7409	3	12
	3.25	C.U.	0.2590 ± 0.0616	0.1007 ± 0.0096	0.3888	3	10
	3.35	C.U.	0.1404 ± 0.0134	0.1249 ± 0.0068	0.8896	5	7
	3.55	C.U.	0.1067 ± 0.0195	0.0953 ± 0.0127	0.8932	3	4
	3.65	C.U.	0.0940 ± 0.0197	0.0898 ± 0.0059	0.9553	5	13
	3.75	C.U.		0.1176 ± 0.0079		0	16
	3.85	C.U.	0.1128 ± 0.0066	0.1110 ± 0.0094	0.9840	4	16
	4.1	C.U.	0.1226 ± 0.0076	0.0827 ± 0.0152	0.6746	13	3
	4.3	C.U.	0.1052 ± 0.1052	0.1101 ± 0.0081	1.0466	19	12

size of the heavy minerals also generally increases upwards (see Figs. IV-5 D and H). The two units which occur in fining-upwards laminae are in units immediately below the base of coarsening-upward laminae. Because of the arbitrary position of the units over which measurements were made there may be some overlap of laminae so that the heavy minerals in association with fining-upward laminae may actually be at the base of coarsening-upward laminae. Another notable feature of the data given in Table IV-3 is that while all of the heavy mineral sheets are prominent in thin section and in outcrop the concentration may be relatively small (as low as 1 opaque grain for 12 light grains in a measured unit). Over distances of greater than 2 mm in thin section the thinnest heavy mineral sheets appear as continuous rows of heavy mineral grains approximately one grain diameter thick (Fig. IV-6). The thickest heavy mineral sheet in sample RM-05 (at 7.9 mm and 8.1 mm in Fig. IV-5B and also shown as the second from the bottom heavy mineral sheets in both photographs in Fig. IV-6) is approximately three grain layers thick and contains secondary pyrite which contributes to its dark colour.

Lateral correlations of laminae in adjacent vertical sections through two samples are shown in figure IV-7 (sample MB-03) and figure IV-8 (sample RM-05). The former shows only laminae (i.e., there are no heavy mineral sheets present) while the latter includes the three uppermost heavy

Figure IV-6. Horizontally laminated sandstone from the Whirlpool Sandstone at the Rice and McHarg quarry as seen in sample RM-05. (a) Polished section, (b) thin section. Note that the top three heavy mineral sheets (arrowed) are also shown in the data in figure IV-8.

5 mm

5 mm

Figure IV-7. Lateral correlation diagram of laminae in sample MB-03. The figure is based on measured vertical sections 1 mm apart through a thin section cut from sample MB-03. The base of each vertical section was a line drawn parallel to the lamination as seen in thin section. The upper diagram shows the actual data and the correlation of boundaries between textural units. The lower diagram shows more clearly the distribution of types of laminae determined from the data.

MB-03

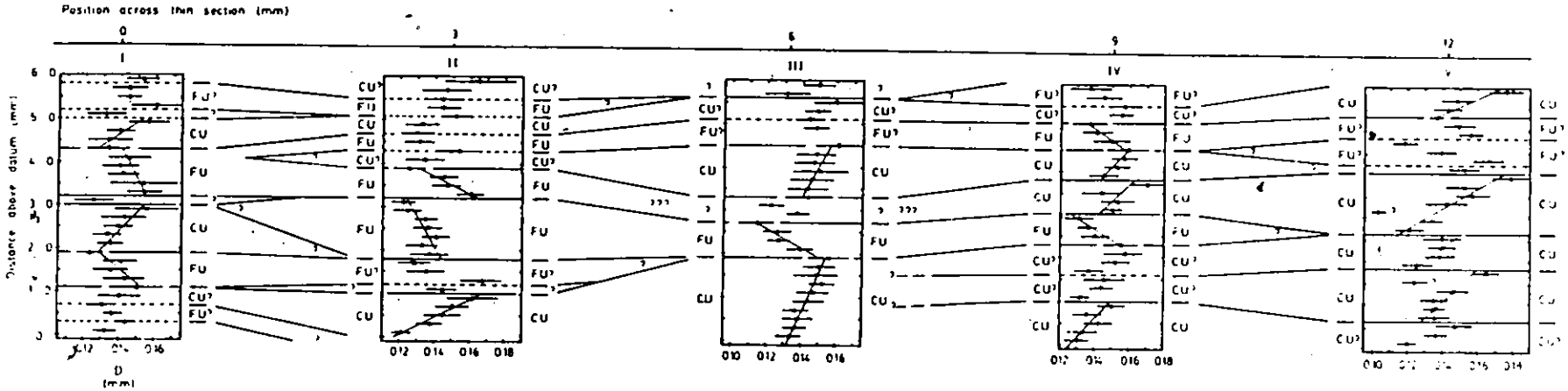

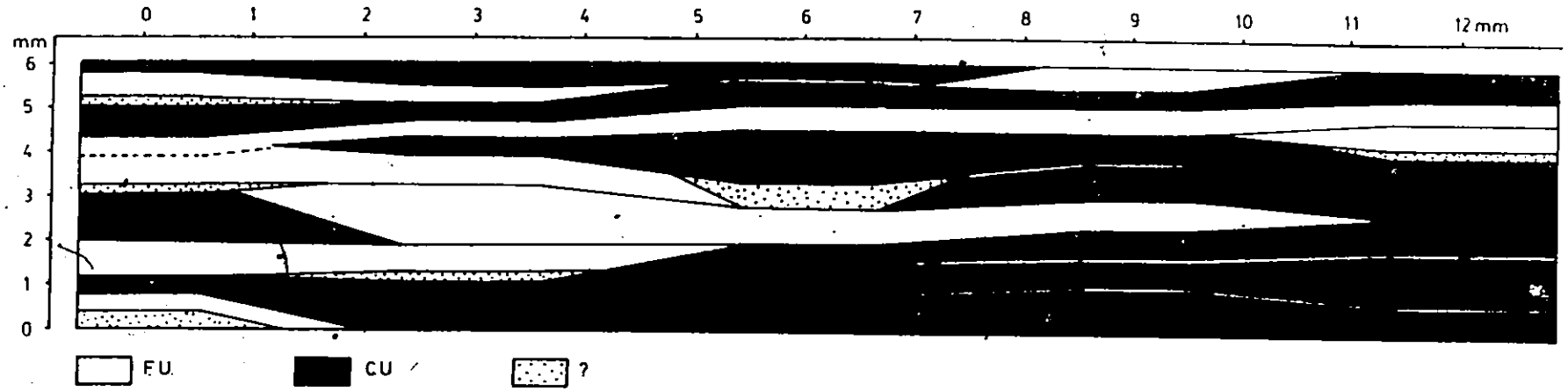

Horizontal exaggeration X3

Figure IV-8. Lateral correlation diagram of laminae in sample RM-05. This figure is similar to figure IV-7 but includes three heavy mineral sheets (also shown in figures IV-5B and IV-6).

RM-05

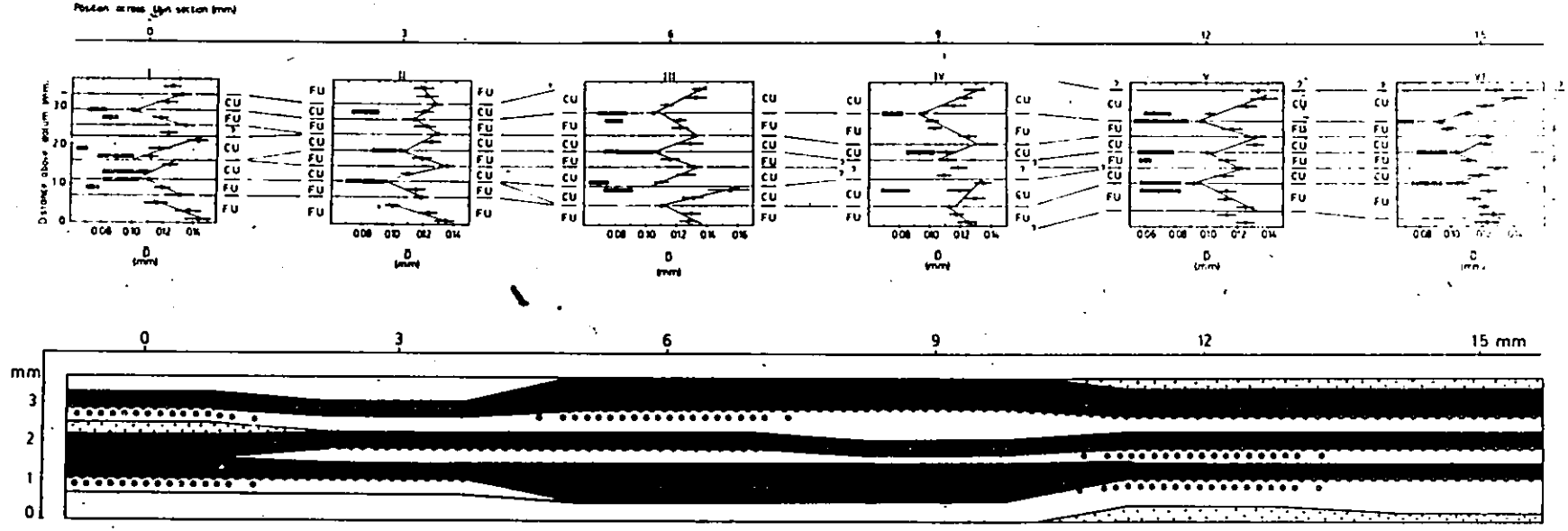

Horizontal exaggeration X 2

mineral sheets in figure IV-5B. In both figures laminae were correlated according to their position (i.e., if two textural units of the same type are present at approximately the same level in adjacent vertical sections it was assumed that they are laterally equivalent).

In figure IV-7 three laminae extend across the full 12 mm length over which the sections were measured, two are completely confined within that length and all of the other laminae terminate at one end within the measured area. The "pinching out" of laminae is reflected by a lateral thinning, in some cases over two adjacent vertical sections (i.e., the coarsening-upward lamination between 3.3 mm and 4.5 mm in section III and the fining-upward lamination between 1.9 mm and 2.7 mm in section III which thins somewhat to the right and thickens to the left and is truncated abruptly between sections I and II). Section III also contains a thick coarsening-upward lamination (from 0 to 1.9 mm on the vertical scale) which appears to be composed of three individual coarsening upward laminae which are distinct in sections IV and V. The thick lamination in section III may be broken up into three individuals, one between 0 and 0.5 mm, another between 0.7 mm and 1.3 mm and the third from 1.5 mm to 1.9 mm, the top of each being marked by a slight increase in the mean grain size between data points.

Laminae in figure IV-7 are generally thicker and

less laterally continuous than those in figure IV-8 where only four laminae terminate at one end over the length of measurement. The most notable feature of figure IV-8 is the position of the opaque heavy mineral sheets. Heavy minerals were present in 27 of the 0.2 mm by 2 mm areas over which measurements were made, 22 were in coarsening-upward laminae (13 at the base of coarsening-upward laminae) and 5 were in fining-upward laminae, just below the base of coarsening-upward laminae with heavy minerals. In general heavy minerals which are plotted in positions other than the base of coarsening-upward laminae do not occur at the same position (relative to the lamination) in adjacent vertical sections. This suggests that where heavy minerals occur above or below the bases of coarsening-upward laminae a single sheet of heavy minerals was incuded in two measured units while the sheet actually occured at the base of the coarsening-upward lamination. The exception to this distribution of heavy minerals occurs in the lowest heavy mineral sheet in vertical section IV which appears to cut across a coarsening-upward lamination. However, the criteria for defining laminae in each section do not allow for laminae to be represented by only two data points. Closer inspection of the data points which comprise the lowermost coarsening-upward lamination in vertical section IV suggests that it may represent the edges of two adjacent coarsening-upward laminae (explaining the shift to a finer

average grain size between 0.7 mm and 0.9 mm in the middle of the lamination). If this is the case the heavy mineral sheet is remaining at the base of two different coarsening-upward laminae and extends across the entire length over which measurements were made.

Both figures IV-7 and IV-8 contribute to the understanding of the significance of the undeterminable layers (labelled "?") in figures IV-5A to H. In figure IV-7, section III, the undeterminable layer between 3.0 mm and 3.3 mm occupies a position between fining-upward and coarsening-upward laminae which are pinching out. The data points in this layer may represent the thinnest edges of the laminae before they pinch out. However, because only two data points are involved the criteria for recognizing a textural trend are not satisfied so that the points are grouped into an undeterminable layer. A similar situation occurs in figure IV-8, section IV, with data points at 1.3mm, 1.5 mm and 1.7 mm. These are interpreted as representing the thinning of a coarsening-upward lamination which pinches out toward section V and the thinning of a fining-upward lamination which thickens in adjacent sections.

In summary, systematic vertical variation in the average grain size in contiguous 0.2 mm by 2 mm areas, measured from thin sections, have been recognized in

horizontally laminated sands and sandstones deposited under upper flow regime plane bed conditions. Individual textural units, generally less than 1 mm thick, may be fining-upward or coarsening-upward and are believed to be the textural expression of laminae. The samples studied indicate that fining-upward laminae are slightly thicker than coarsening-upward laminae and that the two laminae types alternate randomly in vertical sequence. Heavy minerals, in sheets, preferably occur in or make up coarsening-upward laminae. Correlation of laminae across thin sections show many laminae which pinch out laterally, at least at one end across the length over which measurements were made, suggesting that laminae have a lateral extent of only a few tens of millimetres. Heavy mineral sheets, on the other hand, appear to be more laterally extensive than individual laminae, as field observations suggest.

Experimentally Formed Horizontal Laminae

Methods

Box cores were collected from a sand bed which had been aggraded under upper flow regime plane bed conditions in the flume at the Geological Survey of Canada in Ottawa (Appendix II-B). The sand used in the flume was from a local sand and gravel pit into Late Quaternary deposits of distal interchannel facies of subaqueous outwash fans (Cheel, 1982). Figure IV-9 shows the size distribution of

Figure IV-9. Histogram showing the size distribution of light and heavy minerals in the bed material used in the flume experiments designed to produce horizontal laminae.

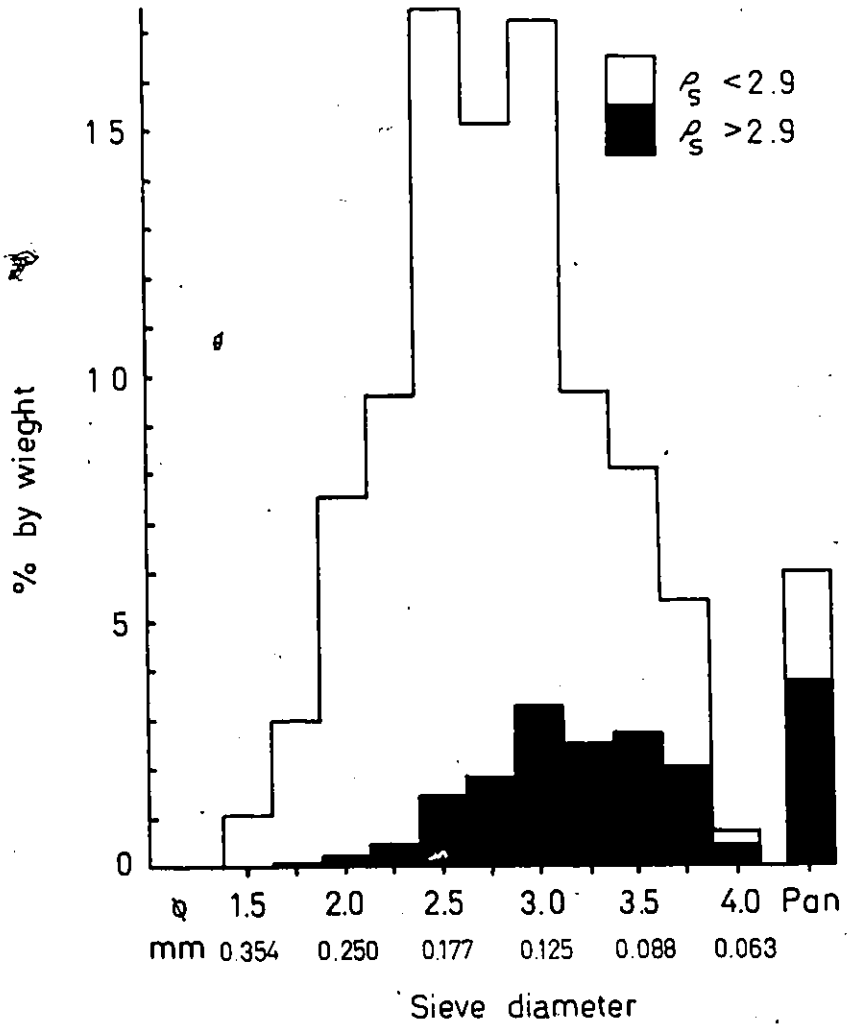
15
10
5
0
% by wieght
ρ_s <2.9
ρ_s >2.9
ø 1.5 2.0 2.5 3.0 3.5 4.0 Pan
mm 0.354 0.250 0.177 0.125 0.088 0.063
Sieve diameter

light minerals (ρ_s less than 2900 kg/m^3) and heavy minerals (ρ_s greater than 2900 kg/m^3). The distinction between light and heavy minerals is based on the method used for mineral separation (i.e., by floatation in tetrabromoethane, ρ= 2900 kg/m^3).

The first step during each flume run was to establish the desired flow depth by setting the tailgate at a suitable height so that the velocity through the channel (at that depth) allowed the development of a stable upper flow regime plane bed. The pitot tube was set at a fixed height above the bed and the velocity at that point was checked periodically to ensure that it was not changing with time. After approximately four hours a velocity profile was taken at 16 m from the entrance and a water surface profile was measured. The slope of the channel was then increased (by 0.00213) by means of electric screw jacks (changing the slope caused increased erosion at the upstream end of the channel and increased deposition downstream so that $\partial\tau_o/\partial x$ was negative along the channel). At 16 m from the entrance aggradation on the bed took place and the process was observed through the glass sidewall. The rate at which the bed aggraded was determined by marking the bed height (as seen through the sidewall) on a piece of paper which was taped to the glass wall, starting at the pre-aggradation bed height. In each run the bed appeared to aggrade vertically and bed waves were not observed. Box cores were collected

and prepared by the method described in Appendix II-C and the textural data derived in the manner described in the previous section of this chapter. The most abundant heavy minerals seen in thin section were measured, including magnetite and garnet which were recorded and plotted separately.

A major problem with the method of aggradation arose due to the acceleration of the flow with increased channel slope. Figures IV-10A to C show the velocity profiles taken for each flume run for which box cores were collected. Figure IV-10A (Run 5) includes both the pre-aggradation and post-aggradation velocity profiles and indicates that the average velocity (at y/d = 0.4) increased from 0.745 m/s to 0.847 m/s during aggradation. This increase is the result of a decrease in the flow depth (because discharge was constant) by approximately 1 cm at 16 m from the entrance (see Fig. IV-11 which shows bed and water surface profiles for the three flume runs). Velocity profiles for Runs 6 and 7 (Figs. IV-10B and C) do not include post-aggradational profiles because during aggradation the water depth decreased to the level where the water surface went below the tailgate. When this happened the pump was immediately shut down because the ensuing acceleration of the flow began to erode the aggraded bed. It was impossible, therefore, to take a post-aggradational velocity profile. However, during aggradation the pitot tube was left in the flow with the

Figure IV-10A to IV-10C. Velocity profiles from flume runs 5, 6 and 7. Note that pre-aggradational and post-aggradational velocities are shown.

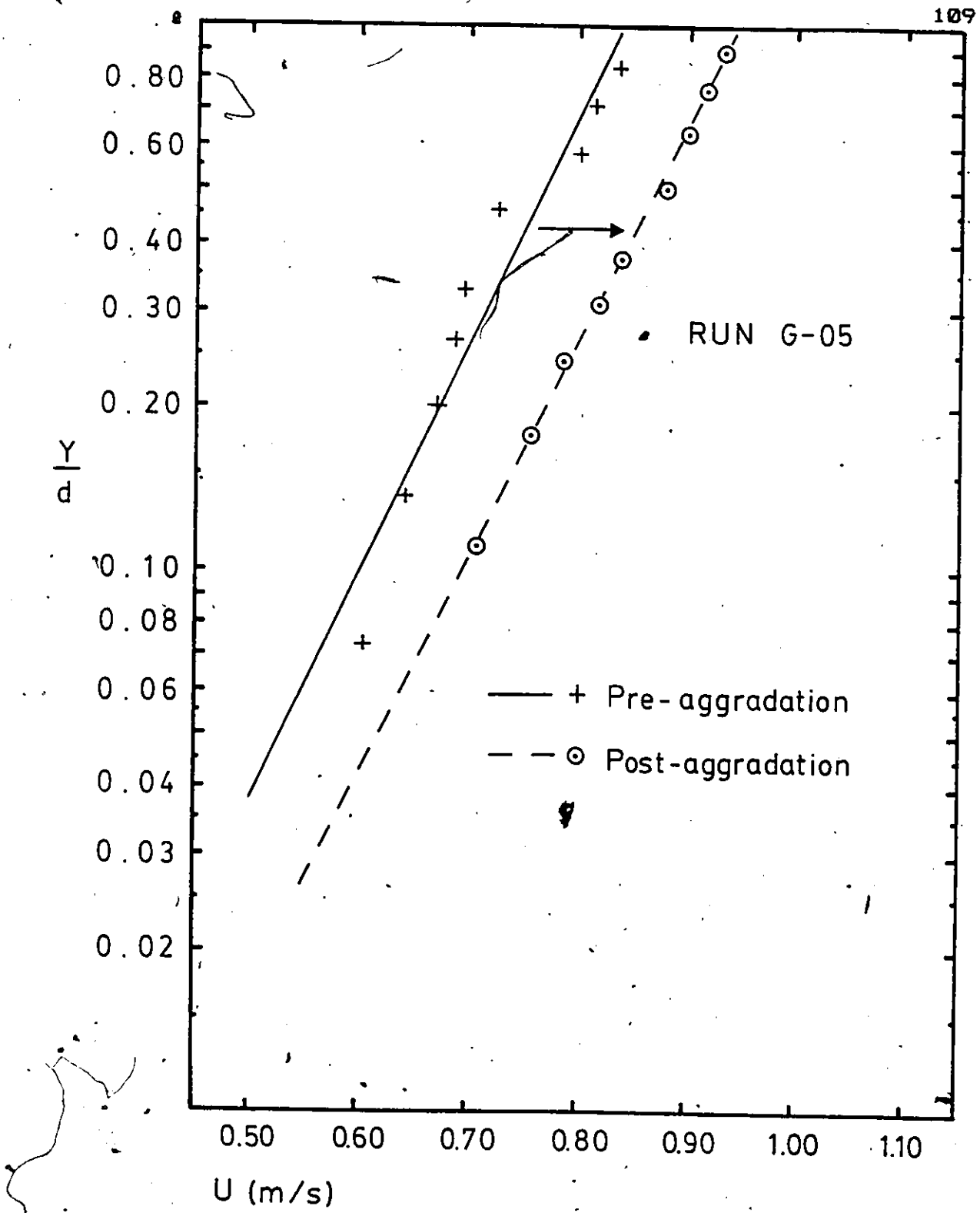
0.80
0.60
0.40
0.30
0.20
Y/d
0.10
0.08
0.06
0.04
0.03
0.02
RUN G-05
+ Pre-aggradation
⊙ Post-aggradation
0.50
0.60
0.70
0.80
0.90
1.00
1.10
U (m/s)

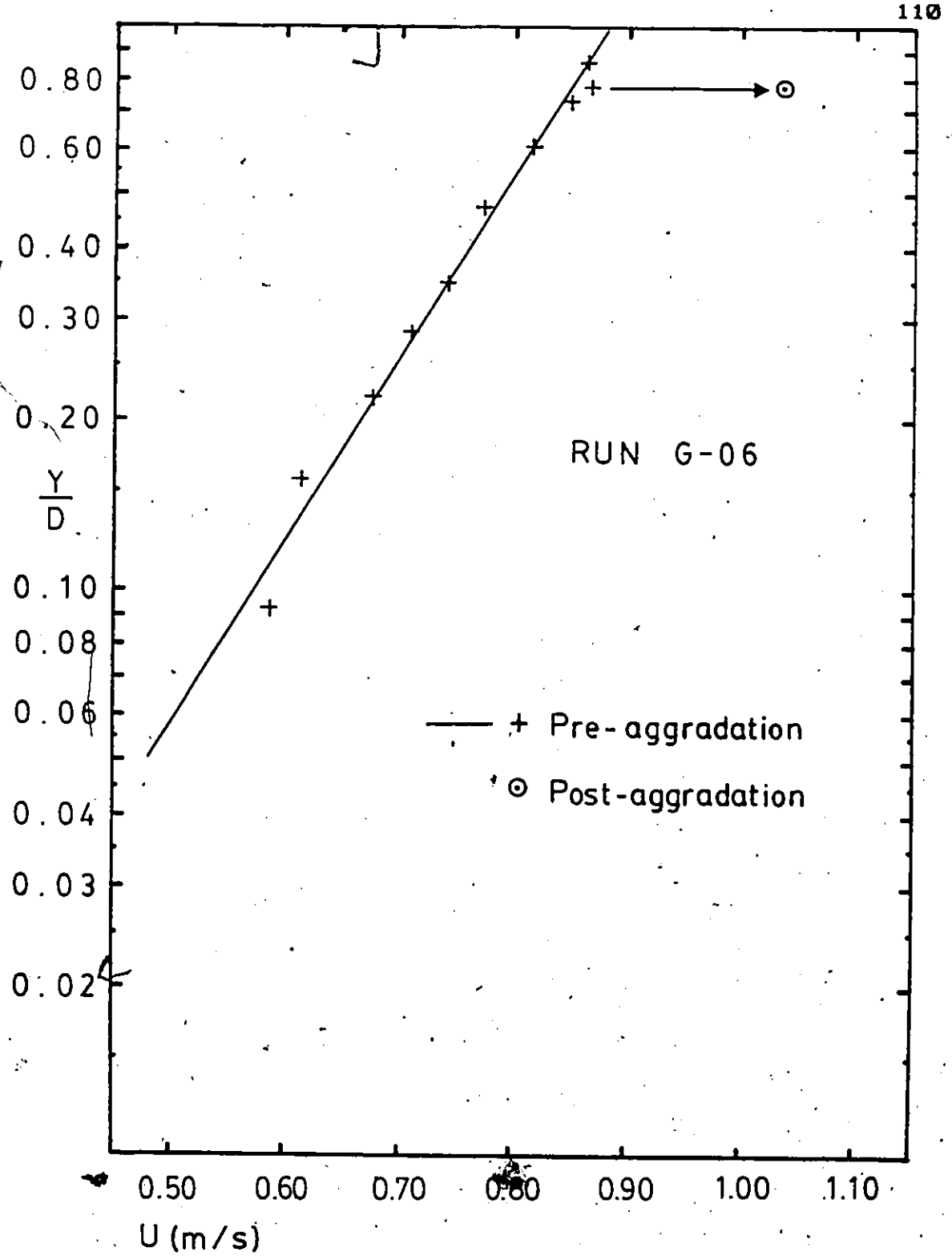
0.80
0.60
0.40
0.30
0.20
Y/D
0.10
0.08
0.06
0.04
0.03
0.02
RUN G-06
+ Pre-aggradation
⊙ Post-aggradation
0.50
0.60
0.70
0.80
0.90
1.00
1.10
U (m/s)

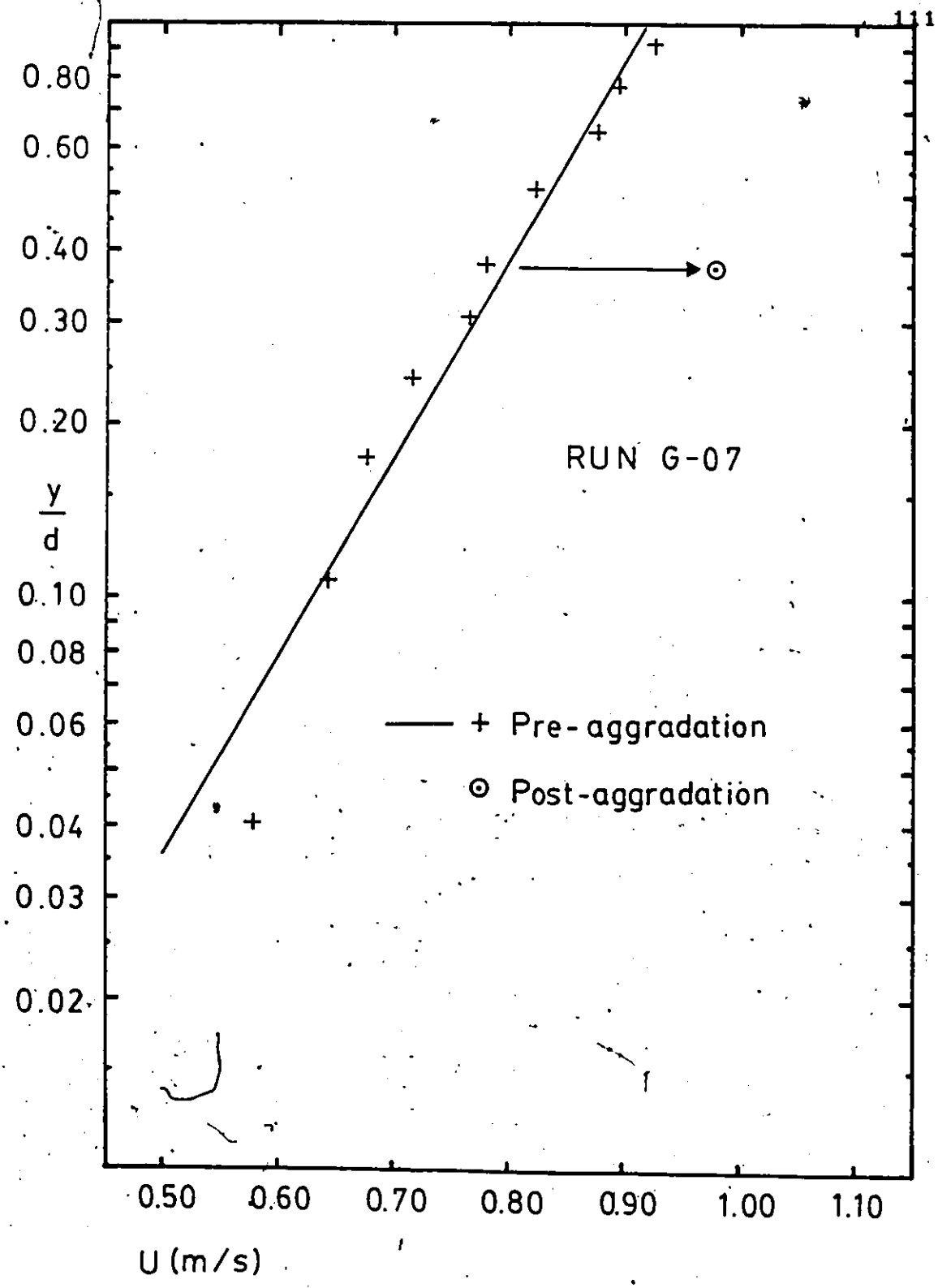
0.80
0.60
0.40
0.30
0.20
y/d
0.10
0.08
0.06
0.04
0.03
0.02
RUN G-07
+ Pre-aggradation
⊙ Post-aggradation
0.50
0.60
0.70
0.80
0.90
1.00
1.10
U (m/s)

Figure IV-11. Longitudinal profiles of pre-aggradation water surface and post-aggradation bed surface for flume runs 5, 6 and 7.

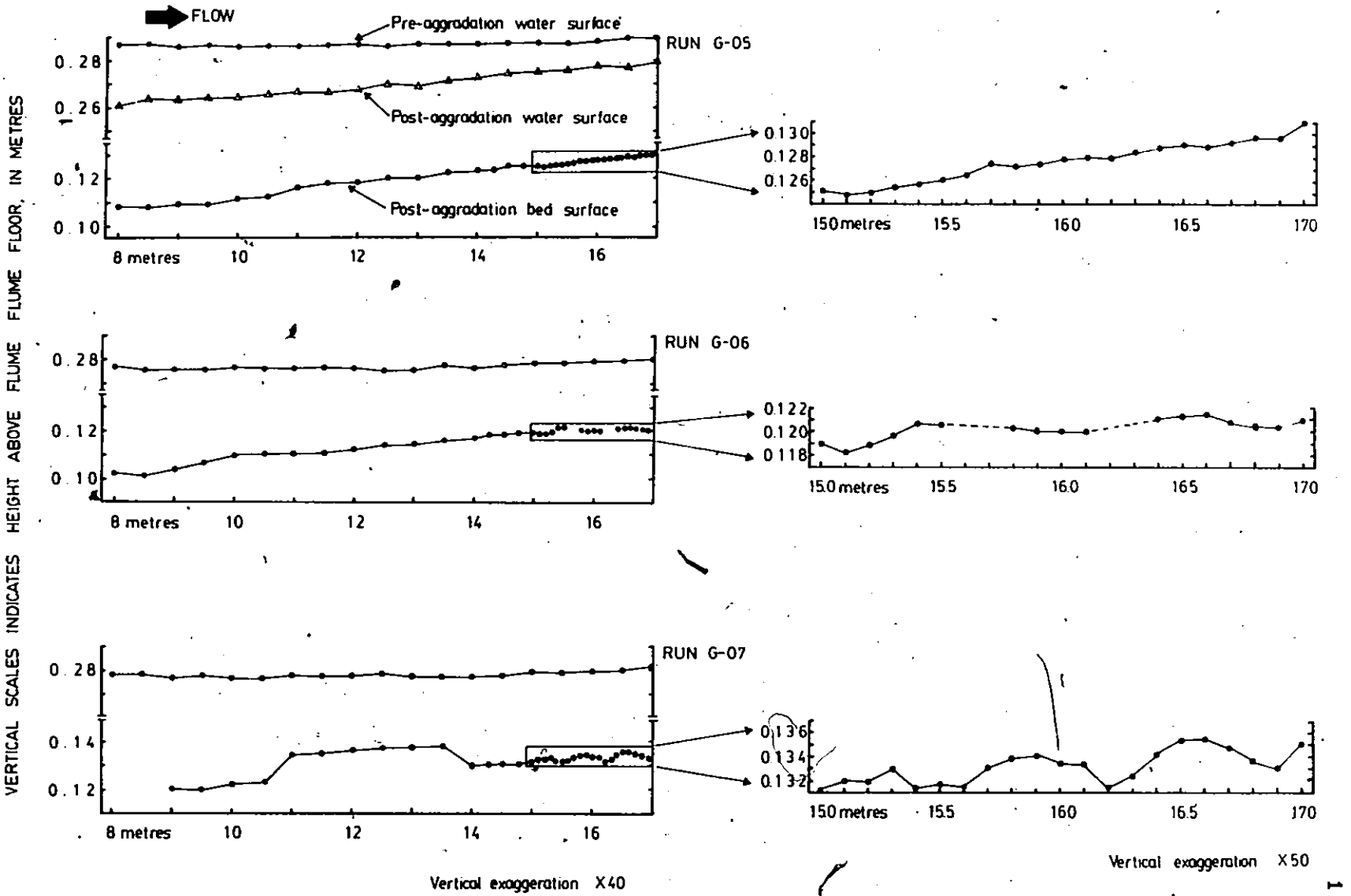
FLOW
Pre-aggradation water surface
Post-aggradation water surface
Post-aggradation bed surface
RUN G-05
RUN G-06
RUN G-07
VERTICAL SCALES INDICATES HEIGHT ABOVE FLUME FLUME FLOOR, IN METRES
0.28
0.26
0.12
0.10
0.14
8 metres
10
12
14
16
0.130
0.128
0.126
0.122
0.120
0.118
0.136
0.134
0.132
150 metres
155
160
165
170
Vertical exaggeration X40
Vertical exaggeration X50

chart recorder running so that the velocity increase was documented for one point at a fixed height above the bed. Figure IV-10B (Run 6) shows that during aggradation the flow velocity, at y/d=0.75, increased from 0.868 m/s to 1.36 m/s and figure IV-10C shows an increase in velocity from 0.800 m/s to 0.980 m/s, at y/d=0.375, during aggradation. Unfortunately it was not possible to complete further flume runs due to the breakdown of the pumping system.

Description of Horizontal Laminae

The flow data for Runs 5, 6, and 7 are summarized in table IV-4. Bed profiles for each run are shown in figure IV-11. Following Run 5 the bed was essentially flat at 16 m where the box core was collected. At the end of Runs 6 and 7, however, low waves were present on the bed. The waves on the bed of Run 6 had heights of less than 2 mm and lengths of approximately 0.9 m and probably formed in response to a water surface wave which was generated by the closing of the tailgate following the run. The bed waves of Run 7 were low symmetrical waves (2 mm to 6 mm high and 0.7 m long) and are probably low standing wave bedforms which developed during the brief period of rapid, relatively shallow flow just after the water surface fell below the tailgate.

Figures IV-12A to C are plots of average grain long axes versus height above a datum derived from thin sections cut from the box cores. Figure IV-12A bears the closest

IV-4. Summary of flow data from flume runs.

	Run 5	Run 6	Run 7
U (m/s)	0.745	0.759	0.800
d (m)	0.1595	0.1591	0.1456
U* (m/s)	0.0405	0.0538	0.0514
F	0.60	0.61	0.59
Rate of aggradation (mm/min)	0.67	0.50	0.59

Note: U* was calculated from the slope of the line through point velocities in figures IV-10A to C using the formula:

$$U^* = \frac{k(U_1 - U_2)}{2.3(\log y_1 - \log y_2)}$$

from Blatt, Middleton and Murray (1980, p. 113) where k is von Karman's constant and is assumed to be equal to 0.4. Rates of aggradation are averages calculated by dividing the total thickness of the aggraded portion of the bed by the time over which aggradation took place.

Figure IV-12A to IV-12C. Plots of average grain size versus distance above a fixed datum from thin sections cut from impregnated box cores of flume beds following runs 5, 6 and 7. Textural units are defined as fining-upward (F.U.), coarsening-upward (C.U.) and ungraded or undeterminable (?). Lines were fitted by eye to sequences which appeared to make up distinct textural units. Error bars represent one standard deviation about the mean.

RUN 5B

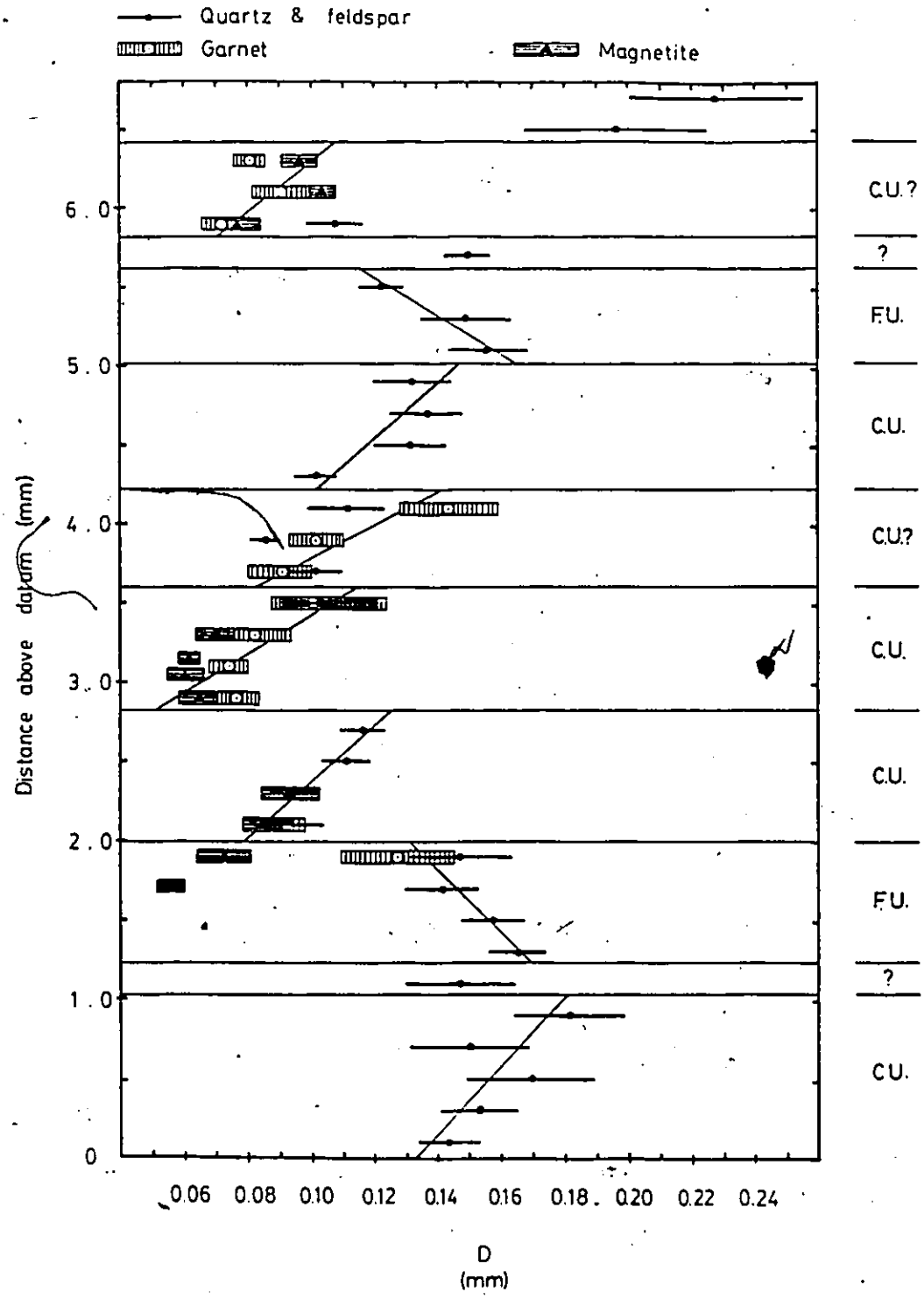
Quartz & feldspar
Garnet
Magnetite
C.U.?
?
F.U.
C.U.
C.U.?
C.U.
C.U.
F.U.
?
C.U.
6.0
5.0
4.0
3.0
2.0
1.0
0
Distance above datum (mm)
0.06
0.08
0.10
0.12
0.14
0.16
0.18
0.20
0.22
0.24
D
(mm)

RUN 6A

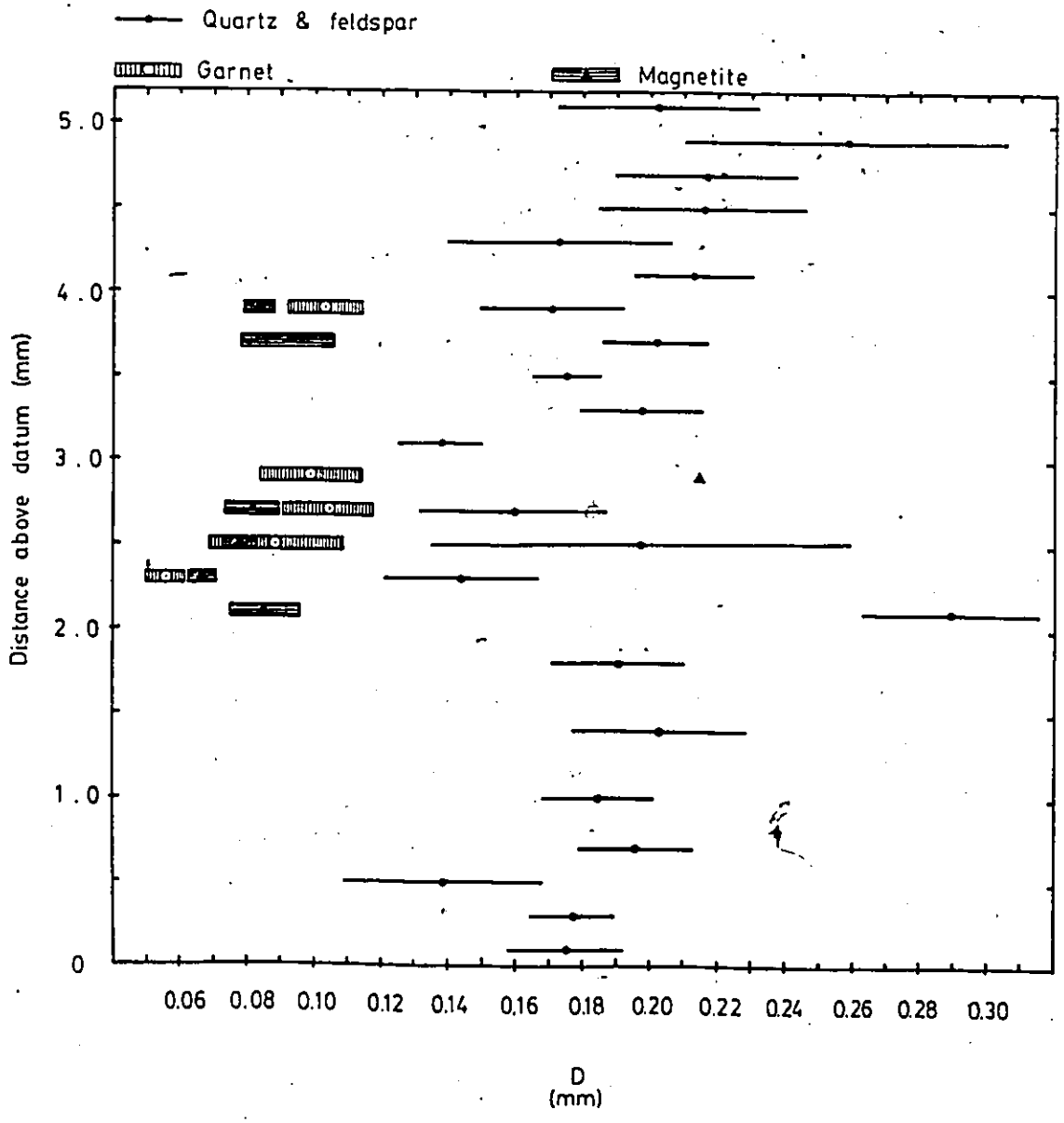
Quartz & feldspar
Garnet
Magnetite
Distance above datum (mm)
5.0
4.0
3.0
2.0
1.0
0
0.06
0.08
0.10
0.12
0.14
0.16
0.18
0.20
0.22
0.24
0.26
0.28
0.30
D
(mm)

RUN 7

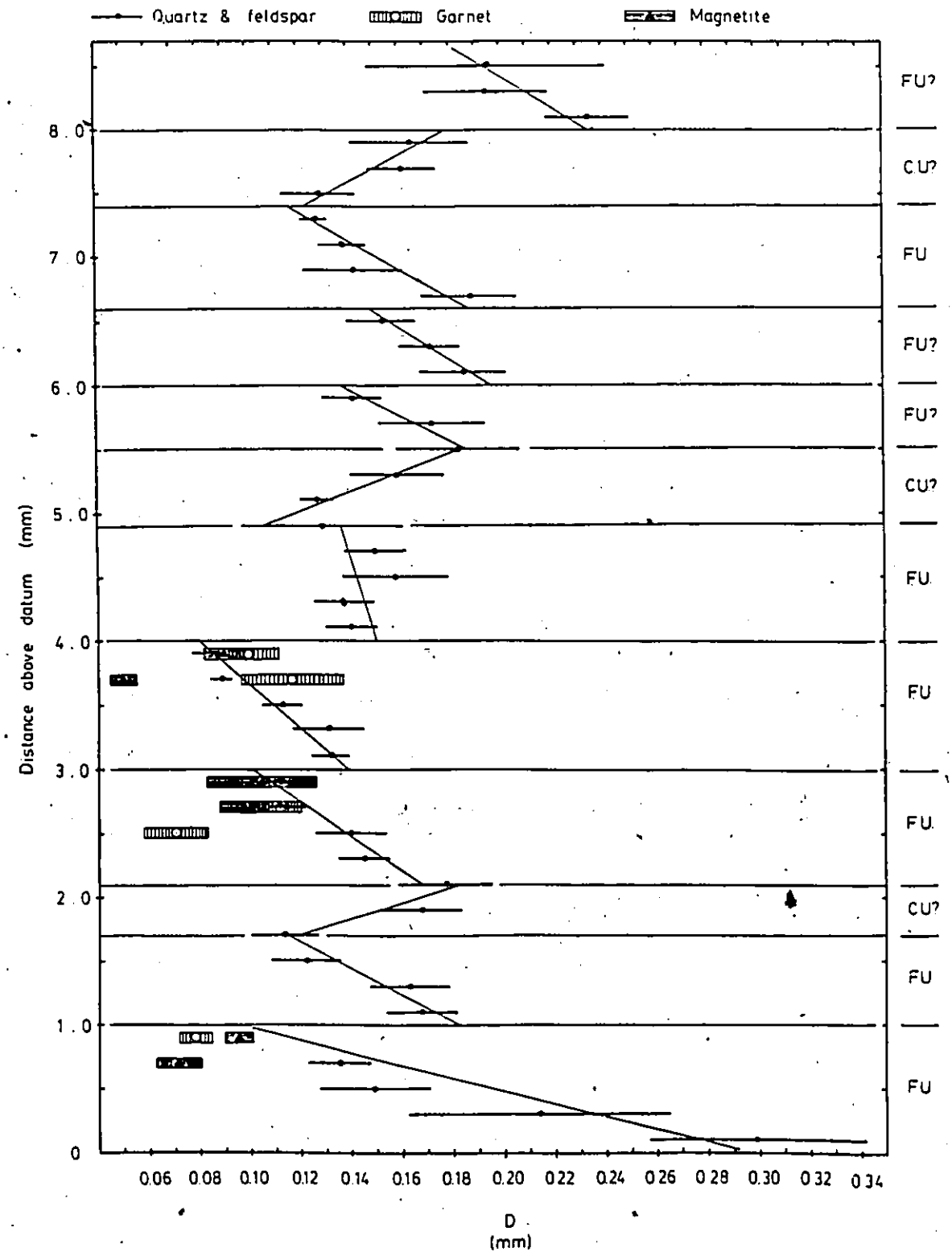
Quartz & feldspar
Garnet
Magnetite
FU?
CU?
FU
FU?
FU?
CU?
FU
FU
FU
CU?
FU
FU
8.0
7.0
6.0
5.0
4.0
3.0
2.0
1.0
0
Distance above datum (mm)
0.06 0.08 0.10 0.12 0.14 0.16 0.18 0.20 0.22 0.24 0.26 0.28 0.30 0.32 0.34
D (mm)

resemblance to figures IV-5A to H, containing both fining- and coarsening-upward laminae. Also, like the laminae described earlier, most of the heavy minerals are associated with (or comprise along with lighter minerals) coarsening-upward laminae. The only exception occurs in the fining-upward laminations from 1.2 mm to 2.0 mm where heavy minerals are present. However, the two units in which magnetite grains were measured fall on the line defining the coarsening-upward trend in the overlying laminae. The thicknesses of the laminae are also comparable to those described earlier with an average fining-upward thickness of 0.68±0.08 mm and an average coarsening upward laminae thickness of 0.78±0.06 mm. The coarsening-upward laminae are somewhat thicker and more abundant than the fining-upward laminae by a ratio of 3 to 1, although the sample size is too small to suggest that they are significantly different from the field examples.

Figure IV-12B (Run 6) does little more than illustrate a random distribution of mean long axis lengths with height above the datum. Lines showing trends were not drawn on this figure because of the randomness of the data. Figure IV-12C (Run 7), shows well developed laminae of comparable thickness to those described earlier (average fining-upward laminae thickness 0.78±0.06 mm; average coarsening-upward laminae thickness o.53±0.07 mm). The striking difference between this set of data and all other

data is that the heavy minerals are found in the upper portion of fining-upward laminae.

In the following discussion the data in figures IV-12B and IV-12C will not be considered because the textural units (or their absence) differs from all other examples in the thesis. The presence of low bedforms following these two runs probably caused these anomalous textural variations and suggest that the data are not relevant to the discussion of horizontal laminae formed on upper flow regime plane beds. The true plane bed of Run 5, however, preserved laminae which are almost identical to those described from the field examples. This supports the proposal that the textural and mineralogical characteristics of laminae described from the field examples, are typical of laminae formed by deposition on upper plane beds.

DISCUSSION

From the descriptions of textural variations in the deposits of upper flow regime plane beds two general types of horizontal structure were recognized: (1) "textural laminae" which are most commonly less than one millimetre thick and display either a fining-upward or coarsening-upward of average grain size within laminae, and (2) "heavy mineral sheets" which are layers of heavy minerals, one to several grain diameters thick, typically associated with textural laminae that are coarsening-upward. From the data presented it appears that both forms of textural laminae occur in approximately equal numbers although a single sample may be dominated by one or the other. On average, fining-upward laminae are slightly thicker than coarsening-upward laminae. In vertical sequence the types of textural laminae alternate randomly, rather than occuring in stacks of the same lamina type. Unfortunately the data are insufficient to discern variation in thickness, frequency, or vertical sequence of laminae due to properties of the depositing flow. In general, the characteristics of laminae appear to be similar in samples from the four different locations and one flume run.

Lateral correlation diagrams showing both types of laminae illustrate that textural laminae recognized in vertical sequence extend laterally across thin sections and in some cases pinch out over less than 10 mm (only the

lateral extent in the direction normal to flow has been documented in this thesis). Heavy mineral sheets, however, appear to be more continuous laterally, occupying a more-or-less horizontal position while, in one case in Fig. IV-8 possibly occuring in two different adjacent textural laminae. In the field it is the heavy mineral sheets which form the distinct horizontal layering while the textural laminae are responsible for the vague sense of horizontal layering where heavy minerals are absent. Figure IV-13 depicts the appearance of horizontal laminae which is suggested by this study.

With these new descriptions of horizontal laminae it is possible to test theories of laminae formation by their ability to explain the characteristics which have been recognized. The shortcomings of Pettijohn's (1957, 1975) "velocity fluctuation" theory have already been discussed. The Moss-Kuenen "like-seeks-like" theory and Jopling's "superposition of current lineation" theory both predict the formation of randomly alternating layers of grains of similar size, shape and density. These theories cannot explain the presence of fining-upward and coarsening-upward laminae which have been described here. The theory put forth by Frostick and Reid (1977), combines the velocity pulsation and like-seeks-like theories, specifically predicts the development of fining-upward laminae in which heavy minerals are concentrated at the top of each

Figure IV-13. A schematic illustration showing the characteristics of horizontal laminae which have been described in the thesis. (a) The overall distribution of fining- and coarsening-upward laminae with one heavy mineral sheet passing laterally from one laminae to another. (b) Specific textural variations within laminae as seen in thin section.

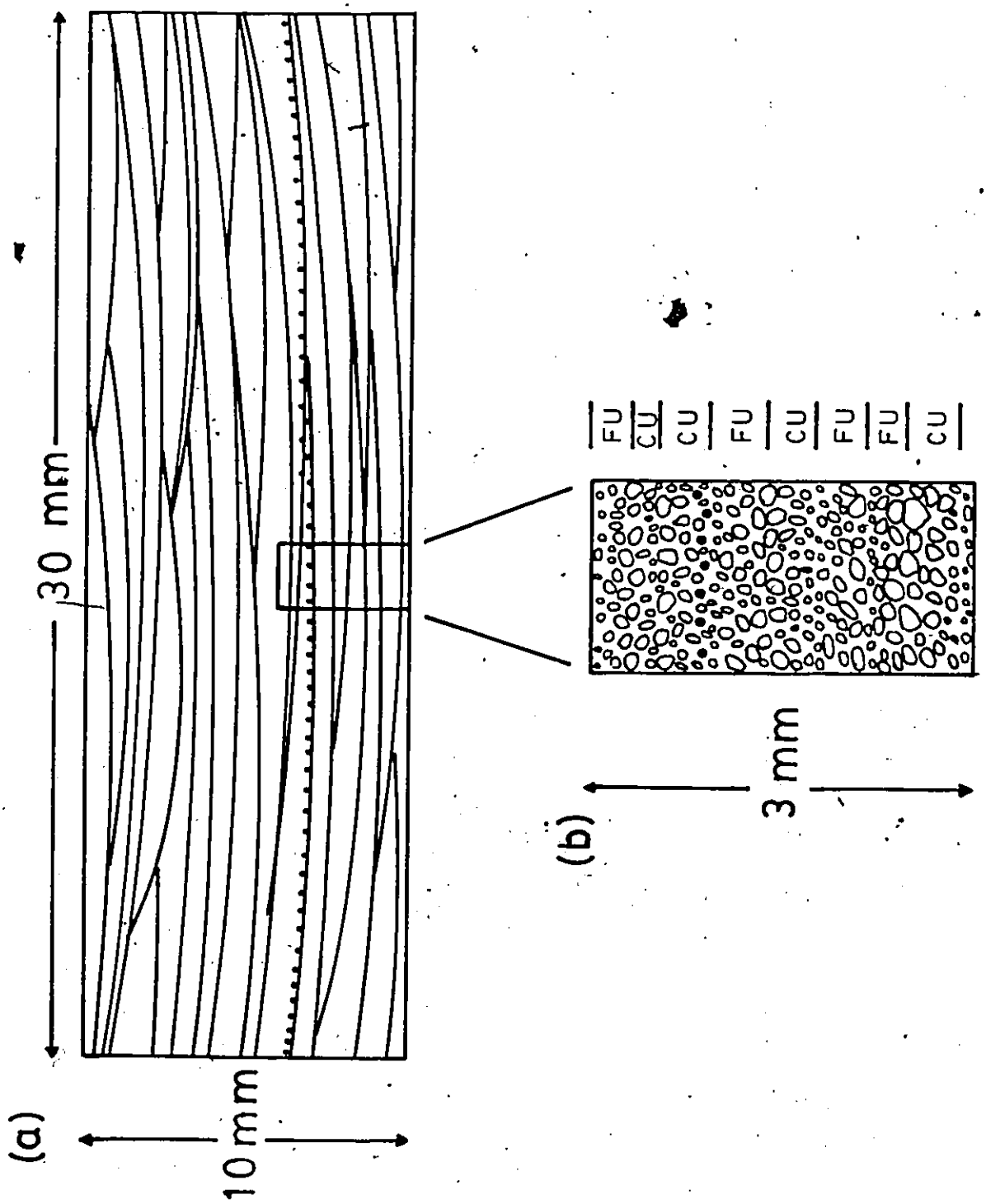
30 mm
10 mm
(a)
FU
CU
3 mm
(b)

lamination. This theory obviously does not explain the close association of heavy minerals with coarsening-upward laminae.

Fining-upward laminae may be explained by the migration of low bedforms, although the absence of bedforms in the bed profile of Run 5 (Fig. IV-11) suggests that some other mechanism is responsible. Furthermore, this mechanism produces significantly thicker laminae than those described here and cannot explain the occurrence of coarsening-upward laminae.

Bridge's (1978) theory provides a possible explanation for the fining-upward laminae (by deposition from decaying sweeps) although a more plausible theory is described below. He also predicted the formation of coarsening-upward laminae in very fine sand and silt in flows where rates of deposition were high. The examples described in this thesis, however, are in fine sand, in which Bridge predicted that only slight coarsening-upward laminae may form on the tops of fining-upward laminae. Bridge (1978, p. 7) also predicted that light and heavy minerals would have equal settling velocities in coarsening-upward laminae formed by the mechanism which he proposed. Figure IV-14 is a plot of the average sizes of light and heavy minerals in measured units from coarsening-upward laminae from samples RM-05, SR-01, SR-02, ShR-01 and Run 5B. The dotted line in Fig. IV-14 (S.E.)

Figure IV-14. Plots of average light and heavy mineral grain axes from the same measured layers in coarsening upward laminae in samples RM-05, SR-01, ShR-01 and Run 5B (see table IV-3). Dotted line represents the size relationship between light and heavy minerals (ρ_s= 2650 Kg/m^3 and 5000 Kg/m^3, respectively) with equal settling velocities (S.E.) based on Stokes' Law. The solid line represents the size relationship predicted for grains subjected to dispersive pressure (D.P.E) and is based on Sallenger (1979, equation 2). The dashed line represents equal light and heavy mineral average long axes (1:1).

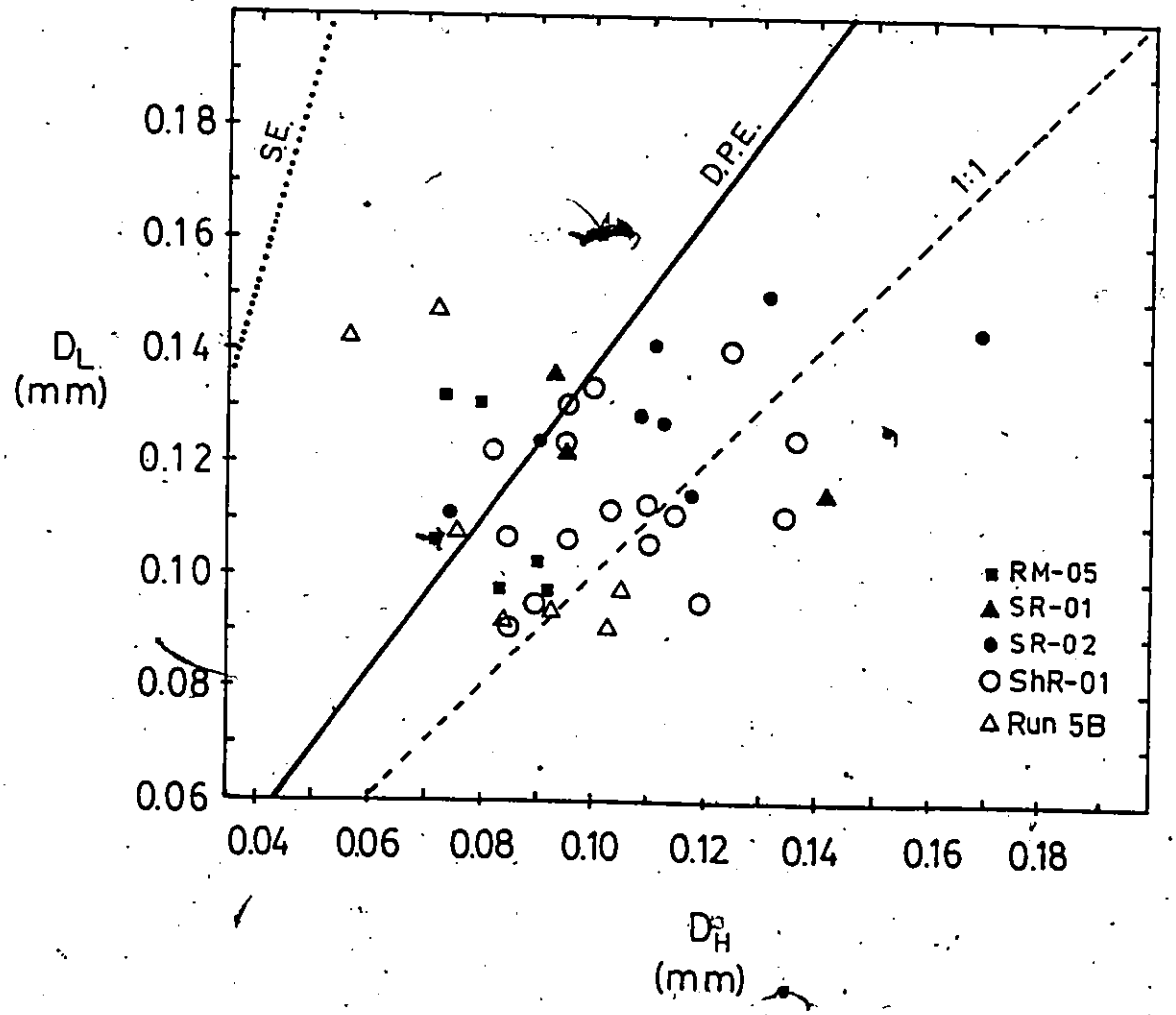
S.E.
D.P.E.
1:1
0.18
0.16
0.14
0.12
0.10
0.08
0.06
D_L (mm)
0.04
0.06
0.08
0.10
0.12
0.14
0.16
0.18
D_H^* (mm)
RM-05
SR-01
SR-02
ShR-01
Run 5B

represents the size relationship between light and heavy minerals (with densities of 2650 kg/m^3 and 5000 kg/^{3}m , approximately that of the light and opaque heavy minerals, respectively, which were included in this study) if the grains are hydraulically equivalent for settling. The data consistently plot well to the right of the dotted line (i.e., the settling velocities of the heavy minerals are much greater than those of associated light minerals) suggesting that some other mechanism is responsible for the formation of coarsening-upward laminae. The multiple bursting mechanism (Hesse an Chough, 1980) is not applicable to the laminae described in this thesis because mud-sized sediment, which is required in their theory, is not present in the laminae.

It is proposed here that the characteristics of textural laminae described earlier in the thesis can be best explained by their formation due to the burst/sweep process. Specifically, it will be shown the sweeps may produce coarsening-upward laminae while bursting may form fining-upward laminae.

Sallenger (1979) has shown inverse grading can develop in response to dispersive pressure in flows in which grains are supported in high concentration in subaerial grainflows and some beach foreshore deposits. Bagnold (1954) predicted that grains which are deposited following support by dispersive pressure would coarsen upwards because

he found that the intensity of dispersive pressure was related to the grain size of the material in transport (see equation 8, Chapter II). Bagnold (1954) suggested that the large grains would be associated with a greater intensity of dispersive pressure than the finer grains and would be pushed upwards through the layer of grains in transport. With deposition the coarsening-upward structure would be preserved.

The formation of coarsening-upward laminae on upper plane beds can also be attributed to the development of dispersive pressure among the grains in transport. When a sweep approaches the bed the local shear stress is increased causing increased sediment transport (i.e., erosion) beneath the accelerated fluid. This will effectively increase the concentration of grains in transport to the level at which dispersive pressure becomes a significant grain support mechanism, causing sorting the bedload into a coarsening-upward layer in transport over the bed. Downstream of the sweep $\partial\tau_o'/\partial x$ (and therefore $\partial q_s/\partial x$) is negative so that a portion of the grains in transport will deposit, forming a coarsening-upward lamination.

The recent work by Sumer and Deigaard (1981) documented how bursting, in flows in which single particles were transported, provides a mechanism which may result in the development of fining-upward laminae. They showed that the ejection fluid from low speed streaks away from the bed

(bursting) can carry a particle upward. Particles which are considerably more dense than the fluid fall out of the ejected mass and settle back to the bed while particles which are only slightly denser than the fluid remain in suspension until the burst breaks up. Although Sumer and Deigaard (1981) used particles of various size and density, in each experiment only one particle was used so that it was not demonstrated that increasingly lighter particles fall out as the ejected fluid moved upward. However, it is reasonable to assume that if a large quantity of grains are lifted away from the bed, out of a moving bed load, the grains with the largest settling velocities will settle out first, followed by grains with decreasing settling velocities. If fallout occurs close to the bed there may not be significant dispersion of the grains before they are re-deposited. Deposition occurs as the settling grains are added back into the bed load, causing an increase in the quantity of grains in transport which is above the capacity of the flow. Deposition from a bed load in which the average grain size is decreasing (due to fallout from the burst) results in a lamination which, on average, is fining-upward. It is stressed that the events described above must occur very near the bed and over a very short span of time so that grains are not sufficiently dispersed downstream to eliminate the possiblity of lamina formation. Even so it is probable that the lamina will become somewhat

finer in the downstream direction due to net downstream transport during fallout from the burst. A particularly important assumption which is made in this theory of fining-upward lamina formation is that the rate of fallout of grains from the ejected fluid exceeds the rate of erosion downstream of the burst. Otherwise the fining-upward laminae could not form.

Returning to the discussion of Bridge's (1978) hypothesis of horizontal laminae formation, it can be shown that if we accept the theory described above that sweeps produce coarsening-upward laminae then fining-upward laminae cannot form by the mechanism proposed by Bridge (i.e., by sweeps). If sweeps did form both types of lamination only those which exerted the greatest bed shear stress would take large enough quantities of sediment into transport so that grain collisions are sufficiently frequent to produce dispersive pressure and the resulting coarsening-upward laminae. Only sweeps which exert a lower shear stress on the bed would cause sediment transport at concentrations low enough so that the grains could settle out relatively freely as the sweep dissipated, forming fining-upward laminae. However, if a larger concentration of sediment is in transport prior to the formation of a coarsening-upward laminae it would be expected that such laminae would be thicker, on average, than the fining-upward laminae. The opposite was found to be true of the laminae described in

this chapter. Formation of fining-upward laminae by bursting (as proposed above) does not necessarily require that these laminae are thinner than coarsening-upward laminae (it is difficult to predict what the relative thickness should be) so that the bursting theory is more acceptable than Bridge's hypothesis.

The distribution of heavy minerals observed in this study can be explained within the context of the proposed mechanisms of laminae formation. Those heavy minerals which were present in the laminae represent those grain sizes, of heavy minerals, which underwent transport on their depositional beds. Figure IV-14 shows the average size of heavy minerals in coarsening-upward laminae (representing their average size of in the bed material) in comparison with the average size of quartz-density minerals with which they were associated. Figure IV-14 also shows that the heavy minerals consistently had greater settling velocities than their associated quartz-density minerals. As a result the heavy minerals are resistant to uplift during the brief period of suspension which occurs with bursting and are largely absent from the fining-upward laminae. Alternatively, heavy minerals with settling velocities which are equal to those of quartz-density grains may not be sufficiently abundant to occur in measurable quantities in fining-upward laminae. Heavy minerals with settling velocities equal to those of light mineral grains in

fining-upward laminae in the samples collected from Run 5 would have diameters of 0.03 mm to 0.04 mm (calculated from Stokes' Law). These grains are present only in the pan fraction of the bed material (i.e., finer than 0.063mm) which makes up much less than 4.5% of the total bed sample.

It was noted in Chapter III (and originally by Brady and Jobson, 1973) that heavy minerals tend to remain in or on the bed while light minerals were in transport. Therefore, heavy minerals are less available for lift-up from the bed load by bursting but are readily available for brief periods of transport by sweeps and become part of coarsening-upward laminae. The absence of heavy minerals in coarsening-upward laminae between laminae with heavy minerals (e.g. Figs. IV-5B, C and D) may reflect their accumulation into patches (shadows?) on the bed. These patches move intermittently in response to large eddies and are frequently disturbed by sweeps. Laminae with heavy minerals may only form when a patch of heavy minerals is located at the site where a sweep approaches the bed. After the patch has passed, few heavy minerals are available on the bed and are absent in coarsening-upward laminae which form before the next patch reaches that site. Patches of heavy minerals may armour the bed from erosion during lift-up by bursts and inhibit the formation of fining-upward laminae. This would explain the absence of fining-upward laminae in Fig. IV-5H where heavy minerals are particularly

abundant (i.e., the laminae may have formed in the presence of an extensive patch of heavy minerals or a series of closely spaced patches).

The random sequence and approximately equal frequency of occurence of fining-upward and coarsening-upward laminae is consistent with the random distribution and equal frequency of bursts and sweeps (Offen and Kline, 1975). This is not to suggest that every sweep and every burst will preserve a lamination. Only partial preservation can be expected, depending on the net rate of deposition on the bed and the periodicity of the burst/sweep events. The lateral scale of the laminae in the direction normal to flow is also consistent with the scales of burst/sweep events. In Fig. IV-7 at least one end of most laminae pinch out within the 12 mm over which measurements were made, suggesting that they are, on average, less than 24 mm wide. Laminae in Fig. IV-8 are more laterally extensive and may be up to 30 or 40 mm wide. Sublayer streak spacing predicted by equation 12, which is thought to be approximately equal to the lateral scale of bursts and sweeps, are only on the order of a few millimetres. However, equation 12 is based on clear fluid flows while Weedman and Slingerland (1983) found that the spacing increased with the concentration of sediment in transport (perhaps due to an increase in "apparent fluid viscosity" due to high grain concentrations as suggested by Allen and Leeder, 1980). The current

lineation on bedding planes in sandstones generally exhibits a greater spacing than clear fluid streaks (Weedman and Slingerland, 1983) with examples ranging from 3 to 25 mm (Allen, 1964). The width of laminae described here, therefore, are fairly consistent with the streak spacing inferred from current lineation. The lateral continuity of heavy mineral sheets (Fig. IV-8) reflects the lateral continuity of the heavy mineral patches on the bed. The heavy mineral sheet which appears in two adjacent coarsening-upward laminae (at approximately 1mm in section IV) may be due to two different sweeps forming coarsening-upward laminae in the presence of the same heavy mineral patch. Downstream continuity of heavy mineral sheets observed in the field may result from (a) areally extensive patches of heavy minerals or (b) the downstream migration of patches over time leaving a lag deposit. The smaller lateral extent of the textural laminae compared to the heavy mineral sheets reflects the smaller scale of the bursts and sweeps compared to the larger eddies which are responsible for the movement of the patches of heavy minerals on the bed.

Eddies probably have an effect on the lighter minerals on the bed but at a scale which is too large to be easily recognized in the manner in which the data is presented. Figure IV-15A shows the variation in the average grain size between laminae through sample MB-02 (Fig.

Figure IV-15. (a) A plot of the average grain size (D) in each lamination versus the relative position of laminae from the base to the top of the measured section from samples MB-02 (Fig. IV-5F). Solid line connects plots of D while the dashed line is drawn by hand to show a possible small scale fluctuation in D through the sample. (b) A record of the ratio of the turbulent bed shear stress to the average bed shear stress (τ_0'/τ_0) over dimensionless time based on measurements made in a wind tunnel (from Brown and Thomas, 1970) showing high frequency, large amplitude fluctuations in τ_0'/τ_0, due to bursting, and small scale variation due to a larger structure in the flow. (Note that this is the same as figure II-5a).

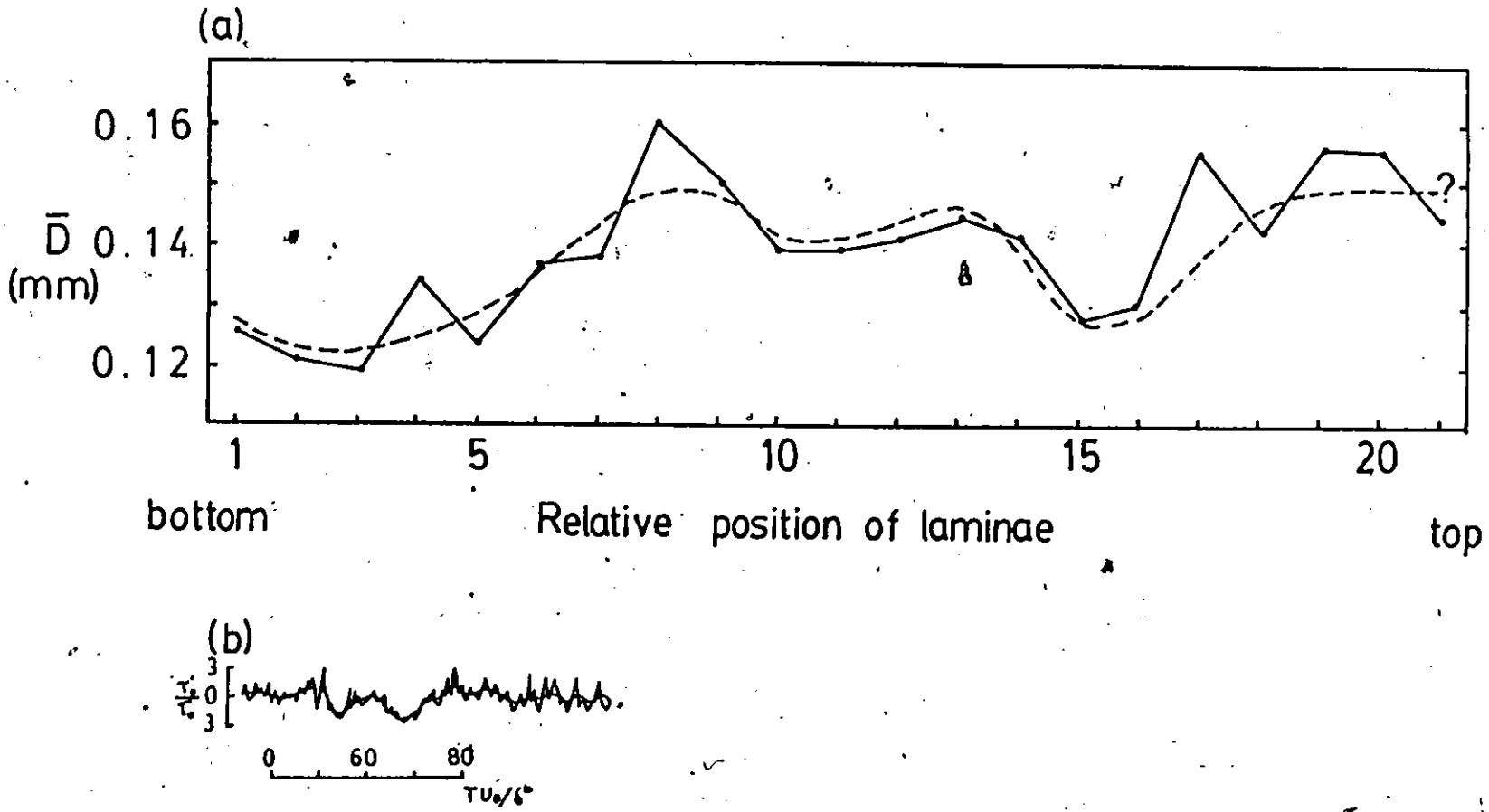
(a)
0.16
$\bar{D}$ 0.14
(mm)
0.12
1
5
10
15
20
bottom
Relative position of laminae
top
(b)
0
60
80

IV-5F). There appears to be a small scale variation in average grain size, from the bottom to the top through the vertical section, onto which is superimposed a larger variation between individual laminae. For comparison, Fig. IV-15B shows the variation in τ_o'/τ_o over dimensionless time (from Fig. II-5A) due to bursts and sweeps and eddies in the outer flow (Brown and Thomas 1971). The similarity between the two figures suggests that the passage of eddies over the bed may cause relatively small scale variations in the average grain size of material in transport. Bursts and sweeps, however, result in a larger scale local variation in the average grain size in transport and preserve the record of both effects in the laminae which they form.

As a test of the hypothesis that coarsening-upward laminae are formed due to sorting by dispersive pressure Fig. IV-14 shows the size of light and heavy minerals in measured units in coarsening-upward laminae. For comparison, also shown in Fig. IV-14 is the line (solid, labled D.P.E.) representing the predicted relationship between light and heavy mineral diameters associated with equal intensities of dispersive pressure (from equation 8). Similar plots by Sallenger (1979) from samples of subaerial grainflow and beach foreshore deposits showed very good agreement between measured and predicted grain size relationships between light and heavy minerals due to sorting by dispersive pressure. The data in Fig. IV-14,

however, show considerable scatter about the line D.P.E., with many points plotting to its right (i.e., heavy minerals are coarser than predicted). The data do not conclusively point to dispersive pressure as the sorting mechanism involved in the formation of coarsening-upward laminae. The scatter may be due to the relatively small sample sizes in the measured units (see table IV-3).

CONCLUSION

The data presented in this chapter have shown that in the deposits of upper flow regime plane beds two general types of structure are responsible for the "lamination" observed in the field: (1) "textural laminae", which include both fining-upward and coarsening-upward laminae less than 1 mm thick and occurring in random vertical sequence. This type of lamination probably accounts for the vague sense of horizontal layering observed in the field. (2) "Heavy mineral sheets" which consist of sheets, one to several grains thick, in which opaque heavy minerals are relatively abundant, occurring in or making up coarsening-upward laminae. It is the heavy mineral sheets which are readily identifiable in the field.

The data provide the first detailed description of horizontal laminae and provides a basis for testing theories of lamination formation. All of the theories decribed at the beginning of this chapter have been rejected in light of the descriptions. However, some theories are probably

correct in their explanation of some reported laminae (e.g., horizontal laminae can form by the migration of low bedforms).

The most likely mechanism which leads to the formation of fining-upward and coarsening-upward laminae with the characteristics described here is the action of bursts and sweeps. Bursting forms fining-upward laminae and coarsening-upward laminae are the products of sweeps. Ejection of a mass of fluid away from the bed (bursting) carries sand grains with it. Grains which are too heavy to continue upward with the ejected mass of fluid will begin to settle out, grains with the largest settling velocity first, followed by grains with increasingly smaller settling velocities. If the addition of these grains to the bedload causes local deposition a fining-upward lamination will form. Coarsening-upward laminae are thought to form as erosion by a sweep increases the concentration of grains in transport near the bed. If this concentration is sufficiently high, grain collisions will result in the development of dispersive pressure as a grain support mechanism forming a coarsening-upward of grain size in the moving mass of sediment. As the sweep dissipates the additional grains in transport will deposit just downstream of the site of erosion and will be preserved as a coarsening-upward lamination. The heavy minerals in the deposits studied here have considerably higher settling

velocities than the lighter minerals and are not responsive to the mechanism which forms fining-upward laminae (i.e., they are too heavy to be lifted by bursting). As a result heavy minerals are largely absent in fining-upward laminae. Heavy minerals are present on the bed (in the form of patches which move intermittently in response to large eddies in the flow) where they are available for brief periods of transport in response to sweeps and become incorporated in coarsening-upward laminae.

CHAPTER V

CONCLUSIONS AND SUGGESTIONS FOR FUTURE WORK

Heavy mineral shadows have been defined in the thesis as irregular patches of heavy minerals, on bedding plane exposures of sandstone (or sand) deposited on an upper flow regime plane bed. They are characterized by the presence of an abrupt upstream boundary with adjacent lighter minerals, and with a gradual transition into the lighter minerals in the downstream direction. This new primary sedimentary structure provides a new tool for interpreting paleoflow direction from bedding plane exposures of horizontally laminated sandstone. Like many other sedimentary structures shadows have gone un-noticed for years. However, after describing the structure to only a few groups of geologists reports have been made to the author of its presence in other quarries in the Whirlpool Sandstone (G.V. Middleton, Personal Communication), in the Thorold Sandstone near Niagara Falls, Ontario (B. Ainsworth, Personal Communication), and in Carboniferous sandstones in New Brunswick (B.R. Rust, Personal Communication). With publication of a modified version of Chapter III (Cheel, in press, 1984) more reports will be forthcoming and the structure will be put to further use in the field.

It was postulated that the shadows form and move in response to the passage of eddies over the bed, on the basis of the relatively large scale of the structure (compared to the scale of bursts and sweeps). Heavy mineral shadows were observed to "wash out" with increasing flow strength and were replaced by flow-parallel windrows of heavy minerals beneath a predominantly quartz sand bed load. At the highest flow strengths heavy mineral were observed primarily on the crests of very low standing waves. The limited range of flow strengths over which heavy mineral shadows are stable and the recognition of other types of heavy mineral accumulations in flume runs with increasing flow strength suggests that the various structures may prove to be useful in the paleohydraulic interpretation of ancient sedimentary rocks.

Further work will be required to better understand the significance of these observations. This work should include flume experiments to determine the effect of the relative size of the light and heavy minerals on the stability of the various types of accumulations (especially shadows). Through this type of work it will be possible to more precisely determine the paleohydraulic implications of the form of heavy mineral accumulation on plane beds in ancient rocks.

The detailed determination of textural variation in sands and sandstones described in Chapter IV have provided

the first precise description of horizontal laminae formed under upper flow regime plane bed conditions. These laminae are made up of both fining- and coarsening-upward textural units, in random sequence, which extend laterally over distance generally less than approximately 40 mm. The descriptions are consistent with the formation of fining-upward and coarsening-upward laminae in response to bursts and sweeps, respectively. Other theories of laminae formation are inadequate in light of the descriptions. Opaque heavy minerals, which are typically associated with coarsening-upward laminae, are believed to form as patches of heavy minerals on the bed are locally disrupted by sweeps. Limited data also suggests that variation in the average grain long axes between laminae may be due to the effects of large eddies in the depositing flow which control the average size of the sediment in transport over the bed on a scale which is larger than that of bursts and sweeps.

Future studies of horizontal laminae should aim to provide more data on the thickness and relative proportions of each type of textural laminae deposited under known flow conditions (e.g. in flumes or on intertidal sand bars where flow measurements can be made). This will provide information on how textural laminae types and sequences may vary with the properties of the depositing flow. It would also be useful to document the distribution of lower density heavy minerals in laminae which include sizes with settling

velocities equal to those of light minerals in fining-upward laminae. The occurrence of minerals of different density and equal settling velocity in fining-upward laminae would strengthen the argument that these laminae form by settling out from suspension. In order to test the proposed theory that both eddies, and bursts and sweeps affect the bed during laminae formation vertical sections through thicker sequences of laminae should be constructed. The samples for these sections should come from beds over which the scale of the eddies can be detemined from instantaneous velocity profiles.

Future work should also include the construction of more lateral correlation diagrams from sections cut normal and parallel to the flow direction. Longer correlation diagrams (normal to the flow) would provide a means of better estimating the lateral extent of laminae than is possible from figures IV-7 and IV-8. Correlation diagrams showing textural variation in laminae in the direction parallel to the flow will show how grain size in laminae varies downstream in laminae (e.g. in Chapter IV it was predicted that average grain size should decrease downstream in fining-upward laminae formed due to bursting).

Finally, the technique developed for the collection of data in Chapter IV provides a new method for studying small scale variation in grain size through other types of lamination. It is important that in future, investigations

be made of horizontal laminae formed by deposition on beaches and from turbidity currents in order to provide a means of differentiating these laminae from those described in the thesis. Application of this technique to ripple and dune cross-stratification, hummocky cross-stratification, and other forms of stratification should prove useful for the interpretation of the specific processes which form those structures also.

REFERENCES CITED

Allen, J.R.L., 1964, Primary current lineation in the Lower Old Red Sandstone (Devonian), Anglo-Welsh Basin: Sedimentology, v. 3, p. 89-108.

_____, 1968, Current Ripples. North-Holland, Amsterdam.

_____, 1970, Physical Processes of Sedimentation. George Allen and Unwin, London.

_____, and M.R. Leeder, 1980, Criteria for the instability of upper-stage plane beds: Sedimentology, v. 27, p. 209-217.

Bagnold, R.A., 1954, Experiments on a gravity-free dispersion of large solid spheres in a Newtonian fluid under shear: Proceedings of the Royal Society of London, v. 225A, p. 49-63.

_____, 1956, The flow of cohesionless grains in fluids: Proceedings of the Royal Society of London, v. 249A, p. 235-297.

_____, 1966, An approach to the sediment transport problem from general physics: U. S. Geological Survey Professional Paper 422-I, 37 pp.

Blatt, H., G. Middleton, and R. Murray, 1980, Origin of Sedimentary Rocks: Prentice-Hall, Inc., Englewood Cliffs, New Jersey, 782 pp.

Bolton, T.E., 1957, Silurian stratigraphy and paleontology of the Niagara escarpment in Ontario: Geological Survey of Canada, Memoir 289, 154 pp.

Bouma, A.H., 1962, Sedimentology of some flysch deposits: Elsevier Publishing Company, Amsterdam, 168 pp.

Brady, L.L., and H.E. Jobson, 1973, An experimental study of heavy-mineral segregation under alluvial-flow conditions: U. S. Geological Survey, Professional Paper 562-K, 38 pp.

Bridge, J.S., 1978, Origin of horizontal lamination under turbulent boundary layers: Sedimentary Geology, v. 20, p. 1-16.

Brown, G.L., and A.S.W. Thomas, 1977, Large structure in a turbulent boundary layer: Physics of fluids, v. 20, p. S243-S252.

Cantwell, B.J., 1981, Organized motion in turbulent flow: Annual Review of Fluid Mechanics, v. 13, p. 457-515.

Cheel, R.J., 1982, The depositional history of an esker near Ottawa, Canada: Canadian Journal of Earth Sciences, v. 19, p. 1417-1427.

_____, In Press, Heavy mineral shadows, a new sedimentary structures formed under upper flow regime plane bed conditions: its directional and hydraulic significance; Journal of Sedimentary Petrology, 19 manuscript pages. Accepted January, 1984.

Coleman, N.L., 1981, Velocity profiles with suspended sediment: Journal of Hydraulic Research, v. 19, p. 211-229.

Collins, M.B. and J.K. Rigler, 1982, The use of settling velocity in defining the initiation of motion of heavy mineral grains under unidirectional flow: Sedimentology, v. 29, p. 419-426.

Crowell, J.C., 1955, Directional-current structures from the Prealpine Flysch, Switzerland: Geological Society of America Bulletin, v. 66, p. 1351-1384.

Dalrymple, R.W., C.L. Amos, and S.B. McCann, 1982, Beach and nearshore depositional enviornments of the Bay of Fundy and southern Gulf of St. Lawrence: International Association of Sedimentologists, Eleventh International Congress On Sedimentology, Guidebook 6A.

Dott, R.H., Jr., and J. Bourgeois, 1982, Hummocky stratification: Significance of its variable bedding sequences: Geological Society of America Bulletin, V. 93, p. 663-680.

Dzulysnki, St., and J.E. Sanders, 1962, Current marks on firm mud bottoms: Connecticut Academy of Arts and Science, Transactions, v. 42, p. 59-96.

Einstein, H.A., and N. Chien, 1955, Effects of heavy sediment concentration near the bed on velocity and sediment distribution: University of California, Berkeley and U.S. Army Corps of Engineers, Missouri River Division, Report #8, 96 pp.

_____, and H. Li, 1958, Secondary currents in straight channels: Transactions of the American Geophysical Union, v. 39, p. 1085.

Engelund, F., and J. Fredsoe, J., 1974, Transition from dunes to plane bed in alluvial channels: Institute of Hydrodynamics and Hydraulic Engineering, Technical University of Denmark, Series Paper No. 4, 56 pp.

_____, and E. Hansen, 1972, A monograph on sediment transport in alluvial streams: Danish Technical Press, Copenhagen.

Everts, C.H., 1973, Particle overpassing on flat granular boundaries: American Society of Civil Engineers, Proceedings, v. 99 WW4, p. 425-438.

Fenton, J.D., and J.E. Abbott, 1977, Initial movement of grains on a stream bed: the effect of relative protrusion: Proceedings of the Royal Society of London, v. 352A, p. 523-537.

Frostick, L.E., and I. Reid, 1977, The origin of horizontal laminae in ephemeral stream channel-fill: Sedimentology, v. 24, p. 1-9.

Gessler, J., 1971, Aggradation and degradation: in River Mechanics, H. W. Shen (editor and publisher), Chapter 8.

Gilbert, G.K., and E.C. Murphy, 1914, The transportation of debris by running water: U. S. Geological Survey Professional Paper 86, 263 pp.

Grass, A.J., 1971, Structural features of turbulent flow over smooth and rough boundaries: Journal of Fluid Mechanics, v. 50, p. 233-255.

Harbaugh, J.W. and G. Bonham-Carter, 1970, Computer simulation in geology: Wiley, New York, 575 pp.

Harms, J.C. and R.K. Fahnestock, 1965, Stratification, bed forms, and flow phenomena (with examples from the Rio Grande): Society of Economic Paleontologists and Mineralogists Special Publication 12, p. 84-115.

_____, J.B. Southard, and R.G. Walker, 1982, Structures and sequences in clastic rocks: Society of Economic Paleontologists and Mineralogists, Short Course Notes, no. 9, p. 8-51.

Hendry, H.E., 1971a, Measurement of discharge in the McMaster recirculating flume: Department of Geology, McMaster University, Technical Memorandum 71-6, 10 pp.

_____, 1971b, Auxiliary equipment used with the McMaster recirculating flume: Department of Geology, McMaster University, Technical Memorandum 71-2, 7 pp.

Hesse, R., and S.K. Chough, 1980, The Northwest Atlantic Mid-Ocean Channel of the Labrador Sea: II. Deposition of parallel laminated levee-muds from the viscous sublayer: Sedimentology, v. 27, p. 697-711.

Hill, H.M., 1966, Bed forms due to a fluid stream: American Society of Civil Engineers, Proceedings, v. 92, No. HY2, p. 127-143.

_____, V.S. Srinvasan and T.E. Unny, Jr., 1969, Instability of flat bed in alluvial channels: American Society of Civil Engineers, Proceedings, v. 95, No. HY5, p. 1545-1558.

Hunter, R.E., 1977, Terminology of cross-stratified sedimentary layers and climbing-ripple structures: Journal of Sedimentary Petrology, v. 47, p. 687-706.

Jackson, R.G., 1976, Sedimentological and fluid dynamic implications of the turbulent bursting phenomenon in geophysical flows: Journal of Fluid Mechanics, v. 77, p. 531-560.

Johnson, J.W., 1942, The importance of side-wall friction and bed-load investigations: Civil Engineering, v. 12, p. 329-331.

Jopling, A.V., 1967, The origin of laminae deposited by the movement of ripples along a streambed: A laboratory study: Journal of Geology, v. 75, p. 287-305.

_____, and D.L. Forbes, 1979, Flume study of silt transportation and deposition: Geografica Annaler, v. 61A, p. 67-85.

Kennedy, J.F., 1963, The mechanics of dunes and antidunes in erodible-bed channels: Journal of Fluid Mechanics, v. 16, p. 521-544.

_____, and the Task Force on Bed Forms in Alluvial Channels, 1966, Nomenclature for bed forms in alluvial channels: Journal of the Hydraulics Division, American Society of Civil Engineers, v. 92, no. HY3, p. 51-64.

Kline, S.J., W.C. Reynolds, F.A. Schraub and P.W. Rundstadler, 1967, The structure of turbulent boundary

layers: Journal of Fluid Mechanics, v. 30, p. 741-773.

Kuenen, Ph.H., 1966, Experimental turbidite lamination in a circular flume: Journal of Geology, v. 74, p. 523-545.

Lambiase, J., 1977, Sediment dynamics in the macrotidal Avon River estuary, Nova Scotia: Unpublished Ph.D. thesis, McMaster University, 415 p.

Leeder, M.R., 1980, On the stability of lower stage plane beds and the absence of current ripples in coarse sands: Journal of the Geological Society of London, v. 137, p. 423-429.

_____, 1983, On the interactions between turbulent flow, sediment transport and bedform mechanics in channelized flows: International Association of Sedimentologists, Special Publication No. 6, p. 5-18.

Lindholm, R.C., 1982, Flat stratification: two ancient examples: Journal of Sedimentary Petrology, v. 52, p. 227-231.

McBride, E.F., and L.S. Yeakel, 1963, Relationship between parting lineation and rock fabric: Journal of Sedimentary Petrology, v. 33, p. 779-782.

_____, R.G. Shepherd and R.A. Crawley, 1975, Origin of parallel, near-horizontal laminae by migration of bed forms in a small flume: Journal of Sedimentary Petrology, v. 45, p. 132-139.

McDonald, B.C., 1972, The Geological Survey of Canada sedimentation flume: Geological Survey of Canda Paper 71-46, 12 p

_____, and J.A. Vincent, 1972, Fluvial sedimentary structures formed experimentally in a pipe, and their implications for interpretation of subglacial sedimentary environments: Geological Survey of Canada, Paper 72-27, 30 pp.

McKee, E.D., E.J. Crosby and H.L. Berryhill, Jr.,1967, Flood deposits, Bijou Creek, Colorado, Journal of Sedimentary Petrology, v. 37, p. 829-851.

McQuivey, R.S., and T.N. Keefer, 1969, The relation of turbulence to deposition of magnetite over ripples: U. S. Geological Survey Professional Paper 650-D, p. 244-247.

Miall, A.D., 1973, Markov chain analysis applied to an

ancient alluvial plain succession: Sedimentology, v. 20, p. 347-364.

Middleton, G.V., 1976, Hydraulic interpretation of grain size distributions: Journal of Geology, v. 84, p. 405-426.

_____, C.J. Salas and I.P. Martini, 1983, Whirlpool Sandstone (Silurian), of Southern Ontario, a braided river deposit?: Geological Society of America, Abstracts with Programmes, v. 15, #13, p. 128.

_____, and J.B. Southard, 1977, Mechanics of sediment movement: Society of Economic Paleontologists and Mineralogists, Short Course No. 3.

Moss, A.J., 1963, The physical nature of common sandy and pebbly deposits, Part II: American Journal of Science, v. 261, p. 197-343.

_____, 1972, Bed-load sediments: Sedimentology, v. 18, p. 159-219.

Offen, G.R., and S.J. Kline, 1975, A proposed model of the bursting process in turbulent bnoundary layers: Journal of Fluid Mechanics, v. 61, p. 209-228.

Pettijohn, F.J., 1975, Sedimentary rocks (Third edition): Harper and Row, Publishers, New York, 628 pp.

Rao, K.N., R. Narasimha, and M.A.B. Narayanan, 1971, The bursting phenomenon in a turbulent boundary layer: Journal of Fluid Mechanics, v. 48, p. 339-352.

Reinson, G.E., 1979, Barrier island systems: in Facies Models, R.G. Walker (editor), Geoscience Canada Reprint Series 1, p. 57-74.

Reynolds, O., 1883, An experimental investigation of the circumstances which determine whether the motion of water shall be direct or sinuous, and the law of resistance in parallel channels: Royal Society of London, Philosophical Transactions, v. 174, p. 935-982.

Sallenger, A.H., 1979, Inverse grading and hydraulic equivalence in grain-flow deposits: Journal of Sedimentary Petrology, v. 49, p. 553-562.

Shields, A., 1936, Anwendung der Ahnlichkeitsmechanik und der turbulenzforschung auf die gechiebebewegung: mitteilungen der preuss: Versuchanst. fur Wasserbau und Schiffbau, Berlin, v. 26, 26 p. English translation as

"Application of similarity principles and turbulence research to bed-load movement", by W.P. Ott and J.C. van Uchelen, U.S. Department of Agriculture, Soil Conservation Service Cooperative Laboratory, California Institute of Technology.,

Saunderson, H.C., and F.P.J. Lockett, 1983, Flume experiments on bedforms and structures at the dune-plane bed transition: International Association of Sedimentologists, Special Publication No. 6, p. 49-58.

Simons, D.B., and E.V. Richardson , 1962, Resistance to flow in alluvial channels: American Society of Civil Engineers Transactions, v. 127, part I, p. 927-954.

_____, 1963, Forms of bed roughness in alluvial channels: American Society of Civil Engineers Transactions, v. 128, Part I, p. 284-302.

_____, E.V. Richardson and C.F. Nordin, Jr., 1965, Sedimentary structures generated by flow in alluvial channels: Society of Economic Paleontologists and Mineralogists, Special Publication 12, p. 34-52.

Smith, N.D., 1971, Pseudo-planar stratification produced by very low amplitude sand waves: Journal of Sedimentary Petrology, v. 41, p. 69-73.

Southard, J.B., 1971, Representation of bed configurations in depth-velocity-size diagrams: Journal of Sedimentary Petrology, v. 41, p. 903-115.

_____, and J.C. Harms, 1972, Sequence of bedform and stratification in silts, based on flume experiments (abstract): American Association of Petroleum Geologists Bulletin, v. 56, p. 654-655.

Southerland, A.J., 1967, Proposed mechanism for sediment entrainment by turbulent flows: Journal of Geophysical Research, v. 72, p. 6183-6194.

Stokes, W.L., 1947, Primary lineation in fluvial sandstones: a criterion of current direction: Journal of Geology, v. 55, p. 52-54.

Stavrakis, N., 1980, Sedimentation of the Katsberg Sandstone and adjacent formations in the south-eastern Karoo Basin: Transactions of the Geological Society of South Africa, v. 83, p. 361-374.

Sumer, B.M., and R. Deigaard, 1981, Particle motions near

the bottom in turbulent flow in an open channel. Part 2: Journal of Fluid Mechanics, v. 109, p. 311-338.

Thorne, C.R., and R.D. Hey, 1979, Direct measurements of secondary currents at a river inflexion point: Nature, v. 280, p. 226-228.

Vanoni, V.A., and N.H. Brooks, 1957, Laboratory studies of the roughness and suspended load of alluvial streams: California Institute of Technology, Sedimentation Laboratory, U. S. Army Corps of Engineers, Missouri River Division, Sediment Series, No. 11, 121 pp..

Walker, R.G, 1979, Shallow marine sands: in Facies Models, R.G. Walker (editor), Geoscience Canada, Reprint Series 1, p. 75-90.

Ward, B.D., 1969, Relative density effects on incipient bed movement: Water Resources Research, v. 5, p. 1090-1096.

Weedman, S.D., and R.L. Slingerland, 1983, Turbulent boundary layer interpretation of parting lineation: Geological Society of America, Abstracts with Programs, v. 15, #6, p. 716.

APPENDICES

APPENDIX I. LIST OF SYMBOLS USED IN THE THESIS

D	Mean grain size (subscript L denotes light minerals, H denotes heavy minerals).
F	Froude number.
L	Average length of standing waves or antidunes.
N	Number of observations.
P	Intensity of dispersive pressure.
R	Flow Reynolds number.
R*	Boundary Reynolds number.
S	Lateral spacing of streaks.
T	Time in seconds.
T*	A dimensionless expression of time.
Th	Thickness of textural laminae.
U	Mean flow velocity.
U_∞	Maximum time average velocity.
U*	Shear velocity.
V	Bulk volume of sediment.
d	Flow depth.
g	Acceleration due to gravity.
h	Bed elevation.
q_s	Sediment transport rate.
t	Time.
w	Settling velocity.

y	Height above bed.
α	An angle related to collision conditions in a grain layer.
β	Shields' beta.
μ	Dynamic viscosity of fluid.
ν	Kinematic viscosity of fluid.
ρ	Density of fluid.
ρ_s	Density of sediment.
λ	Linear concentration of grains.
τ_o	Boundary shear stress (subscript "crit" denotes critical value for the initiation of movement of bed material).
τ_o'	Turbulent shear stress at a bed.
$\partial G/\partial y$	Shear strain in a moving grain layer.
T	Periodicity of the burst/sweep process.

APPENDIX II. DESCRIPTION OF EXPERIMENTAL APPARATUS AND EQUIPMENT

A. 12.2 metre McMaster recirculating flume.

The flume used for the work described in Chapter III (Heavy mineral shadows...) is a closed circuit (no free overfall at the downstream end of the channel) recirculating flume with a channel 12.2 m long (the central 6 m of which is glass-walled), 0.3 m wide and 0.6 m deep (Fig. IIA-1). Sand and water are recirculated through the flume via a variable speed axial flow pump, beneath the downstream end of the channel, through a 0.10 m inner diameter return pipe. The capacity of the pump is 0.0217 m^3/s. Discharge through the channel is calculated from the difference in pressure head (Δh) measured on manometres attached to a venturi meter which is built into the downstream end of the return pipe (see Hendry, 1971a). The relationship between the discharge and Δh is given by:

$$Q = 5.837 \times 10^{-3} \sqrt{2g\Delta h} \qquad (16)$$

where Q is the discharge in cubic metres per second.

The slope of the channel is adjustable by means of scissor jacks which support the upstream end of the flume. The water surface slope is determined from water levels in peizometer tubes which are linked by clear Tygon tubing to taps in the floor of the flume spaced at 0.914 m intervals along the channel. A point gage, mounted on a mobile

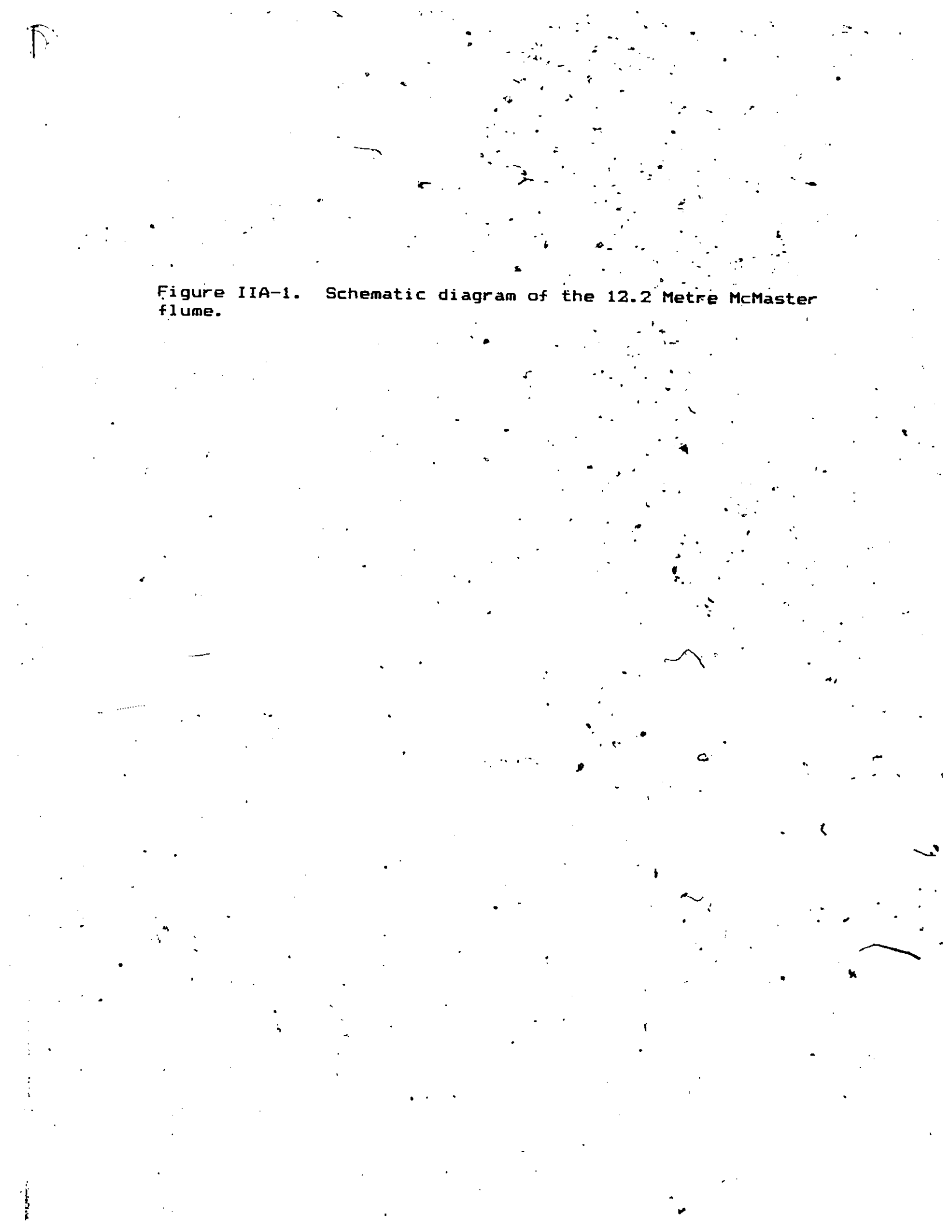

Figure IIA-1. Schematic diagram of the 12.2 Metre McMaster flume.

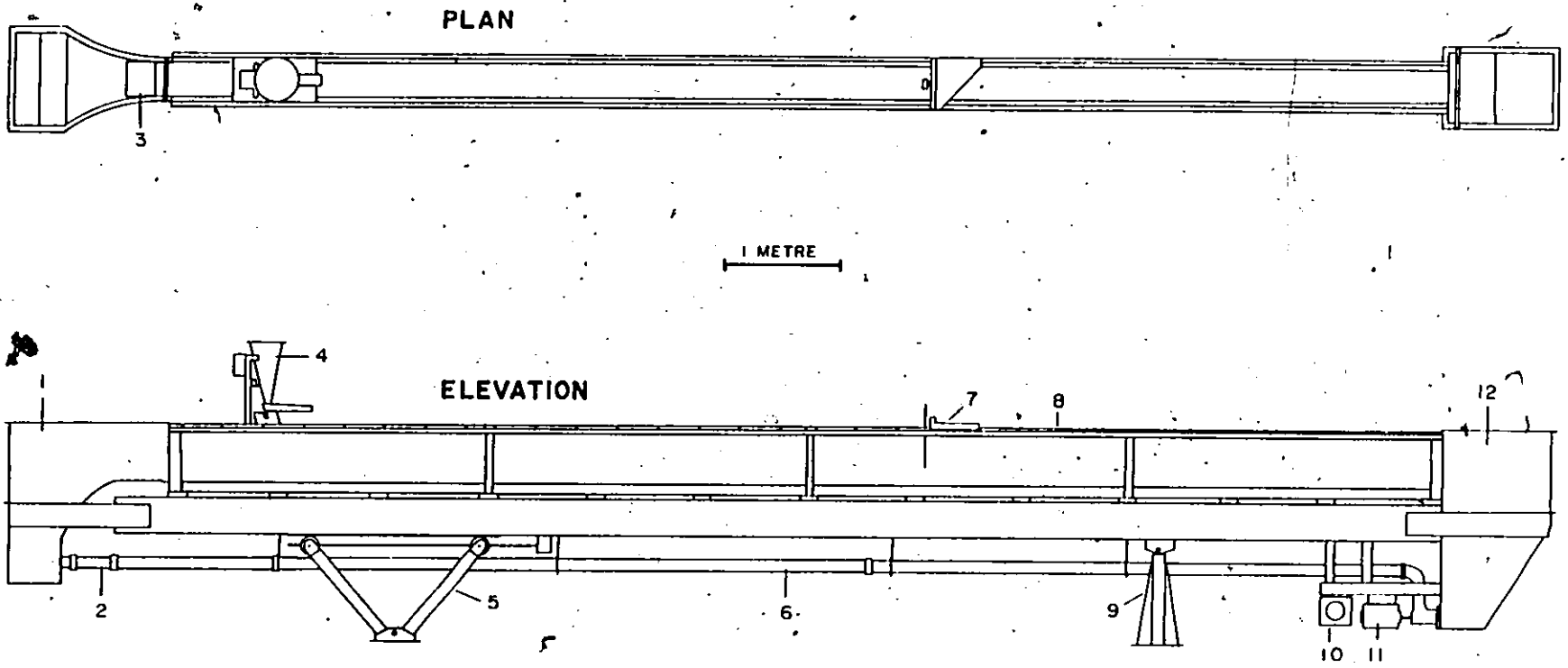

LEGEND

1	Head-box.	7	Instrument carriage & point gage
2	Venturi metre	8	Rails
3	Baffles	9	Pivot support
4	Syntron sediment feeder	10	Pump speed control
5	Scissor-jack support	11	Pump
6	Return pipe	12	Tail-box

instrument carriage which slides along rails attached to the top of the channel walls, allows accurate measurement of water and bed surface elevations to within 0.1mm. The temperature of the water in the channel is measured to within 0.5 degrees Celsius by a thermometer suspended to the tail box. A chicken wire baffle in the channel at its upstream end acts to break up the turbulent structure of the flow leaving the head box. A board, cut to the plan shape of the head box is floated on the water surface in the entrance to suppress waves which may have affected the flow (and bed) in the channel.

A Prandtl pitot tube, attached to the instrument carriage, is used to measure point velocites in the flow by the method outlined by Hendry (1971c and d). A pressure transducer attached to plastic tube leading from the pitot tube, produces a small electrical current, the intensity of which is proportional to the difference in static and dynamic pressure in the pitot tube. The intensity of the current is recorded on a chart recorder. To determine the velocity at a point in the flow the pitot tube is lowered to the desired depth and the output from the transducer is recorded for one to two minutes. The average voltage is determined from the chart recorder trace and the difference in pressure head (in metres of water) is found from calibration curves derived by finding the voltage produced by the transducer in response to small differences in water

pressure while attached to two manometers. The velocity at any depth is calculated from:

$$U = \sqrt{2g\Delta h} \qquad (17)$$

Other auxiliary equipment for use with this flume are decribed in Hendry (1971b).

B. The Geological Survey of Canada Sedimentation Flume

This free-overfall recirculating sediment flume has been described in detail by McDonald (1972). The channel is 18.3 m long, 0.76 m wide and 0.6 m deep (Figure IIB-1). The slope of the channel may be adjusted by means of electric jacks at a rate of 0.000125 per second. Flow through the channel falls into a 2.9 m long, 2.4 m wide and 1.5 m deep tail box which is flanked on both sides by 1.9 m long, 2.4 m wide and 1.5 m deep secondary boxes. During flume runs desribed in the thesis false walls were built into the central box in order to reduce overflow and resulting loss of sediment into the side boxes.

Sediment and water is recirculated through the system by two constant speed electric axial flow pumps, one with a capacity of 0.230 m^3/s and the other with a capacity of 0.115 m^3/s. The larger pump supplies a 0.305 m (inner diameter) return pipe and the smaller pump a 0.254 m (I.D.) pipe, both are mounted beneath the channel. Flow through each pipe is controlled by two valves which alter the proportion of the total discharge through the pumps which is sent through the pipe to the head box or back into the tail box. During the flume runs described in this thesis the 0.305 m return pipe was broken so that only the smaller pump and return pipe could be used to recirculate sediment and water to the channel. The larger pump, however, was used to recirculate all of its discharge back

Figure IIB-1. Schematic diagram illustrating the Geological Survey of Canada sedimentation flume in plan (top) and elevation (bottom) after McDonald (1972).

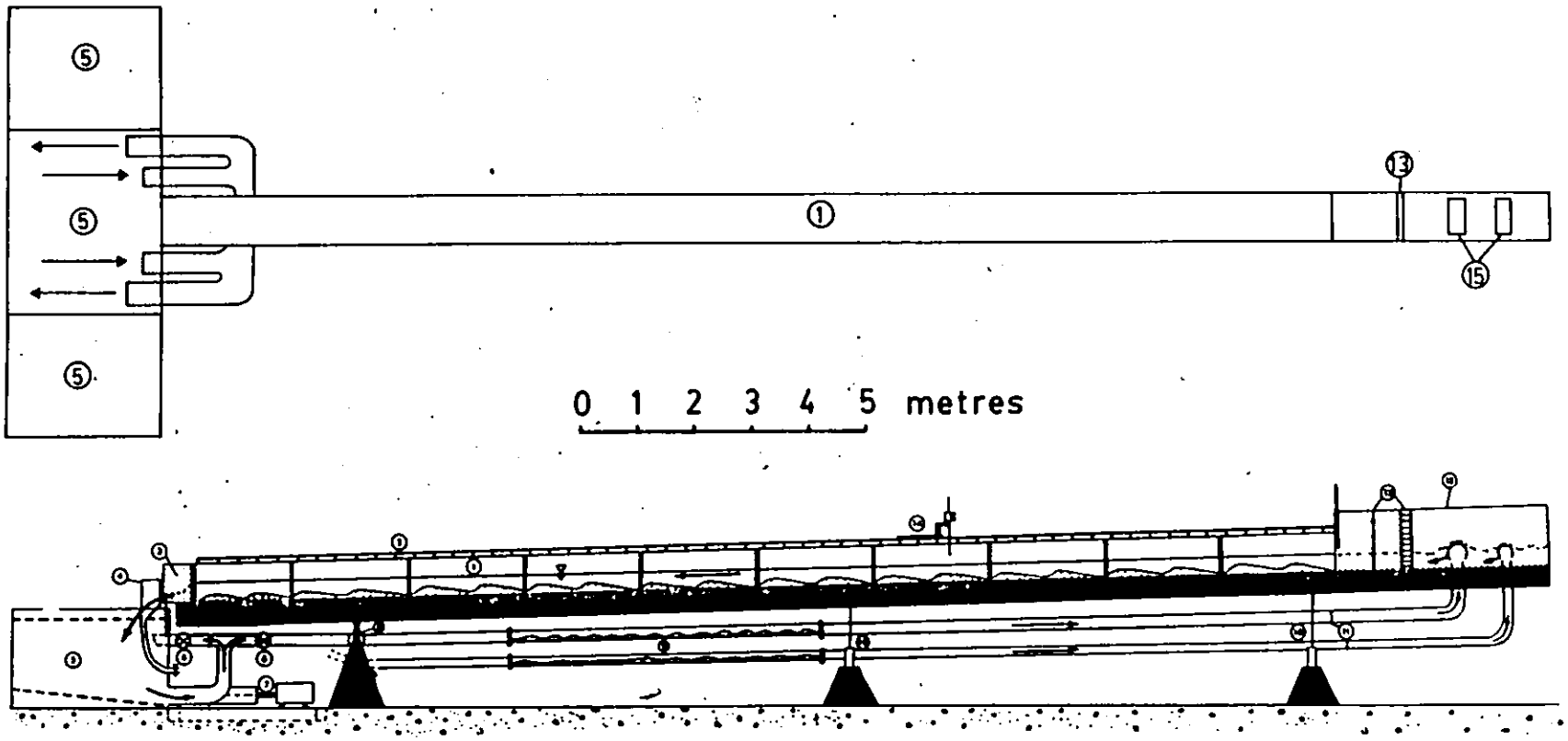

1. main channel
2. rails
3. tailgate assembly
4. total lead sampler
5. tail tank
6. flow-control valves
7. pump and motor
   (small pump, not shown, feeds the 25cm return pipe)
8. pivot support
9. transparent sections of return pipe
10. jack supports
11. orifice plates
12. headbox
13. baffles
14. instrument carriage

into he tailbox where a high intensity of turbulence was maintained to keep sediment in suspension in the box thereby inhibiting losses due to deposition on the floor of the box.

At the entrance to the channel flow leaves the return pipes through vertical T-pipes and then passes into the channel through a 0.15m thick grid baffle which extends across the channel. To further enhance the development of a logarithmic velocity profile a block of impregnated gravel which was as wide as the channel and 1 m long was placed on the floor of the channel just downstream of the entrance. A board (as wide as the channel) was laid on the water surface over the gravel block to inhibit the development of water surface waves which might affect the mobile sand bed which covered the rest of the channel floor. Hydraulic conditions in the flume were varied by maintaining maximum discharge through the smaller of the two pumps and changing the flow depth by means of a knife edge gate which could be lowered into the flow at the downstream end of the channel. The water temperature was measured with a thermometer suspended in the flow in the head box.

A sliding instrument carriage was mounted on the flume rails. To measure the water surface slope a point gage was attached to the carriage. A flat plate (foot) was fixed onto the point gage for measurement of the bed surface height. The same pitot tube that was used with the McMaster flume was attached to the instrument carriage for the

measurement of point velocities in the flow. Figure IIB-2 shows a series of vertical and cross channel profiles taken along the length of the flume. Note that near the entrance (at 5m) both the vertical and cross-channel profiles are not well developed. However, by 11 m from the entrance the vertical profile is logarithmic and the cross-channel profile is two dimensional.

Figure IIB-2. Vertical (top) and cross-channel (bottom) velocity profiles measured at various distances from the flume entrance.

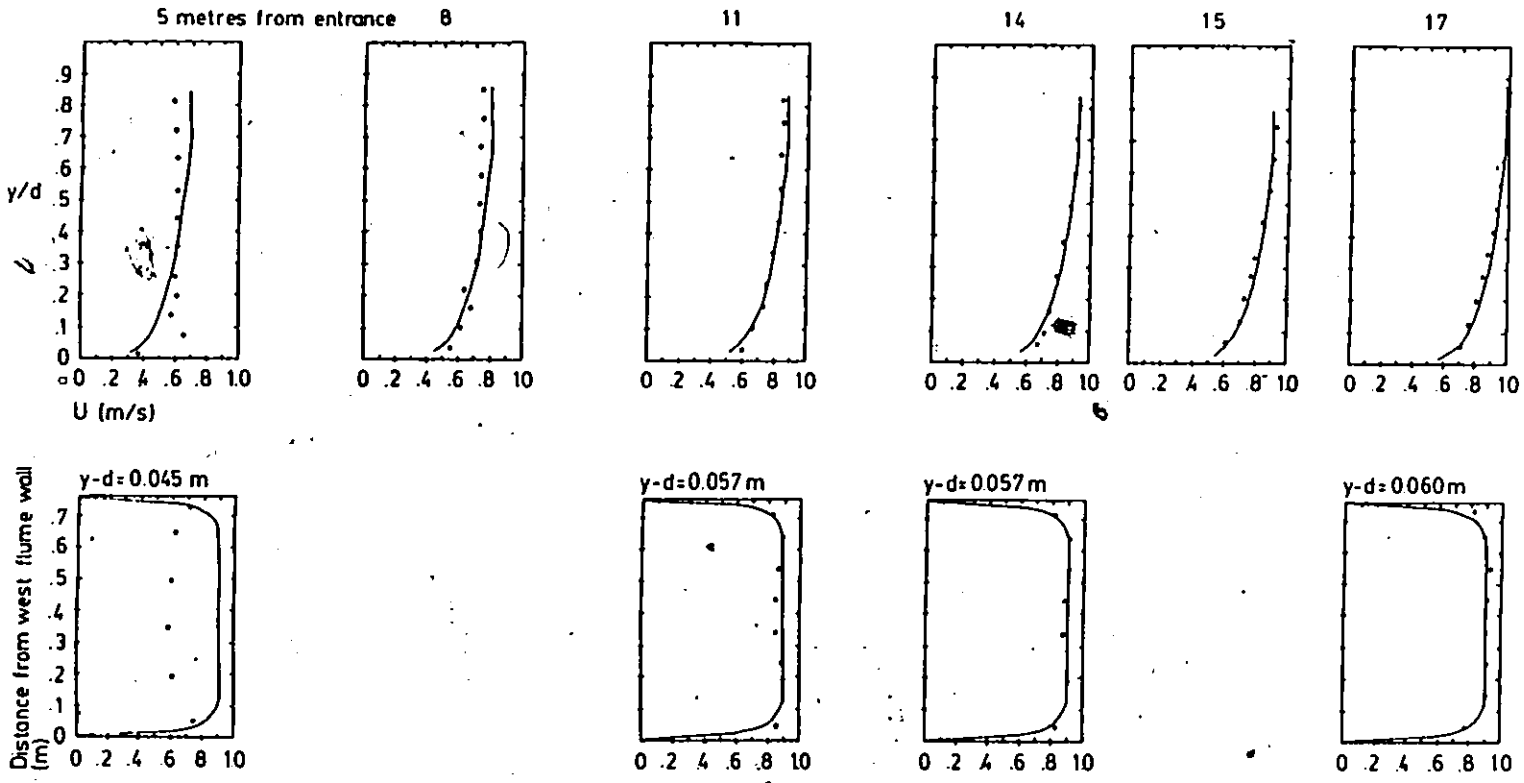
5 metres from entrance
8
11
14
15
17
y/d
U (m/s)
y-d=0.045 m
y-d=0.057 m
y-d=0.057 m
y-d=0.060 m
Distance from west flume wall (m)
U (m/s)

C. Impregnated box cores.

Box cores were collected from flume beds and sand bars in Nova Scotia using the same technique. Rectangular boxes (0.1 m x 0.06 m x 0.06 m) were constructed from galvanized steel (approximately 0.5 mm thick). The top and one end of each box was left open and covers for the open ends were constructed out of the same galvanized steel. To collect a sample a trench, with a face oriented normal to the flow direction, was cut into the sand bed (in the flume this was done after several hours of drying). With its long axis parallel to the flow direction the box was carefully pushed into the sand with its base parallel to the plane of the bedding. When the closed end of the box was in contact with and parallel to the vertical face of the trench the sand at the open end was cut with a knife so that its surface was flush with the walls of the box. The core was then removed from the bed and the cover placed on the open end and secured with masking tape.

Box cores were placed in an oven for several hours until all interstitial water had evaporated. While still warm from the oven they were impregnated with Araldite 502 epoxy resin* (mixed with HY956 hardener at a ratio of 5 to 2). The mixture of hardener and resin was poured onto the sand in each box while in an evacuated vacuum jar by means of a funnel, with a stop-cock in its stem, which passed into the vacuum jar through a rubber stopper in the glass lid.

(The vacuum increased the extent of the impregnation by reducing the need for the resin to displace air from the pore spaces of the sand.) The resin was allowed to harden for 24 hours before the sample was removed from the metal boxes. Impregnation was never complete, extending generally less than 0.1m on the top of the sample and several centimetres at the ends where the the resin ran down the walls of the boxes. Thin sections were normally cut from the ends of the samples for later textural analysis.

* Resin and hardener are available from:

Canadian Hanson Ltd.,
45 Vansco Rd.,
Toronto, Ontario,
M8Z 5J7

At the time of writing a new epoxy resin is available from Canadian Hanson Ltd. which is of lower viscosity (and lower toxicity) than the one used in this work. This new resin is Araldite 509 epoxy resin and will be tested by the author to determine if better impregnation will be possible in future work.

APPENDIX III. TEXTURAL DATA

Sample RM-01

Height below datum (mm)	N	D(min) (mm)	D(max) (mm)	$\bar{D}$ (mm)	S (mm)	$S/\sqrt{N}$ (mm)
0.1	9	0.0600	0.2500	0.1378	0.0533	0.0178
0.3	11	0.1300	0.2500	0.1591	0.0359	0.0108
0.5	8	0.1200	0.2400	0.1575	0.0392	0.0139
0.7	14	0.0500	0.2400	0.1450	0.0511	0.0137
0.9	14	0.1100	0.2300	0.1557	0.0394	0.0105
1.1	12	0.1200	0.2100	0.1725	0.0286	0.0083
1.3	17	0.0500	0.2000	0.1059	0.0345	0.0084
1.5	17	0.0500	0.2000	0.1165	0.0431	0.0098
1.7	18	0.0700	0.2200	0.1217	0.0415	0.0098
1.9	21	0.0600	0.2000	0.1286	0.0411	0.0090
2.1	22	0.0600	0.2000	0.1273	0.0365	0.0078
2.3	20	0.1100	0.2600	0.1390	0.0391	0.0087
2.5	23	0.0600	0.1600	0.1083	0.0285	0.0060
2.7	19	0.0700	0.1400	0.1105	0.0175	0.0040
2.9	19	0.0500	0.1900	0.1095	0.0303	0.0069
3.1	22	0.0700	0.1800	0.1214	0.0311	0.0066
3.3	20	0.0500	0.1700	0.1270	0.0303	0.0068
3.5	24	0.0400	0.2000	0.1038	0.0389	0.0079
3.7	23	0.0600	0.1900	0.1204	0.0336	0.0070
3.9	24	0.0700	0.2200	0.1204	0.0384	0.0078
4.1	26	0.0600	0.1900	0.1173	0.0329	0.0065
4.3	20	0.0700	0.1900	0.1385	0.0392	0.0076
4.5	18	0.0600	0.3200	0.1522	0.0639	0.0143
4.7	21	0.0400	0.1600	0.1110	0.0264	0.0058
4.9	23	0.0700	0.1700	0.1135	0.0298	0.0062
5.1	20	0.0500	0.1800	0.1170	0.0361	0.0081
5.3	24	0.0600	0.1800	0.1179	0.0277	0.0056
5.5	25	0.0600	0.2200	0.1188	0.0327	0.0065
5.7	19	0.0700	0.2200	0.1353	0.0398	0.0091
5.9	26	0.0800	0.1800	0.1192	0.0299	0.0059
6.1	26	0.0600	0.2300	0.1185	0.0466	0.0091
6.3	26	0.0700	0.2300	0.1265	0.0434	0.0085
6.5	16	0.0800	0.2100	0.1363	0.0413	0.0103

Sample RM-01

Height below datum (mm)	N	D(min) (mm)	D(max) (mm)	$\bar{D}$ (mm)	S (mm)	$S/\sqrt{N}$ (mm)
6.7	21	0.0800	0.2700	0.1400	0.0515	0.0112
6.9	11	0.1000	0.2600	0.1582	0.0517	0.0156
7.1	13	0.0700	0.2700	0.1469	0.0506	0.0140
7.3	15	0.0700	0.2800	0.1533	0.0475	0.0123
7.5	19	0.0700	0.1700	0.1258	0.0287	0.0066
7.7	25	0.0600	0.1700	0.1080	0.0257	0.0051
7.9	16	0.0700	0.2400	0.1350	0.0434	0.0108
8.1	12	0.1000	0.2000	0.1433	0.0331	0.0096
8.3	17	0.0700	0.2000	0.1276	0.0342	0.0083
8.5	22	0.0700	0.1600	0.1073	0.0262	0.0056
8.7	27	0.0500	0.1700	0.0963	0.0288	0.0056
8.9	21	0.0600	0.2300	0.1271	0.0414	0.0090
9.1	19	0.0800	0.2300	0.1374	0.0409	0.0094
9.3	18	0.0900	0.2100	0.1444	0.0367	0.0086
9.5	19	0.0400	0.1900	0.1353	0.0366	0.0084
9.7	21	0.0600	0.2100	0.1281	0.0410	0.0087
9.9	19	0.0800	0.1700	0.1305	0.0257	0.0059
10.1	15	0.0800	0.2300	0.1367	0.0445	0.0149
10.3	18	0.0800	0.2900	0.1339	0.0475	0.0111
10.5	16	0.0800	0.2000	0.1419	0.0437	0.0109
10.7	20	0.0700	0.2500	0.1310	0.0451	0.0101
10.9	18	0.0900	0.2200	0.1317	0.0303	0.0072
11.1	20	0.0500	0.2000	0.1110	0.0384	0.0086
11.3	26	0.0700	0.2000	0.1165	0.0321	0.0063
11.5	18	0.0800	0.2000	0.1350	0.0294	0.0069
11.7	18	0.0900	0.2300	0.1494	0.0349	0.0082
11.9	17	0.0800	0.1800	0.1141	0.0312	0.0076
12.1	28	0.0700	0.1900	0.1089	0.0313	0.0059
12.3	23	0.0700	0.2100	0.1278	0.0374	0.0078
12.5	15	0.1000	0.2200	0.1440	0.0292	0.0075
12.7	18	0.0800	0.1900	0.1302	0.0369	0.0087
12.9	19	0.0700	0.2200	0.1416	0.0380	0.0087
13.1	17	0.0500	0.2000	0.1141	0.0381	0.0092

Sample RM-01

Height below datum (mm)	N	D(min) (mm)	D(max) (mm)	$\bar{D}$ (mm)	S (mm)	$S/\sqrt{N}$ (mm)
13.3	18	0.0700	0.2000	0.1117	0.0328	0.0077
13.5	20	0.0600	0.1700	0.1180	0.0311	0.0069
13.7	19	0.0700	0.2100	0.1374	0.0354	0.0081
13.9	19	0.0400	0.2500	0.1353	0.0475	0.0109
14.1	21	0.0600	0.2600	0.1319	0.0456	0.0099
14.3	21	0.0600	0.1700	0.1186	0.0307	0.0067
14.5	26	0.0600	0.2000	0.1115	0.0361	0.0071
14.7	20	0.0700	0.2100	0.1195	0.0293	0.0065
14.9	21	0.0600	0.1400	0.0967	0.0221	0.0048

Sample RM-05

Height below datum (mm)	N	D(min) (mm)	D(max) (mm)	$\bar{D}$ (mm)	S (mm)	$S/\sqrt{N}$ (mm)
0.1	15	0.0900	0.2200	0.1360	0.0391	0.0101
0.3	17	0.0600	0.2900	0.1529	0.0621	0.0151
0.5	15	0.0800	0.2100	0.1380	0.0393	0.0102
0.7	18	0.1100	0.2000	0.1489	0.0355	0.0084
0.9	17	0.0800	0.2000	0.1247	0.0322	0.0078
1.1	18	0.0600	0.2100	0.1178	0.0362	0.0085
1.3	19	0.0800	0.2100	0.1474	0.0380	0.0087
1.5	17	0.0700	0.2100	0.1335	0.0348	0.0084
1.7	23	0.0800	0.1500	0.1174	0.0245	0.0051
1.9(L)	27	0.0400	0.1800	0.1026	0.0381	0.0073
1.9(H)	6	0.0600	0.1200	0.0900	0.0253	0.0103
2.1	22	0.0600	0.1300	0.1132	0.0201	0.0043
2.3	15	0.0800	0.2100	0.1340	0.0368	0.0095
2.5	20	0.0900	0.2500	0.1400	0.0415	0.0093
2.7	23	0.0500	0.2500	0.1113	0.0442	0.0088
2.9(L)	24	0.0700	0.1500	0.1063	0.0243	0.0050
2.9(H)	5	0.0600	0.0900	0.0720	0.0164	0.0073
3.1	22	0.0600	0.2500	0.1305	0.0416	0.0091
3.3	25	0.0600	0.1800	0.1296	0.0309	0.0062
3.5	24	0.0600	0.2000	0.1221	0.0319	0.0065
3.7(L)	16	0.0800	0.1800	0.1306	0.0279	0.0070
3.7(H)	4	0.0600	0.1000	0.0800	0.0183	0.0091
3.9	22	0.0500	0.2000	0.1177	0.0364	0.0078
4.1	24	0.0700	0.2000	0.1275	0.0359	0.0073
4.3	20	0.0700	0.1800	0.1320	0.0309	0.0069
4.5	23	0.0600	0.2100	0.1335	0.0433	0.0090
4.7	23	0.0800	0.2000	0.1196	0.0287	0.0060
4.9	24	0.0600	0.1800	0.1158	0.0354	0.0072
5.1	19	0.0700	0.2500	0.1511	0.0509	0.0117
5.3	19	0.0500	0.2200	0.1316	0.0450	0.0103
5.5	16	0.0900	0.2700	0.1525	0.0497	0.0124
5.7	19	0.0800	0.2300	0.1274	0.0357	0.0082
5.9	26	0.0600	0.1800	0.1177	0.0358	0.0070

Sample RM-05

Height above datum (mm)	N	D(min) (mm)	D(max) (mm)	$\bar{D}$ (mm)	S (mm)	$S/\sqrt{N}$ (mm)
6.1	23	0.0600	0.2100	0.1252	0.0334	0.0070
6.3	20	0.0700	0.2100	0.1320	0.0356	0.0080
6.5	28	0.0400	0.2100	0.1121	0.0402	0.0076
6.7	25	0.0600	0.2000	0.1192	0.0383	0.0077
6.9	25	0.0900	0.2000	0.1268	0.0357	0.0071
7.1	16	0.0700	0.2000	0.1288	0.0388	0.0097
7.3	21	0.0500	0.1800	0.1233	0.0343	0.0075
7.5	18	0.0500	0.2700	0.1339	0.0520	0.0123
7.7	20	0.0500	0.2000	0.1235	0.0369	0.0082
7.9(L)	22	0.0300	0.1600	0.0973	0.0334	0.0071
7.9(H)	11	0.0500	0.1300	0.0918	0.0232	0.0092
8.1(L)	14	0.0700	0.2100	0.1329	0.0356	0.0095
8.1(H)	6	0.0500	0.0900	0.0733	0.0163	0.0067
8.3	27	0.0700	0.2000	0.1119	0.0325	0.0062
8.5(L)	31	0.0500	0.1500	0.0977	0.0256	0.0049
8.5(H)	6	0.0600	0.1200	0.0833	0.0207	0.0084
8.7	24	0.0800	0.1600	0.1196	0.0256	0.0052
8.9	27	0.0600	0.1900	0.1174	0.0360	0.0069
9.1	27	0.0500	0.1700	0.1133	0.0406	0.0074
9.3	23	0.0700	0.2000	0.1239	0.0385	0.0076
9.5	22	0.0600	0.1800	0.1241	0.0371	0.0079
9.7	24	0.0400	0.2000	0.1200	0.0458	0.0093
9.9	24	0.0400	0.2100	0.1200	0.0449	0.0092

Sample RM-05I

Height above datum (mm)	N	D(min) (mm)	D(max) (mm)	$\bar{D}$ (mm)	S (mm)	$S/\sqrt{N}$ (mm)
0.1	22	0.0700	0.2100	0.1432	0.0409	0.0087
0.3	23	0.0700	0.2400	0.1370	0.0423	0.0088
0.5	31	0.0600	0.3000	0.1158	0.0466	0.0084
0.7	24	0.0800	0.2200	0.1308	0.0496	0.0101
0.9(L)	28	0.0700	0.1800	0.1182	0.0275	0.0052
0.9(H)	5	0.0700	0.0900	0.0740	0.0089	0.0040
1.1(L)	25	0.0400	0.2000	0.1108	0.0311	0.0062
1.1(H)	6	0.0600	0.1300	0.0917	0.0293	0.0119
1.3(L)	30	0.0500	0.1500	0.1077	0.0265	0.0048
1.3(H)	2	0.0800	0.1100	0.0950	0.0212	0.0150
1.5	24	0.0700	0.2000	0.1246	0.0277	0.0056
1.7(L)	28	0.0700	0.1800	0.1111	0.0328	0.0062
1.7(H)	5	0.0500	0.1200	0.0880	0.0259	0.0116
1.9(L)	24	0.0600	0.2000	0.1175	0.0361	0.0074
1.9(H)	3	0.0600	0.0700	0.0667	0.0058	0.0033
2.1(L)	29	0.0900	0.2100	0.1424	0.0397	0.0074
2.1(H)	1	0.1100	0.1100	0.1100		
2.3	28	0.0500	0.2000	0.1232	0.0339	0.0064
2.5	26	0.0800	0.2100	0.1346	0.0388	0.0076
2.7(L)	32	0.0700	0.1800	0.1184	0.0293	0.0052
2.7(H)	2	0.0800	0.0900	0.0850	0.0071	0.0050
2.9(L)	24	0.0600	0.1600	0.1004	0.0256	0.0052
2.9(H)	13	0.0600	0.1100	0.0769	0.0193	0.0054
3.1	26	0.0700	0.1900	0.1227	0.0358	0.0070
3.3	27	0.0900	0.2000	0.1315	0.0358	0.0069
3.5	23	0.0500	0.1800	0.1257	0.0324	0.0068

Sample RM-05II

Height above datum (mm)	N	D(min) (mm)	D(max) (mm)	$\bar{D}$ (mm)	S (mm)	$S/\sqrt{N}$ (mm)
0.1	26	0.0800	0.2200	0.1346	0.0385	0.0075
0.3	27	0.0700	0.1800	0.1237	0.0321	0.0062
0.5	29	0.0600	0.1600	0.1000	0.0256	0.0048
0.7	33	0.0600	0.2000	0.1182	0.0321	0.0056
0.9	28	0.0600	0.2100	0.1150	0.0348	0.0066
1.1(L)	26	0.0500	0.1500	0.0919	0.0243	0.0048
1.1(H)	5	0.0500	0.1200	0.0820	0.0286	0.0128
1.3	31	0.0600	0.1600	0.1090	0.0240	0.0043
1.5	24	0.0900	0.2200	0.1354	0.0260	0.0053
1.7	21	0.0600	0.1700	0.1186	0.0329	0.0072
1.9(L)	17	0.0700	0.1400	0.1041	0.0221	0.0054
1.9(H)	5	0.0700	0.1100	0.0940	0.0182	0.0081
2.1	27	0.0700	0.2300	0.1248	0.0332	0.0064
2.3	25	0.0700	0.2200	0.1288	0.0380	0.0076
2.5	23	0.0800	0.2100	0.1213	0.0316	0.0066
2.7	24	0.0600	0.2000	0.1129	0.0382	0.0078
2.9(L)	25	0.0700	0.2200	0.1192	0.0341	0.0068
2.9(H)	8	0.0400	0.1300	0.0813	0.0247	0.0087
3.1	26	0.0700	0.1800	0.1265	0.0298	0.0058
3.3	29	0.0600	0.2000	0.1214	0.0392	0.0073
3.5	26	0.0600	0.1800	0.1188	0.0339	0.0066

Sample RM-05III

Height above datum (mm)	N	D(min) (mm)	D(max) (mm)	$\bar{D}$ (mm)	S (mm)	$S/\sqrt{N}$ (mm)
0.1	33	0.0800	0.2000	0.1273	0.0344	0.0060
0.3	26	0.0700	0.2000	0.1296	0.0350	0.0069
0.5	26	0.0600	0.1500	0.1100	0.0242	0.0047
0.7	24	0.0800	0.2200	0.1308	0.0348	0.0071
0.9(L)	17	0.0800	0.2400	0.1547	0.0598	0.0145
0.9(H)	5	0.0500	0.1000	0.0691	0.0207	0.0062
1.1(L)	24	0.0500	0.1700	0.1100	0.0265	0.0054
1.1(H)	11	0.0400	0.1000	0.0880	0.0342	0.0153
1.3	23	0.0700	0.1800	0.1261	0.0327	0.0068
1.5	25	0.0800	0.2200	0.1316	0.0308	0.0062
1.7	28	0.0700	0.2000	0.1157	0.0323	0.0061
1.9(L)	26	0.0600	0.2000	0.1038	0.0320	0.0063
1.9(H)	5	0.0400	0.1300	0.0880	0.0342	0.0153
2.1	26	0.0800	0.2400	0.1285	0.0458	0.0090
2.3	23	0.0800	0.2500	0.1304	0.0425	0.0089
2.5	29	0.0900	0.2100	0.1220	0.0324	0.0060
2.7(L)	24	0.0900	0.1700	0.1221	0.0234	0.0048
2.7(H)	9	0.0500	0.1000	0.0789	0.0162	0.0054
2.9(L)	24	0.0600	0.1400	0.1046	0.0221	0.0045
2.9(H)	8	0.0500	0.1200	0.0775	0.0271	0.0096
3.1	33	0.0600	0.1800	0.1133	0.0272	0.0047
3.3	27	0.0700	0.2100	0.1322	0.0392	0.0075
3.5	25	0.0700	0.2000	0.1344	0.0290	0.0058

Sample RM-05IV

Height above datum (mm)	N	D(min) (mm)	D(max) (mm)	$\bar{D}$ (mm)	S (mm)	$S/\sqrt{N}$ (mm)
0.1	29	0.0600	0.1900	0.1245	0.0377	0.0070
0.3	33	0.0600	0.1700	0.1176	0.0313	0.0055
0.5	33	0.0600	0.2100	0.1127	0.0319	0.0056
0.7	26	0.0500	0.1900	0.1282	0.0344	0.0067
0.9(L)	21	0.0700	0.2200	0.1181	0.0393	0.0086
0.9(H)	7	0.0600	0.1100	0.0771	0.0243	0.0092
1.1	29	0.0500	0.1800	0.1348	0.0318	0.0059
1.3	31	0.0700	0.2200	0.1090	0.0270	0.0048
1.5	36	0.0600	0.2200	0.1186	0.0347	0.0058
1.7	30	0.0500	0.2100	0.1113	0.0323	0.0059
1.9(L)	27	0.0700	0.2000	0.1104	0.0345	0.0064
1.9(H)	6	0.0700	0.1200	0.0933	0.0225	0.0092
2.1	19	0.0700	0.2000	0.1421	0.0324	0.0079
2.3	24	0.0700	0.1800	0.1250	0.0341	0.0070
2.5	34	0.0500	0.2000	0.1013	0.0283	0.0050
2.7	32	0.0500	0.1500	0.1013	0.0283	0.0050
2.9(L)	27	0.0700	0.1400	0.0956	0.0185	0.0036
2.9(H)	8	0.0500	0.1200	0.0750	0.0207	0.0073
3.1	23	0.0500	0.2200	0.1152	0.0394	0.0082
3.3	26	0.0700	0.1700	0.1227	0.0284	0.0056
3.5	21	0.0700	0.1900	0.1290	0.0353	0.0077

Sample RM-05V

Height above datum (mm)	N	D(min) (mm)	D(max) (mm)	$\bar{D}$ (mm)	S (mm)	$S/\sqrt{N}$ (mm)
0.1	29	0.0800	0.2200	0.1252	0.0342	0.0063
0.3	29	0.0600	0.1700	0.1131	0.0309	0.0057
0.5	23	0.0600	0.1600	0.1208	0.0297	0.0062
0.7	34	0.0600	0.1800	0.1124	0.0295	0.0051
0.9(L)	21	0.0600	0.1500	0.1133	0.0294	0.0064
0.9(H)	4	0.0500	0.1100	0.0700	0.0271	0.0135
1.1(L)	24	0.0600	0.1600	0.0917	0.0238	0.0048
1.1(H)	6	0.0300	0.1100	0.0700	0.0329	0.0134
1.3	25	0.0800	0.1600	0.1120	0.0260	0.0052
1.5	26	0.0500	0.1800	0.1223	0.0322	0.0063
1.7(L)	25	0.0700	0.2200	0.1136	0.0319	0.0064
1.7(H)	4	0.0500	0.0700	0.0600	0.0082	0.0041
1.9(L)	21	0.0700	0.1500	0.1005	0.0256	0.0056
1.9(H)	3	0.0500	0.0900	0.0667	0.0208	0.0120
2.1	22	0.0600	0.1800	0.1318	0.0319	0.0068
2.3	23	0.0500	0.2400	0.1313	0.0379	0.0079
2.5	28	0.0600	0.1700	0.1161	0.0296	0.0056
2.7(L)	34	0.0600	0.1500	0.0962	0.0245	0.0042
2.7(H)	4	0.0400	0.1200	0.0700	0.0356	0.0178
2.9(L)	34	0.0600	0.1600	0.1026	0.0203	0.0035
2.9(H)	5	0.0400	0.0900	0.0680	0.0192	0.0086
3.1	26	0.0800	0.2000	0.1262	0.0328	0.0064
3.3	24	0.0600	0.2300	0.1371	0.0413	0.0084
3.5	26	0.0800	0.1900	0.1335	0.0295	0.0058

Sample RM-05VI

Height above datum (mm)	N	D(min) (mm)	D(max) (mm)	$\bar{D}$ (mm)	S (mm)	$S/\sqrt{N}$ (mm)
0.1	25	0.0700	0.2300	0.1228	0.0435	0.0087
0.3	27	0.0700	0.2300	0.1270	0.0466	0.0090
0.5	30	0.0700	0.1700	0.1210	0.0209	0.0038
0.7	27	0.0700	0.1600	0.1148	0.0255	0.0049
0.9	29	0.0800	0.2100	0.1238	0.0320	0.0059
1.1(L)	22	0.0600	0.2200	0.1041	0.0376	0.0080
1.1(H)	10	0.0500	0.1400	0.0840	0.0317	0.0100
1.3	15	0.0800	0.1900	0.1180	0.0303	0.0078
1.5	16	0.0900	0.2100	0.1306	0.0307	0.0077
1.7	19	0.0700	0.1500	0.1111	0.0223	0.0051
1.9(L)	22	0.0700	0.1500	0.1032	0.0223	0.0048
1.9(H)	8	0.0500	0.1100	0.0875	0.0287	0.0101
2.1	26	0.0900	0.1800	0.1227	0.0207	0.0041
2.3	27	0.0900	0.1600	0.1233	0.0245	0.0047
2.5	22	0.0700	0.1300	0.0977	0.0202	0.0043
2.7(L)	25	0.0600	0.1400	0.0924	0.0231	0.0046
2.7(H)	12	0.0500	0.1000	0.0700	0.0200	0.0058
2.9	23	0.0700	0.1400	0.1100	0.0217	0.0045
3.1	24	0.0700	0.1700	0.1221	0.0219	0.0045
3.3	18	0.0900	0.2300	0.1417	0.0378	0.0089
3.5	23	0.0700	0.2100	0.1283	0.0352	0.0073

Sample SR-01

Height above datum (mm)	N	D(min) (mm)	D(max) (mm)	$\bar{D}$ (mm)	S (mm)	$S/\sqrt{N}$ (mm)
0.1	17	0.0595	0.2713	0.1373	0.0670	0.0162
0.3	13	0.0921	0.3212	0.1730	0.0631	0.0175
0.5	13	0.0867	0.2557	0.1503	0.0423	0.0117
0.7	14	0.0785	0.3335	0.1626	0.0688	0.0185
0.9	13	0.0801	0.2309	0.1424	0.0430	0.0119
1.1	15	0.0681	0.2715	0.1342	0.0534	0.0138
1.3	18	0.0545	0.2038	0.1305	0.0430	0.0101
1.5	17	0.0982	0.2726	0.1566	0.0595	0.0145
1.7	20	0.0386	0.2696	0.1410	0.0549	0.0123
1.9	23	0.0813	0.2683	0.1398	0.0465	0.0097
2.1(L)	21	0.0845	0.1847	0.1361	0.0323	0.0161
2.1(H)	3	0.0387	0.1195	0.0927	0.0457	0.0264
2.3(L)	24	0.0458	0.2813	0.1220	0.0501	0.0102
2.3(H)	5	0.0578	0.1323	0.0950	0.0274	0.0123
2.5	19	0.0696	0.2537	0.1373	0.0423	0.0097
2.7	30	0.0600	0.1885	0.1225	0.0331	0.0060
2.9	19	0.0719	0.2157	0.1422	0.0419	0.0096
3.1	28	0.0518	0.2211	0.1146	0.0343	0.0065
3.3	24	0.0699	0.1938	0.1149	0.0290	0.0059
3.5	22	0.0378	0.2150	0.1367	0.0413	0.0088
3.7	21	0.0681	0.2386	0.1708	0.0357	0.0078
3.9	17	0.0723	0.2776	0.1717	0.0564	0.0137
4.1	23	0.0737	0.2638	0.1557	0.0594	0.0124
4.3(L)	21	0.0499	0.2068	0.1164	0.0434	0.0095
4.3(H)	3	0.1058	0.1657	0.1418	0.0317	0.0183
4.5	23	0.0777	0.2317	0.1249	0.0404	0.0084
4.7	22	0.0834	0.2870	0.1467	0.0490	0.0104
4.9	20	0.0751	0.2140	0.1398	0.0417	0.0093
5.1	16	0.0779	0.2450	0.1557	0.0462	0.0115
5.3	25	0.0499	0.2229	0.1252	0.0474	0.0095
5.5	23	0.0633	0.2318	0.1234	0.0382	0.0080
5.7	21	0.0378	0.2235	0.1297	0.0500	0.0109

Sample SR-01

Height above datum (mm)	N	D(min) (mm)	D(max) (mm)	$\overline{D}$ (mm)	S (mm)	$S/\sqrt{N}$ (mm)
5.9	17	0.1020	0.2159	0.1614	0.0438	0.0106
6.1	25	0.0659	0.1938	0.1267	0.0391	0.0078
6.3	21	0.0705	0.2123	0.1343	0.0369	0.0081
6.5	19	0.0848	0.1957	0.1433	0.0343	0.0079
6.7	15	0.0807	0.2414	0.1478	0.0480	0.0124
6.9	25	0.0691	0.1853	0.1312	0.0366	0.0073
7.1	22	0.0560	0.2069	0.1282	0.0349	0.0074
7.3	17	0.0847	0.2226	0.1637	0.0376	0.0091
7.5	16	0.1053	0.2373	0.1689	0.0383	0.0096
7.7	24	0.0656	0.2353	0.1480	0.0444	0.0091
7.9	23	0.0845	0.1865	0.1256	0.0275	0.0057
8.1	24	0.0832	0.2017	0.1352	0.0337	0.0069
8.3	20	0.0643	0.2678	0.1308	0.0521	0.0116
8.5	21	0.0597	0.1639	0.1127	0.0288	0.0063
8.7	21	0.0739	0.2047	0.1370	0.0297	0.0065
8.9	20	0.0687	0.1747	0.1207	0.0333	0.0074
9.1	16	0.1036	0.2259	0.1514	0.0352	0.0088
9.3	17	0.0594	0.2276	0.1322	0.0456	0.0111
9.5	14	0.0844	0.3869	0.1649	0.0773	0.0207
9.7	14	0.0477	0.2776	0.1598	0.0652	0.0174
9.9	19	0.0647	0.2710	0.1384	0.0489	0.0112
10.1	20	0.0826	0.2202	0.1460	0.0412	0.0092
10.3	27	0.0614	0.2159	0.1172	0.0364	0.0070
10.5	17	0.0921	0.1881	0.1377	0.0266	0.0064
10.7	14	0.0518	0.2667	0.1306	0.0519	0.0139
10.9	23	0.0502	0.1776	0.1189	0.0388	0.0081
11.1	20	0.0571	0.2035	0.1209	0.0342	0.0077
11.3	16	0.0705	0.1791	0.1241	0.0449	0.0112
11.5	10	0.0785	0.2608	0.1526	0.0535	0.0169
11.7	15	0.0854	0.2637	0.1643	0.0491	0.0127
11.9	15	0.0880	0.2394	0.1600	0.0476	0.0122
12.1	16	0.1123	0.1906	0.1461	0.0245	0.0061

Sample SR-01

Height above datum (mm)	N	D(min) (mm)	D(max) (mm)	$\overline{D}$ (mm)	S (mm)	$S/\sqrt{N}$ (mm)
12.3	12	0.0910	0.3267	0.1978	0.0793	0.0229
12.5	12	0.1328	0.3007	0.1832	0.0489	0.0141
12.7	14	0.0743	0.3088	0.1584	0.0746	0.0199
12.9	16	0.0777	0.2529	0.1539	0.0534	0.0133
13.1	13	0.0785	0.2605	0.1476	0.0528	0.0147
13.3	17	0.0730	0.2285	0.1468	0.0468	0.0114
13.5	12	0.0723	0.4001	0.1953	0.0950	0.0274
13.7	19	0.0730	0.2260	0.1422	0.0445	0.0102
13.9	18	0.0854	0.2423	0.1594	0.0493	0.0116
14.1	22	0.0723	0.3297	0.1502	0.0665	0.0142
14.3	15	0.0102	0.2751	0.1764	0.0481	0.0124
14.5	19	0.0810	0.2596	0.1715	0.0504	0.0116
14.7	19	0.0428	0.2433	0.1587	0.0549	0.0126
14.9	19	0.1012	0.2189	0.1449	0.0330	0.0076
15.1	17	0.0702	0.2108	0.1437	0.0385	0.0093

Sample SR-02

Height above datum (mm)	N	D(min) (mm)	D(max) (mm)	$\bar{D}$ (mm)	S (mm)	$S/\sqrt{N}$ (mm)
0.1	19	0.0885	0.1969	0.1337	0.0287	0.0066
0.3	17	0.0936	0.2048	0.1327	0.0328	0.0080
0.5	17	0.0562	0.1727	0.1344	0.0291	0.0071
0.7	18	0.0776	0.2307	0.1400	0.0409	0.0096
0.9	15	0.0665	0.2009	0.1496	0.0405	0.0105
1.1	19	0.0914	0.1938	0.1324	0.0253	0.0058
1.3	18	0.0708	0.1712	0.1189	0.0290	0.0068
1.5	23	0.0353	0.2453	0.1090	0.0418	0.0087
1.7(L)	18	0.0600	0.2084	0.1292	0.0407	0.0096
1.7(H)	4	0.0647	0.1348	0.1082	0.0316	0.0158
1.9	17	0.0703	0.2330	0.1417	0.0414	0.0101
2.1	17	0.0660	0.2302	0.1460	0.0438	0.0106
2.3(L)	13	0.0574	0.1784	0.1314	0.0368	0.0102
2.5	21	0.0777	0.0194	0.1266	0.0303	0.0066
2.7	21	0.0742	0.2519	0.1489	0.0397	0.0087
2.9	20	0.0735	0.2520	0.1458	0.0480	0.0107
3.1	19	0.0921	0.1898	0.1407	0.0250	0.0057
3.3	21	0.0687	0.2248	0.1371	0.0409	0.0089
3.5	19	0.0698	0.2075	0.1317	0.0317	0.0073
3.7	17	0.0895	0.3183	0.1453	0.0625	0.0152
3.9	21	0.0764	0.2174	0.1342	0.0361	0.0079
4.1	15	0.0977	0.2547	0.1494	0.0434	0.0112
4.3	19	0.0810	0.1746	0.1327	0.0303	0.0070
4.5	14	0.0934	0.1911	0.1413	0.0290	0.0077
4.7	22	0.0491	0.1826	0.1265	0.0383	0.0082
4.9	18	0.0889	0.1877	0.1300	0.0328	0.0077
5.1	15	0.0590	0.2042	0.1276	0.0395	0.0102
5.3	13	0.1012	0.2135	0.1489	0.0351	0.0097
5.5	16	0.0210	0.2210	0.1487	0.0525	0.0131
5.7	18	0.0647	0.1870	0.1368	0.0381	0.0090
5.9	14	0.0871	0.2407	0.1446	0.0416	0.0111
6.1(L)	14	0.0807	0.2255	0.1413	0.0392	0.0105

Sample SR-02

Height above datum (mm)	N	D(min) (mm)	D(max) (mm)	$\bar{D}$ (mm)	S (mm)	S/ N (mm)
6.1(H)	2	0.0957	0.1259	0.1108	0.0213	0.0151
6.3(L)	20	0.0645	0.1724	0.1149	0.0292	0.0065
6.3(H)	4	0.1002	0.1579	0.1175	0.0274	0.0137
6.5(L)	16	0.0910	0.1582	0.1274	0.0225	0.0056
6.5(H)	6	0.0643	0.1441	0.1123	0.0336	0.0137
6.7(L)	11	0.0878	0.2521	0.1507	0.0465	0.0140
6.7(H)	4	0.1078	0.1435	0.1311	0.0159	0.0080
6.9(L)	16	0.1107	0.1927	0.1443	0.0268	0.0067
6.9(H)	4	0.1291	0.2455	0.1689	0.0534	0.0267
7.1(L)	24	0.0657	0.1728	0.1119	0.0207	0.0055
7.1(H)	2	0.0668	0.0817	0.0742	0.0105	0.0074
7.3(L)	18	0.0883	0.1887	0.1246	0.0258	0.0061
7.3(H)	2	0.0891	0.0918	0.0904	0.0019	0.0013
7.5	20	0.0827	0.1706	0.1288	0.0210	0.0047
7.7	16	0.0921	0.1950	0.1358	0.0300	0.0075
7.9	18	0.0739	0.1887	0.1288	0.0288	0.0068
8.1	20	0.0174	0.2306	0.1232	0.0484	0.0108
8.3	15	0.0606	0.1553	0.1044	0.0304	0.0078
8.5	16	0.0647	0.1865	0.1457	0.0323	0.0081
8.7	20	0.0457	0.2197	0.1244	0.0421	0.0094
8.9	18	0.0958	0.1838	0.1390	0.0246	0.0058
9.1	14	0.0692	0.2145	0.1554	0.0392	0.0105
9.3	10	0.0810	0.2296	0.1634	0.0440	0.0139
9.5	15	0.0723	0.2035	0.1439	0.0361	0.0093
9.7	11	0.0680	0.2071	0.1448	0.0460	0.0139
9.9	12	0.0565	0.2148	0.1238	0.0491	0.0142
10.1	14	0.0962	0.2070	0.1495	0.0383	0.0102
10.3	14	0.0471	0.2982	0.1507	0.0674	0.0180
10.5	14	0.0820	0.2506	0.1372	0.0504	0.0135
10.7	18	0.0612	0.2346	0.1297	0.0483	0.0114

Sample SR-02

Height above datum (mm)	N	D(min) (mm)	D(max) (mm)	$\bar{D}$ (mm)	S (mm)	$S/\sqrt{N}$ (mm)
10.9	15	0.0280	0.2255	0.1376	0.0549	0.0142
11.1	26	0.0595	0.2084	0.1278	0.0365	0.0072
11.3	22	0.0792	0.2297	0.1364	0.0418	0.0089
11.5	20	0.0720	0.2191	0.1162	0.0374	0.0084
11.7	22	0.0543	0.2362	0.1196	0.0468	0.0100
11.9	21	0.0581	0.2543	0.1337	0.0457	0.0100
12.1	15	0.0930	0.1719	0.1315	0.0229	0.0059
12.3	15	0.0644	0.3030	0.1372	0.0549	0.0142
12.5	20	0.0575	0.1840	0.1404	0.0298	0.0067
12.7	20	0.0632	0.2042	0.1223	0.0421	0.0094
12.9	18	0.0698	0.2222	0.1387	0.0432	0.0102
13.1	17	0.0740	0.1714	0.1268	0.0261	0.0063
13.3	15	0.0877	0.2691	0.1411	0.0487	0.0126
13.5	18	0.0643	0.1904	0.1348	0.0411	0.0097
13.7	13	0.1119	0.3273	0.1762	0.0678	0.0188
13.9	16	0.0675	0.2787	0.1454	0.0577	0.0144
14.1	14	0.0988	0.2517	0.1599	0.0442	0.0118
14.3	16	0.0667	0.2584	0.1514	0.0476	0.0119
14.5	16	0.0802	0.2294	0.1396	0.0489	0.0122
14.7	16	0.0818	0.2003	0.1304	0.0404	0.0101
14.9	16	0.0877	0.3163	0.1576	0.0593	0.0148

Sample MB-01

Height below datum (mm)	N	D(min) (mm)	D(max) (mm)	$\bar{D}$ (mm)	S (mm)	$S/\sqrt{N}$ (mm)
0.1	16	0.0845	0.2089	0.1354	0.0388	0.0097
0.3	20	0.0561	0.1576	0.1118	0.0345	0.0077
0.5	27	0.0541	0.1767	0.0937	0.0297	0.0057
0.7	20	0.0515	0.1890	0.1178	0.0391	0.0088
0.9	20	0.0932	0.2392	0.1415	0.0427	0.0095
1.1	18	0.0564	0.1788	0.1324	0.0424	0.0100
1.3	13	0.0483	0.2189	0.1297	0.0483	0.0134
1.5	11	0.0655	0.2328	0.1270	0.0479	0.0145
1.7	10	0.0895	0.1540	0.1185	0.0226	0.0071
1.9	11	0.0791	0.1810	0.1264	0.0285	0.0086
2.1	8	0.1018	0.1941	0.1561	0.0271	0.0096
2.3	12	0.1014	0.1859	0.1363	0.0283	0.0082
2.5	11	0.1001	0.2078	0.1500	0.0319	0.0096
2.7	15	0.0615	0.2048	0.1369	0.0491	0.0127
2.9	16	0.0827	0.2267	0.1321	0.0272	0.0068
3.1	20	0.0867	0.2069	0.1361	0.0272	0.0061
3.3	17	0.0623	0.2557	0.1307	0.0600	0.0146
3.5	17	0.0725	0.2813	0.1321	0.0553	0.0134
3.7	18	0.0751	0.2028	0.1315	0.0345	0.0081
3.9	17	0.0607	0.1994	0.1314	0.0358	0.0087
4.1	12	0.0634	0.2065	0.1259	0.0495	0.0143
4.3	18	0.0960	0.2504	0.1518	0.0440	0.0104
4.5	17	0.1072	0.2267	0.1493	0.0403	0.0099
4.7	16	0.0671	0.2308	0.1304	0.0456	0.0114
4.9	19	0.0618	0.1926	0.1283	0.0412	0.0094
5.1	18	0.0208	0.2102	0.1353	0.0461	0.0109
5.3	17	0.0735	0.2338	0.1317	0.0360	0.0087
5.5	21	0.0737	0.1827	0.1146	0.0282	0.0062
5.7	17	0.0561	0.2333	0.1462	0.0465	0.0113
5.9	18	0.0737	0.2343	0.1445	0.0462	0.0109
6.1	17	0.0737	0.1696	0.1259	0.0293	0.0071
6.3	18	0.0582	0.1849	0.1248	0.0388	0.0091
6.5	17	0.1277	0.2157	0.1567	0.0270	0.0065

Sample MB-01

Height above datum (mm)	N	D(min) (mm)	D(max) (mm)	$\bar{D}$ (mm)	S (mm)	$S/\sqrt{N}$ (mm)
6.7	18	0.0593	0.1798	0.1217	0.0400	0.0094
6.9	16	0.0626	0.3286	0.1443	0.0630	0.0157
7.1	16	0.0582	0.1879	0.1363	0.0407	0.0102
7.3	14	0.0987	0.2736	0.1820	0.0485	0.0130
7.5	13	0.0817	0.2704	0.1590	0.0650	0.0180
7.7	20	0.0549	0.2179	0.1208	0.0434	0.0097
7.9	19	0.0738	0.2818	0.1283	0.0490	0.0113
8.1	19	0.0695	0.2065	0.1301	0.0374	0.0086
8.3	18	0.0698	0.2989	0.1270	0.0561	0.0132
8.5	13	0.0900	0.2670	0.1672	0.0576	0.0160
8.7	12	0.1010	0.3870	0.1514	0.0803	0.0232
8.9	18	0.0980	0.2470	0.1609	0.0410	0.0097
9.1	17	0.0830	0.1910	0.1318	0.0325	0.0079
9.3	21	0.0640	0.2320	0.1256	0.0409	0.0089
9.5	16	0.0690	0.1790	0.1228	0.0389	0.0097
9.7	19	0.0640	0.2660	0.1364	0.0512	0.0117
9.9	16	0.0620	0.2600	0.1374	0.0536	0.0134
10.1	10	0.1010	0.2390	0.1752	0.0497	0.0157
10.3	16	0.0620	0.2430	0.1367	0.0456	0.0114
10.5	13	0.1070	0.1810	0.1431	0.0227	0.0063
10.7	17	0.0730	0.2510	0.1521	0.0445	0.0108
10.9	14	0.0740	0.2010	0.1231	0.0393	0.0105
11.1	17	0.0870	0.2130	0.1337	0.0324	0.0079
11.3	19	0.0790	0.3750	0.1477	0.0616	0.0141
11.5	20	0.0710	0.2090	0.1373	0.0342	0.0076
11.7	14	0.0820	0.2470	0.1627	0.0480	0.0128
11.9	12	0.0900	0.1920	0.1533	0.0275	0.0079
12.1	16	0.0730	0.3140	0.1331	0.0586	0.0147
12.3	17	0.0620	0.2080	0.1424	0.0386	0.0094
12.5	11	0.1150	0.2450	0.1787	0.0420	0.0127
12.7	14	0.1250	0.2290	0.1634	0.0353	0.0094
12.9	14	0.1010	0.3300	0.1789	0.0614	0.0164
13.1	12	0.0740	0.2620	0.1525	0.0609	0.0176

Sample MB-01

Height above datum (mm)	N	D(min) (mm)	D(max) (mm)	$\bar{D}$ (mm)	S (mm)	$S/\sqrt{N}$ (mm)
13.3	18	0.0620	0.2230	0.1429	0.0461	0.0109
13.5	16	0.0990	0.2670	0.1543	0.0441	0.0110
13.7	21	0.0800	0.1950	0.1331	0.0271	0.0059
13.9	15	0.0710	0.2590	0.1543	0.0489	0.0126
14.1	12	0.0810	0.2500	0.1442	0.0416	0.0120
14.3	14	0.0960	0.1710	0.1406	0.0268	0.0072
14.5	15	0.0850	0.2140	0.1481	0.0376	0.0097
14.7	17	0.0860	0.2380	0.1257	0.0349	0.0085
14.9	15	0.0760	0.1590	0.1318	0.0248	0.0064
15.1	15	0.1030	0.1860	0.1296	0.0208	0.0054

Sample MB-02

Height above datum (mm)	N	D(min) (mm)	D(max) (mm)	$\bar{D}$ (mm)	S (mm)	$S/\sqrt{N}$ (mm)
0.1	20	0.0640	0.1170	0.1205	0.0352	0.0079
0.3	17	0.0780	0.2150	0.1241	0.0352	0.0086
0.5	22	0.0890	0.2070	0.1194	0.0273	0.0058
0.7	18	0.0730	0.2130	0.1344	0.0352	0.0083
0.9	24	0.0640	0.0208	0.1152	0.0316	0.0064
1.1	22	0.0620	0.1900	0.1210	0.0339	0.0072
1.3	20	0.0470	0.1900	0.1168	0.0377	0.0084
1.5	17	0.0660	0.1970	0.1367	0.0445	0.0108
1.7	15	0.0180	0.2310	0.1081	0.0480	0.0124
1.9	17	0.0590	0.1910	0.1308	0.0284	0.0069
2.1	20	0.0700	0.1820	0.1242	0.0313	0.0070
2.3	21	0.0700	0.2180	0.1260	0.0382	0.0083
2.5	20	0.0640	0.3300	0.1307	0.0543	0.0122
2.7	13	0.0710	0.1940	0.1491	0.0420	0.0116
2.9	15	0.0760	0.2050	0.1308	0.0333	0.0086
3.1	15	0.0456	0.1853	0.1183	0.0398	0.0103
3.3	22	0.0592	0.2170	0.1160	0.0375	0.0080
3.5	19	0.0490	0.2108	0.1373	0.0492	0.0113
3.7	23	0.0647	0.2052	0.1261	0.0332	0.0069
3.9	25	0.0490	0.1789	0.1133	0.0368	0.0074
4.1	23	0.0690	0.1750	0.1079	0.0316	0.0066
4.3	20	0.0490	0.1480	0.1009	0.0275	0.0062
4.5	18	0.0710	0.1770	0.1229	0.0334	0.0079
4.7	18	0.0630	0.2250	0.1284	0.0314	0.0074
4.9	20	0.0730	0.2590	0.1268	0.0526	0.0118
5.1	18	0.0860	0.2360	0.1446	0.0394	0.0093
5.3	13	0.0990	0.2180	0.1463	0.0356	0.0099
5.5	12	0.0730	0.3500	0.1503	0.0753	0.0217
5.7	15	0.0760	0.2360	0.1458	0.0437	0.0113
5.9	20	0.0800	0.2790	0.1364	0.0449	0.0100
6.1	22	0.0470	0.1840	0.1180	0.0382	0.0081
6.3	14	0.1050	0.2400	0.1581	0.0376	0.0101

Sample MB-02

Height above datum (mm)	N	D(min) (mm)	D(max) (mm)	$\bar{D}$ (mm)	S (mm)	$S/\sqrt{N}$ (mm)
6.5	17	0.0540	0.2010	0.1290	0.0357	0.0086
6.7	16	0.0570	0.2730	0.1489	0.0496	0.0124
6.9	16	0.0920	0.2520	0.1460	0.0452	0.0113
7.1	14	0.1090	0.2670	0.1754	0.0495	0.0132
7.3	18	0.0640	0.1960	0.1218	0.0403	0.0095
7.5	18	0.0670	0.2070	0.1316	0.0350	0.0083
7.7	15	0.0610	0.2000	0.1307	0.0392	0.0101
7.9	15	0.0920	0.2390	0.1516	0.0424	0.0109
8.1	16	0.0620	0.2470	0.1569	0.0562	0.0140
8.3	15	0.0740	0.2160	0.1376	0.0522	0.0135
8.5	17	0.0700	0.1970	0.1233	0.0321	0.0078
8.7	20	0.0700	0.2220	0.1331	0.0443	0.0099
8.9	13	0.0900	0.2050	0.1423	0.0330	0.0092
9.1	11	0.0610	0.2640	0.1638	0.0626	0.0189
9.3	17	0.0690	0.1890	0.1312	0.0333	0.0081
9.5	18	0.0790	0.1770	0.1329	0.0218	0.0051
9.7	15	0.0770	0.2000	0.1339	0.0344	0.0089
9.9	17	0.0824	0.2403	0.1576	0.0455	0.0110
10.1	13	0.0714	0.2476	0.1677	0.0569	0.0158
10.3	24	0.0660	0.2500	0.1324	0.0442	0.0090
10.5	16	0.0710	0.2320	0.1369	0.0428	0.0107
10.7	17	0.0900	0.1910	0.1451	0.0314	0.0076
10.9	14	0.0990	0.2260	0.1511	0.0378	0.0101
11.1	22	0.0740	0.2630	0.1323	0.0487	0.0104
11.3	20	0.0660	0.1940	0.1301	0.0329	0.0074
11.5	22	0.0760	0.1740	0.1155	0.0274	0.0058
11.7	24	0.0550	0.1700	0.1094	0.0313	0.0064
11.9	20	0.0870	0.1810	0.1318	0.0286	0.0064
12.1	21	0.0760	0.2160	0.1344	0.0356	0.0078
12.3	15	0.0870	0.2270	0.1492	0.0360	0.0093
12.5	18	0.0620	0.2840	0.1396	0.0517	0.0122
12.7	13	0.1130	0.2470	0.1768	0.0438	0.0122

Sample MB-02

Height above datum (mm)	N	D(min) (mm)	D(max) (mm)	$\bar{D}$ (mm)	S (mm)	$S/\sqrt{N}$ (mm)
12.9	9	0.0910	0.2580	0.1650	0.0657	0.0122
13.1	17	0.0690	0.2180	0.1468	0.0358	0.0219
13.3	19	0.0770	0.1860	0.1302	0.0321	0.0074
13.5	17	0.0910	0.2040	0.1422	0.0327	0.0088
13.7	12	0.0880	0.2880	0.1557	0.0555	0.0160
13.9	18	0.0880	0.2110	0.1341	0.0360	0.0085
14.1	14	0.1010	0.2150	0.1634	0.0332	0.0089
14.3	13	0.1280	0.2860	0.1724	0.0439	0.0122
14.5	17	0.0990	0.2340	0.1482	0.0358	0.0087
14.7	16	0.1030	0.2280	0.1473	0.0329	0.0082
14.9	17	0.1110	0.2240	0.1654	0.0321	0.0078
15.1	18	0.0610	0.2000	0.1372	0.0410	0.0097
15.3	18	0.0580	0.2090	0.1319	0.0429	0.0101

Sample MB-03I

Height above datum (mm)	N	D(min) (mm)	D(max) (mm)	$\bar{D}$ (mm)	S (mm)	$S/\sqrt{N}$ (mm)
0.1	14	0.0930	0.1870	0.1326	0.0244	0.0065
0.3	17	0.1110	0.2080	0.1439	0.0256	0.0062
0.5	13	0.1160	0.1740	0.1361	0.0159	0.0044
0.7	11	0.0700	0.2080	0.1305	0.0411	0.0124
0.9	12	0.0770	0.2080	0.1404	0.0420	0.0121
1.1	12	0.0640	0.2530	0.1581	0.0535	0.0155
1.3	18	0.0470	0.2330	0.1428	0.0495	0.0117
1.5	13	0.0750	0.2280	0.1352	0.0456	0.0125
1.7	16	0.0660	0.2000	0.1411	0.0399	0.0100
1.9	21	0.0630	0.1810	0.1235	0.0342	0.0075
2.1	17	0.0770	0.2130	0.1351	0.0316	0.0077
2.3	17	0.0790	0.1930	0.1332	0.0342	0.0083
2.5	15	0.0830	0.1900	0.1395	0.0330	0.0085
2.7	11	0.0860	0.1980	0.1427	0.0414	0.0125
2.9	15	0.0810	0.3820	0.1554	0.0708	0.0183
3.1	13	0.0710	0.1880	0.1252	0.0402	0.0111
3.3	14	0.1030	0.2190	0.1536	0.0385	0.0103
3.5	10	0.1040	0.3070	0.1536	0.0615	0.0194
3.7	15	0.0890	0.2050	0.1416	0.0360	0.0093
3.9	15	0.0520	0.2230	0.1399	0.0423	0.0109
4.1	14	0.075	0.2440	0.1458	0.0460	0.0123
4.3	14	0.0680	0.2220	0.1336	0.0469	0.0125
4.5	11	0.0540	0.1970	0.1368	0.0440	0.0133
4.7	17	0.0960	0.2040	0.1400	0.0340	0.0083
4.9	19	0.0790	0.2990	0.1560	0.0517	0.0119
5.1	14	0.0750	0.2160	0.1316	0.0438	0.0117
5.3	13	0.1140	0.3140	0.1603	0.0530	0.0147
5.5	17	0.0980	0.2120	0.1452	0.0299	0.0073
5.7	13	0.0880	0.2180	0.1453	0.0380	0.0105
5.9	10	0.1050	0.1930	0.1528	0.0319	0.0101
6.1	14	0.0840	0.2360	0.1493	0.0393	0.0105
6.3	14	0.1110	0.2560	0.1573	0.0478	0.0128
6.5	13	0.1080	0.2530	0.1687	0.0407	0.0113

Sample MB-03I

Height above datum (mm)	N	D(min) (mm)	D(max) (mm)	$\bar{D}$ (mm)	S (mm)	$S/\sqrt{N}$ (mm)
6.7	17	0.0750	0.1890	0.1313	0.0293	0.0071
6.9	18	0.0600	0.2320	0.1414	0.0501	0.0118
7.1	11	0.0820	0.1940	0.1321	0.0359	0.0108
7.3	16	0.0840	0.2820	0.1583	0.0471	0.0118
7.5	16	0.0770	0.2150	0.1388	0.0398	0.0099
7.7	14	0.0820	0.2360	0.1525	0.0445	0.0119
7.9	23	0.0730	0.2090	0.1257	0.0328	0.0068
8.1	9	0.1120	0.2150	0.1819	0.0357	0.0119
8.3	16	0.0870	0.2060	0.1406	0.0354	0.0088
8.5	18	0.0770	0.1560	0.1190	0.0233	0.0055
8.7	17	0.0820	0.1840	0.1206	0.02840	0.0069
8.9	16	0.0990	0.2370	0.1583	0.0386	0.0096
9.1	16	0.0570	0.2740	0.1622	0.0620	0.0155
9.3	18	0.0860	0.2270	0.1525	0.0379	0.0089
9.5	16	0.0790	0.2300	0.1491	0.0424	0.0106
9.7	16	0.1090	0.1890	0.1463	0.0219	0.0055
9.9	17	0.0690	0.2210	0.1272	0.0376	0.0091
10.1	15	0.0590	0.2700	0.1501	0.0550	0.0142
10.3	14	0.0910	0.2540	0.1507	0.0503	0.0134
10.5	19	0.0150	0.2300	0.1397	0.0513	0.0118
10.7	15	0.0690	0.2710	0.1488	0.0516	0.0133
10.9	16	0.0840	0.2290	0.1497	0.0394	0.0099
11.1	14	0.0610	0.2850	0.1557	0.0568	0.0152
11.3	13	0.0640	0.1990	0.1308	0.0354	0.0098
11.5	14	0.0950	0.2880	0.1581	0.0512	0.0137
11.7	16	0.0790	0.2230	0.1471	0.0404	0.0101
11.9	14	0.1150	0.2250	0.1516	0.0351	0.0094
12.1	16	0.0670	0.2760	0.1558	0.0461	0.0115
12.3	21	0.0770	0.2430	0.1219	0.0421	0.0092
12.5	20	0.0720	0.1680	0.1284	0.0236	0.0053
12.7	20	0.0740	0.1790	0.1315	0.0276	0.0062
12.9	14	0.0970	0.2410	0.1514	0.0453	0.0121
13.1	16	0.0760	0.2530	0.1430	0.0529	0.0132

Sample MB-03I

Height above datum (mm)	N	D(min) (mm)	D(max) (mm)	$\bar{D}$ (mm)	S (mm)	$S/\sqrt{N}$ (mm)
13.3	14	0.0490	0.2070	0.1269	0.0398	0.0106
13.5	23	0.0560	0.2050	0.1115	0.0335	0.0070
13.7	18	0.0960	0.1810	0.1388	0.0227	0.0054
13.9	16	0.0720	0.1970	0.1419	0.0329	0.0082
14.1	15	0.0800	0.3090	0.1693	0.0588	0.0152
14.3						
14.5	15	0.0520	0.2240	0.1431	0.0530	0.0137
14.7	15	0.0950	0.2120	0.1517	0.0382	0.0099
14.9	20	0.0800	0.2270	0.1395	0.0417	0.0093

Sample MB-03II

Height above datum (mm)	N	D(min) (mm)	D(max) (mm)	$\bar{D}$ (mm)	S (mm)	$S/\sqrt{N}$ (mm)
0.1	19	0.0900	0.1820	0.1214	0.0240	0.0055
0.3	17	0.0920	0.1910	0.1376	0.0314	0.0076
0.5	14	0.0910	0.2590	0.1447	0.0411	0.0110
0.7	12	0.0940	0.2040	0.1503	0.0343	0.0099
0.9	12	0.0960	0.2840	0.1620	0.0509	0.0147
1.1	13	0.1000	0.2160	0.1445	0.0314	0.0087
1.3	12	0.1140	0.2620	0.1673	0.0434	0.0125
1.5	11	0.0860	0.2020	0.1350	0.0351	0.0106
1.7	14	0.0690	0.1720	0.1283	0.0363	0.0097
1.9	15	0.0670	0.2060	0.1373	0.0443	0.0118
2.1	13	0.0660	0.1870	0.1329	0.0342	0.0095
2.3	17	0.0940	0.2150	0.1412	0.0342	0.0083
2.5	13	0.1110	0.2250	0.1358	0.0294	0.0082
2.7	16	0.0800	0.1780	0.1349	0.0282	0.0071
2.9	14	0.0700	0.1830	0.1242	0.0309	0.0083
3.1	20	0.0590	0.1770	0.1219	0.0331	0.0074
3.3	12	0.1230	0.2330	0.1599	0.0300	0.0086
3.5	14	0.0910	0.1980	0.1465	0.0321	0.0086
3.7	13	0.0760	0.2140	0.1453	0.0381	0.0083
3.9	20	0.0760	0.1930	0.1255	0.0406	0.0091
4.1	11	0.0800	0.1850	0.1339	0.0383	0.0115
4.3	12	0.0820	0.2390	0.1535	0.0480	0.0138
4.5	19	0.0800	0.2120	0.1314	0.0391	0.0090
4.7	13	0.0710	0.2050	0.1299	0.0358	0.0099
4.9	13	0.0900	0.1930	0.1325	0.0356	0.0099
5.1	16	0.0840	0.2150	0.1519	0.0382	0.0095
5.3	12	0.0910	0.2250	0.1447	0.0351	0.0101
5.5	15	0.0810	0.2180	0.1452	0.0448	0.0116
5.7	13	0.0860	0.2840	0.1465	0.0537	0.0149
5.9	12	0.1010	0.3830	0.1652	0.0726	0.0210

Sample MB-03III

Height above datum (mm)	N	D(min) (mm)	D(max) (mm)	$\bar{D}$ (mm)	S (mm)	$S/\sqrt{N}$ (mm)
0.1	18	0.0710	0.2050	0.1337	0.0339	0.0080
0.3	17	0.0910	0.2100	0.1365	0.0298	0.0072
0.5	15	0.0840	0.2010	0.1383	0.0351	0.0091
0.7	19	0.0800	0.2030	0.1367	0.0327	0.0075
0.9	14	0.0870	0.2050	0.1443	0.0359	0.0096
1.1	14	0.0850	0.2140	0.1469	0.0368	0.0098
1.3	19	0.0940	0.2050	0.1518	0.0330	0.0076
1.5	13	0.0930	0.2430	0.1487	0.0469	0.0130
1.7	17	0.0900	0.2410	0.1504	0.0392	0.0095
1.9	15	0.0910	0.2380	0.1561	0.0465	0.0120
2.1	16	0.0820	0.2020	0.1392	0.0318	0.0080
2.3	19	0.0640	0.1800	0.1268	0.0292	0.0067
2.5	23	0.0640	0.2120	0.1263	0.0385	0.0080
2.7	21	0.0560	0.1720	0.1141	0.0235	0.0110
2.9	17	0.1000	0.1830	0.1377	0.0262	0.0064
3.1	17	0.0770	0.1860	0.1220	0.0292	0.0071
3.3	11	0.0940	0.2130	0.1434	0.0460	0.0139
3.5	16	0.0690	0.2270	0.1432	0.0481	0.0120
3.7	16	0.0670	0.2750	0.1452	0.0510	0.0128
3.9	14	0.0600	0.3000	0.1507	0.0611	0.0163
4.1	14	0.0590	0.2090	0.1468	0.0446	0.0119
4.3	14	0.0920	0.2320	0.1480	0.0430	0.0115
4.5	17	0.0790	0.2680	0.1612	0.0576	0.0140
4.7						
4.9	17	0.0910	0.2010	0.1479	0.0309	0.0075
5.1	18	0.0800	0.2430	0.1439	0.0377	0.0089
5.3	14	0.1120	0.2080	0.1481	0.0290	0.0077
5.5	14	0.0680	0.2590	0.1596	0.0520	0.0139
5.7	17	0.0540	0.2830	0.1310	0.0532	0.0129
5.9	16	0.0960	0.2140	0.1493	0.0379	0.0095

Sample MB-03IV

Height above datum (mm)	N	D(min) (mm)	D(max) (mm)	$\bar{D}$ (mm)	S (mm)	$S/\sqrt{N}$ (mm)
0.1	19	0.0820	0.1970	0.1308	0.0323	0.0074
0.3	16	0.0660	0.1940	0.1333	0.0372	0.0093
0.5	20	0.0750	0.2360	0.1428	0.0402	0.0090
0.7	20	0.0760	0.2110	0.1361	0.0386	0.0086
0.9	15	0.0970	0.2290	0.1502	0.0333	0.0086
1.1	22	0.0880	0.2010	0.1321	0.0286	0.0061
1.3	17	0.0890	0.2080	0.1445	0.0298	0.0072
1.5	16	0.0940	0.2570	0.1459	0.0497	0.0124
1.7	18	0.0830	0.2150	0.1374	0.0383	0.0090
1.9	19	0.0960	0.2470	0.1520	0.0383	0.0088
2.1	16	0.0990	0.2490	0.1573	0.0451	0.0113
2.3	15	0.1020	0.2360	0.1551	0.0398	0.0103
2.5	20	0.0750	0.1960	0.1399	0.0381	0.0085
2.7	22	0.0780	0.1750	0.1364	0.0294	0.0063
2.9	19	0.0860	0.2300	0.1311	0.0357	0.0082
3.1	19	0.1090	0.1980	0.1501	0.0254	0.0058
3.3	15	0.0980	0.2260	0.1535	0.0400	0.0103
3.5	18	0.0770	0.2650	0.1438	0.0509	0.0120
3.7	14	0.1190	0.2450	0.1703	0.0378	0.0101
3.9	17	0.0820	0.2670	0.1449	0.0402	0.0098
4.1	18	0.0970	0.2080	0.1529	0.0345	0.0081
4.3	17	0.0870	0.2110	0.1571	0.0326	0.0079
4.5	19	0.0940	0.2970	0.1586	0.0547	0.0125
4.7	17	0.0880	0.2460	0.1494	0.0469	0.0114
4.9	18	0.0900	0.2310	0.1413	0.0385	0.0091
5.1	18	0.0680	0.2090	0.1372	0.0433	0.0102
5.3	17	0.0970	0.2230	0.1554	0.0298	0.0072
5.5	18	0.0860	0.2510	0.1567	0.0435	0.0103
5.7	20	0.0800	0.2450	0.1451	0.0478	0.0107
5.9	17	0.0610	0.2290	0.1374	0.0502	0.0122

Sample MB-03V

Height above datum (mm)	N	D(min) (mm)	D(max) (mm)	$\bar{D}$ (mm)	S (mm)	$S/\sqrt{N}$ (mm)
0.1	24	0.0770	0.1860	0.1198	0.0270	0.0055
0.3	24	0.0850	0.1980	0.1365	0.0304	0.0062
0.5	21	0.0620	0.2700	0.1473	0.0494	0.0108
0.7	24	0.0570	0.2090	0.1355	0.0462	0.0094
0.9	24	0.0740	0.2080	0.1355	0.0311	0.0064
1.1	20	0.0810	0.2400	0.1351	0.0371	0.0083
1.3	26	0.0730	0.2580	0.1462	0.0487	0.0096
1.5	21	0.0670	0.1870	0.1240	0.0367	0.0080
1.7	20	0.1040	0.2520	0.1649	0.0378	0.0085
1.9	31	0.0470	0.2470	0.1255	0.0536	0.0096
2.1	23	0.0860	0.2590	0.1385	0.0398	0.0083
2.3	22	0.0730	0.2560	0.1404	0.0404	0.0086
2.5	21	0.0620	0.2530	0.1394	0.0531	0.0116
2.7	25	0.0640	0.2250	0.1212	0.0434	0.0087
2.9	26	0.0830	0.2000	0.1343	0.0316	0.0062
3.1	30	0.0450	0.1610	0.1033	0.0262	0.0048
3.3	27	0.0570	0.3940	0.1427	0.0630	0.0121
3.5	18	0.0900	0.2300	0.1572	0.0431	0.0102
3.7	19	0.0750	0.2100	0.1522	0.0442	0.0101
3.9	15	0.0820	0.2410	0.1788	0.0403	0.0104
4.1	20	0.0590	0.2260	0.1524	0.0427	0.0095
4.3	17	0.1150	0.2500	0.1668	0.0376	0.0091
4.5	27	0.0550	0.2560	0.1396	0.0475	0.0091
4.7	24	0.0640	0.2040	0.1183	0.0348	0.0071
4.9	25	0.1000	0.2190	0.1562	0.0372	0.0074
5.1	20	0.0910	0.2470	0.1494	0.0428	0.0096
5.3	25	0.0950	0.2000	0.1363	0.0219	0.0044
5.5	19	0.0860	0.2250	0.1431	0.0371	0.0085
5.7	21	0.0810	0.2310	0.1482	0.0424	0.0093
5.9	16	0.0960	0.2840	0.1768	0.0413	0.0103

Sample ShR-01

Height above datum (mm)	N	D(min) (mm)	D(max) (mm)	$\bar{D}$ (mm)	S (mm)	$S/\sqrt{N}$ (mm)
0.1	17	0.0620	0.2000	0.1189	0.0360	0.0087
0.3	21	0.0370	0.2000	0.1210	0.0419	0.0091
0.5	21	0.0810	0.2160	0.1196	0.0325	0.0071
0.7	21	0.0590	0.2070	0.1299	0.0380	0.0083
0.9	16	0.0890	0.1980	0.1390	0.0341	0.0085
1.1(L)	15	0.0560	0.1910	0.1070	0.0396	0.0102
1.1(H)	13	0.0530	0.1240	0.0849	0.0228	0.0063
1.3(L)	17	0.0630	0.1920	0.1116	0.0360	0.0087
1.3(H)	8	0.0520	0.1710	0.1033	0.0381	0.0135
1.5(L)	14	0.0680	0.1700	0.1235	0.0288	0.0077
1.5(H)	4	0.0640	0.1350	0.0950	0.0295	0.0147
1.7	21	0.0640	0.1540	0.1117	0.0289	0.0063
1.9	23	0.0570	0.2080	0.1156	0.0377	0.0079
2.1	17	0.0420	0.2290	0.1167	0.0397	0.0096
2.25(L)	11	0.0370	0.1340	0.0908	0.0290	0.0087
2.25(H)	12	0.0420	0.1630	0.0853	0.0370	0.0107
2.35(L)	5	0.0640	0.1360	0.0954	0.0307	0.0137
2.35(H)	10	0.0420	0.1790	0.1197	0.0391	0.0124
2.5(L)	12	0.0620	0.1580	0.1110	0.0315	0.0091
2.5(H)	8	0.0840	0.1350	0.1151	0.0196	0.0069
2.7(L)	12	0.0660	0.1830	0.1243	0.0327	0.0094
2.7(H)	8	0.0390	0.2300	0.1370	0.0565	0.0200
2.9(L)	15	0.0680	0.2430	0.1309	0.0502	0.0130
2.9(H)	7	0.0500	0.1330	0.0956	0.0298	0.0113
3.05(L)	3	0.0740	0.1160	0.0920	0.0216	0.0125
3.05(H)	13	0.0740	0.1500	0.1112	0.0192	0.0053
3.15(L)	3	0.0870	0.1590	0.1347	0.0413	0.0238
3.15(H)	12	0.0350	0.1300	0.0998	0.0241	0.0069
3.25(L)	3	0.1780	0.3800	0.2590	0.1068	0.0616
3.25(H)	10	0.0500	0.1460	0.1007	0.0304	0.0096
3.35(L)	5	0.0920	0.1690	0.1404	0.0300	0.0134
3.35(H)	7	0.0930	0.1500	0.1249	0.0180	0.0068
3.45	8	0.0860	0.2010	0.1338	0.0316	0.0112

Sample ShR-01

Height above datum (mm)	N	D(min) (mm)	D(max) (mm)	$\bar{D}$ (mm)	S (mm)	$S/\sqrt{N}$ (mm)
3.55(L)	3	0.0780	0.1440	0.1067	0.0338	0.0195
3.55(H)	4	0.0670	0.1210	0.0953	0.0255	0.0127
3.65(L)	5	0.0400	0.1480	0.0940	0.0440	0.0197
3.65(H)	13	0.0560	0.1250	0.0898	0.0213	0.0059
3.75(H)	16	0.0580	0.1620	0.1176	0.0316	0.0079
3.85(L)	4	0.0980	0.1300	0.1128	0.0132	0.0066
3.85(H)	16	0.0530	0.2090	0.1110	0.0378	0.0094
3.95(L)	8	0.1080	0.1680	0.1326	0.0174	0.0062
4.1(L)	14	0.0830	0.1830	0.1226	0.0283	0.0076
4.1(H)	3	0.0660	0.1130	0.0827	0.0263	0.0152
4.3(L)	19	0.0690	0.1850	0.1052	0.0278	0.0064
4.3(H)	12	0.0740	0.1510	0.1101	0.0281	0.0081
4.5	11	0.1110	0.1710	0.1338	0.0167	0.0050
4.7	11	0.0799	0.1857	0.1358	0.0274	0.0083
4.9	13	0.0790	0.2130	0.1224	0.0358	0.0099
5.1	14	0.0620	0.2090	0.1410	0.0405	0.0108
5.3	17	0.0830	0.1690	0.1234	0.0222	0.0054
5.5	17	0.0510	0.2500	0.1207	0.0480	0.0116
5.7	14	0.0830	0.2060	0.1411	0.0334	0.0089
5.9	20	0.0540	0.2030	0.1040	0.0373	0.0083

Sample G-05B

Height above datum (mm)	N	D(min) (mm)	D(max) (mm)	$\bar{D}$ (mm)	S (mm)	$S/\sqrt{N}$ (mm)
0.1	10	0.0930	0.1930	0.1438	0.0318	0.0101
0.3	11	0.1040	0.2310	0.1531	0.0400	0.0121
0.5	10	0.0790	0.2680	0.1695	0.0634	0.0200
0.7	5	0.1040	0.2110	0.1502	0.0425	0.0190
0.9	8	0.1144	0.2455	0.1810	0.0488	0.0173
1.1	10	0.0992	0.2674	0.1469	0.0538	0.0171
1.3	12	0.1130	0.2270	0.1651	0.0320	0.0092
1.5	14	0.1180	0.2370	0.1576	0.0372	0.0099
1.7(L)	9	0.0900	0.2070	0.1412	0.0358	0.0119
1.7(H)	5	0.0440	0.0700	0.0564	0.0010	0.0042
1.9(L)	7	0.1050	0.2170	0.1470	0.0438	0.0166
1.9(H)	14	0.0330	0.1550	0.0726	0.0319	0.0085
1.9(I)	4	0.0880	0.1750	0.1258	0.0362	0.0181
2.1(L)	6	0.0420	0.1300	0.0922	0.0288	0.0118
2.1(H)	12	0.0490	0.1240	0.0848	0.0211	0.0061
2.1(I)	10	0.0680	0.1250	0.0921	0.0182	0.0058
2.3(L)	17	0.0520	0.1600	0.0941	0.0306	0.0074
2.3(H)	9	0.0470	0.1410	0.0937	0.0272	0.0091
2.5	14	0.0670	0.1720	0.1112	0.0296	0.0079
2.7	15	0.0560	0.1700	0.1163	0.0291	0.0075
2.9(H)	11	0.0390	0.1090	0.0658	0.0242	0.0073
2.9(I)	13	0.0390	0.1180	0.0768	0.0236	0.0074
3.1(I)	21	0.0250	0.1430	0.0741	0.0282	0.0062
3.05(H)	21	0.0220	0.1210	0.0603	0.0270	0.0059
3.15(H)	23	0.0280	0.0970	0.0616	0.0163	0.0034
3.3(H)	18	0.0300	0.1240	0.0697	0.0249	0.0059
3.3(I)	7	0.0370	0.1230	0.0820	0.0297	0.0112
3.5(L)	8	0.0647	0.1262	0.0978	0.0204	0.0072
3.5(H)	4	0.0714	0.1320	0.1059	0.0302	0.0151
3.5(I)	7	0.0570	0.2010	0.1006	0.0481	0.0182
3.7(L)	12	0.0550	0.1560	0.1014	0.0288	0.0083
3.7(I)	9	0.0540	0.1290	0.0907	0.0299	0.0100
3.9(L)	10	0.0620	0.1040	0.0855	0.0156	0.0049

Sample G-05B

Height above datum (mm)	N	D(min) (mm)	D(max) (mm)	$\bar{D}$ (mm)	S (mm)	$S/\sqrt{N}$ (mm)
3.9(I)	6	0.0830	0.1310	0.1018	0.0217	0.0088
4.1(L)	10	0.0520	0.1570	0.1117	0.0396	0.0125
4.1(I)	5	0.1000	0.1980	0.1436	0.0353	0.0158
4.3(L)	15	0.0640	0.1570	0.1017	0.0265	0.0069
4.5	15	0.0660	0.2140	0.1314	0.0408	0.0105
4.7	13	0.0960	0.2250	0.1368	0.0414	0.0115
4.9	9	0.0530	0.1970	0.1332	0.0388	0.0129
5.1	14	0.1000	0.2690	0.1557	0.0481	0.0129
5.3	15	0.0620	0.2410	0.1491	0.0553	0.0143
5.5	16	0.0620	0.1820	0.1224	0.0281	0.0070
5.7	16	0.0940	0.1930	0.1499	0.0307	0.0077
5.9(L)	10	0.0620	0.1630	0.1078	0.0288	0.0091
5.9(H)	25	0.0360	0.1460	0.0767	0.0286	0.0057
5.9(I)	10	0.0490	0.1000	0.0719	0.0189	0.0060
6.1(L)	4	0.0490	0.1020	0.0910	0.0098	0.0049
6.1(H)	24	0.0640	0.1360	0.1037	0.0206	0.0042
6.1(I)	8	0.0560	0.1350	0.0906	0.0263	0.0093
6.3(H)	29	0.0420	0.1450	0.0966	0.0314	0.0059
6.3(I)	9	0.0520	0.1050	0.0810	0.0151	0.0050
6.5	8	0.0960	0.3460	0.1969	0.0816	0.0288
7.6	8	0.0990	0.3500	0.2278	0.0783	0.0277

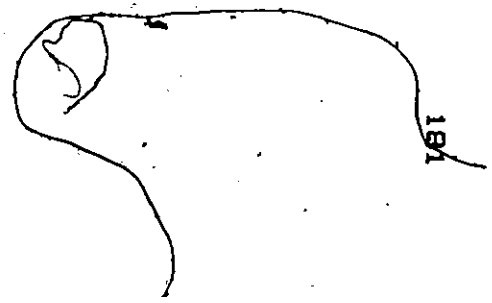

Sample G-06A

Height above datum (mm)	N	D(min) (mm)	D(max) (mm)	$\bar{D}$ (mm)	S (mm)	$S/\sqrt{N}$ (mm)
0.1	13	0.1061	0.3058	0.1752	0.0631	0.0175
0.3	15	0.1192	0.2776	0.1771	0.0503	0.0130
0.5	9	0.0409	0.3070	0.1384	0.0896	0.0299
0.7	12	0.1100	0.3287	0.1955	0.0594	0.0172
1.0	14	0.0910	0.2780	0.1848	0.0629	0.0168
1.4	19	0.0880	0.3540	0.2027	0.1133	0.0260
1.8	18	0.0598	0.3140	0.1907	0.0846	0.0199
2.1(L)	7	0.1921	0.3841	0.2892	0.0709	0.0268
2.1(H)	2	0.0744	0.0953	0.0848	0.0148	0.0105
2.3(L)	8	0.0753	0.2574	0.1437	0.0667	0.0236
2.3(H)	13	0.0392	0.0854	0.0665	0.0153	0.0042
2.5(L)	5	0.0806	0.4248	0.1968	0.1413	0.0632
2.5(H)	23	0.0410	0.1369	0.0776	0.0262	0.0055
2.5(I)	16	0.0409	0.2070	0.0988	0.0498	0.0203
2.7(L)	6	0.0535	0.2606	0.1597	0.0690	0.0285
2.7(H)	4	0.0603	0.0957	0.0819	0.0170	0.0085
2.7(I)	13	0.0157	0.2032	0.1043	0.0491	0.0136
2.9(L)						
2.9(H)	1	0.2141	0.2141	0.2141		
2.9(I)	5	0.0632	0.1533	0.0990	0.0338	0.0151
3.1	12	0.0841	0.2407	0.1379	0.0452	0.0130
3.3	10	0.1038	0.2961	0.1977	0.0588	0.0186
3.5	14	0.1097	0.2483	0.1754	0.0399	0.0107
3.7(L)	10	0.1413	0.2900	0.2017	0.0517	0.0163
3.7(H)	2	0.0779	0.1067	0.0923	0.0204	0.0144
3.9(L)	13	0.0598	0.2953	0.1707	0.0808	0.0224
3.9(H)	2	0.0775	0.0888	0.0832	0.0080	0.0057
3.9(I)	3	0.0808	0.1146	0.1033	0.0195	0.0113
4.1	13	0.0895	0.3623	0.2126	0.0669	0.0186
4.3	5	0.0849	0.2532	0.1719	0.0759	0.0339
4.5	7	0.0836	0.3332	0.2157	0.0762	0.0311
4.7	6	0.1563	0.3388	0.2167	0.0676	0.0276
4.9	8	0.1439	0.5233	0.2589	0.1378	0.0487
5.1	9	0.0681	0.3998	0.2022	0.0922	0.0307

Sample G-07B

Height above datum (mm)	N	D(min) (mm)	D(max) (mm)	$\bar{D}$ (mm)	S (mm)	$S/\sqrt{N}$ (mm)
0.1	5	0.2090	0.4030	0.2896	0.0941	0.0421
0.3	6	0.0940	0.4470	0.2135	0.1261	0.0515
0.5	11	0.0830	0.3090	0.1487	0.0723	0.0218
0.7(L)	11	0.0590	0.2100	0.1350	0.0417	0.0126
0.7(H)	14	0.0250	0.1430	0.0711	0.0341	0.0091
0.9(H)	29	0.0480	0.1660	0.0957	0.0313	0.0058
0.9(I)	15	0.0370	0.1150	0.0781	0.0239	0.0062
1.1	10	0.0910	0.2270	0.1677	0.0447	0.0141
1.3	9	0.1030	0.2300	0.1629	0.0472	0.0157
1.5	13	0.0220	0.2210	0.1222	0.0500	0.0139
1.7	12	0.0620	0.2080	0.1135	0.0454	0.0131
1.9	15	0.0750	0.3190	0.1677	0.0607	0.0157
2.1	12	0.0730	0.2910	0.1772	0.0638	0.0189
2.3	20	0.0820	0.2480	0.1451	0.0453	0.0101
2.5(L)	14	0.0590	0.2290	0.1402	0.0532	0.0142
2.5(I)	6	0.0460	0.1310	0.0710	0.0311	0.0127
2.7(L)	8	0.0700	0.1390	0.1145	0.0224	0.0079
2.7(H)	11	0.0490	0.1690	0.0979	0.0321	0.0097
2.7(I)	11	0.0700	0.1460	0.1122	0.0272	0.0082
2.9(L)	20	0.0500	0.1840	0.1120	0.0344	0.0077
2.9(H)	6	0.0400	0.1610	0.1053	0.0523	0.0214
3.1	20	0.0810	0.1950	0.1325	0.0335	0.0075
3.3	19	0.0500	0.1560	0.1028	0.0262	0.0060
3.5	15	0.0570	0.1730	0.1132	0.0307	0.0079
3.7(L)	17	0.0590	0.1370	0.0892	0.0185	0.0045
3.7(H)	7	0.0320	0.0740	0.0504	0.0146	0.0055
3.7(I)	4	0.0740	0.1660	0.1173	0.0406	0.0203
3.9(L)	15	0.0420	0.1320	0.0840	0.0254	0.0066
3.9(H)	7	0.0620	0.1210	0.0899	0.0204	0.0077
3.9(I)	8	0.0490	0.1570	0.9978	0.0340	0.0120
4.1	16	0.0900	0.2220	0.1403	0.0413	0.0103
4.3	12	0.0780	0.2060	0.1378	0.0432	0.0119
4.5	10	0.0910	0.2980	0.1577	0.0660	0.0209

Sample G-07B

Height above datum (mm)	N	D(min) (mm)	D(max) (mm)	$\bar{D}$ (mm)	S (mm)	$S/\sqrt{N}$ (mm)
4.7	12	0.1040	0.2670	0.1583	0.0414	0.0120
4.9	8	0.0400	0.2990	0.1296	0.0893	0.0316
5.1	13	0.0840	0.1660	0.1173	0.0239	0.0066
5.3	10	0.1020	0.3010	0.1587	0.0586	0.0185
5.5	7	0.0820	0.2780	0.1826	0.0645	0.0244
5.7	12	0.0700	0.3570	0.1725	0.0720	0.0208
5.9	12	0.0760	0.2350	0.1315	0.0390	0.0113
6.1	10	0.1250	0.2850	0.1851	0.0547	0.0173
6.3	8	0.1400	0.2350	0.1718	0.0338	0.0120
6.5	12	0.0780	0.2620	0.1534	0.0465	0.0134
6.7	11	0.1090	0.3340	0.1877	0.0637	0.0192
6.9	12	0.0700	0.2630	0.1424	0.0684	0.0198
7.1	8	0.1026	0.1906	0.1379	0.0265	0.0094
7.3	8	0.0990	0.1446	0.1270	0.0150	0.0053
7.5						
7.7	8	0.0700	0.1940	0.1285	0.0416	0.0147
7.9	13	0.0870	0.2620	0.1614	0.0484	0.0134
8.1	9	0.0810	0.2750	0.1647	0.0703	0.0234
8.3	8	0.1430	0.2940	0.2348	0.0473	0.0167
8.5	9	0.0127	0.3500	0.1942	0.0728	0.0243
8.7	11	0.0970	0.5880	0.1947	0.1548	0.0467